Eel Density Analysis (EDA 2.3)

Escapement of silver eels (*Anguilla anguilla*) from French, Spanish and Portuguese rivers

GT4 - deliverable E4.1.1

Cédric Briand (1), María Mateo (2), Hilaire Drouineau(3), María Korta (2), Estibaliz Díaz (2), Laurent Beaulaton (4)

(1) EPTB-Vilaine, (2) AZTI, (3) INRAE, (4) OFB

version 2.3 final, February 8, 2022

Eel Density Analysis (EDA 2.3)

Escapement of silver eels (*Anguilla anguilla*)
from French, Spanish and Portugese rivers

1 Introduction

The European eel (*Anguilla anguilla*) range extends from the Baltic Sea to the Mediterranean Sea (Tesch and White, 2008). Reproduction takes place in the Sargasso Sea (Schmidt, 1922; Miller et al., 2014). European eel leptocephalus larvae cross the Atlantic Sea and later transform into glass eel when they reach the continental slope (Tesch, 1980; Schmidt, 1909). Glass eel will, using tide currents, colonize coastal areas, estuaries and possibly when conditions are favourable, progress inland during a short colonization of fresh water. The glass eel then turn into yellow eels, and this stage will gradually achieve colonization of the continental freshwater habitats (Naismith and Knights, 1988; Feunteun et al., 2003). The distribution of eels is naturally concentrated in the downstream part of water basins (Ibbotson et al., 2002). Upon reaching a size of 30 cm, eels will settle and most of them will remain confined in a reduced home range territory for the remainder of their continental life (Laffaille et al., 2005a; Tesch and White, 2008; Imbert et al., 2010). After a variable number of year (Svedäng et al., 1996) yellow eels will metamorphose into silver eels (Durif et al., 2006). The male silver eels mature at a lower size and age than their female counterparts, the size limit between the two sexes is about 45 cm (Tesch and White, 2008).

The European eel is outside safe biological limits (ICES et al., 2019) and is currently on the Red List of the International Union for the Conservation of Nature (IUCN), the world authority on the state of nature and natural resources, classified as "Critically Endangered" (IUCN, 2018). From the end of the 1980's, the arrival of European glass eel has diminished to a minimum level in 2009 of about 1 to 5 % of their level before the decline. Since 2010, but the level of glass eel arrival has remained low, between 4 and 12 % of the reference level of the 1960's-1970's (ICES et al., 2019). Several effects of global change have been proposed to explain these declines (Drouineau et al., 2018), including changes in oceanic conditions, contamination and habitat degradation, parasitism, fishing pressure, fragmentation including habitat loss, and hydroelectricity-induced mortality. For that reason, the EU regulation 1100/2007 established a management framework whose objective is to restore the eel stock. EU Member States have developed Eel Management Plans (EMPs) for their river basin districts to allow at least 40 % of the silver eel biomass to escape to the sea with high probability, relative to the best estimate of escapement that would have existed if no anthropogenic pressures had impacted the stock.

To test whether management objectives set by the EU regulation 1100/2007 have been met, the biomass of spawners produced by the different management units from EU Member States must be assessed, but also the mortality rates caused by anthropogenic sources. However, the review of the Member States EMPs ICES (2013) concluded that data and knowledge gaps, variability in data collection formats, level of detail and coverage restricted the value of international stock assessment. This problem also occurs in the SUDOE area: the eel in Spain, France and Portugal constitutes a single stock but it is assessed at national and regional level as if it were an isolated stock (Figure 1.1). The French EMP estimated the escapement using the Eel Density Analysis (EDA) model. For Portugal, no single actual value was used and reference values for escapement from the River Rhone were extrapolated to all its basins. In Spain, each of the Autonomous Communities that constitute an Eel Management Unit (EMU) carried out estimates using different methodologies: gross extrapolations with real or reference values. As such, the escapement estimates are incomparable, and in some cases even unreliable, making it difficult to manage the population based on escapement rates.

Comprehensive assessment and management of the species requires the greatest possible coordination and standardization of data collection and assessment methods among the different states. For that reason, one of the major objectives of the SUDOANG project is to apply the Eel Density Analysis (EDA) model (Briand et al., 2018; de Eyto et al., 2016; Jouanin et al., 2012a; Walker et al., 2011) as a common tool at the scale of the SUDOE area to harmonize the silver eel predictions between France, Portugal and Spain. This model uses electrofishing data to predict the average silver eel output from the different portions of the basins using a spatial model based on river stretch characteristics, and in particular the anthropogenic pressures (mainly dams) applied to the river segments.

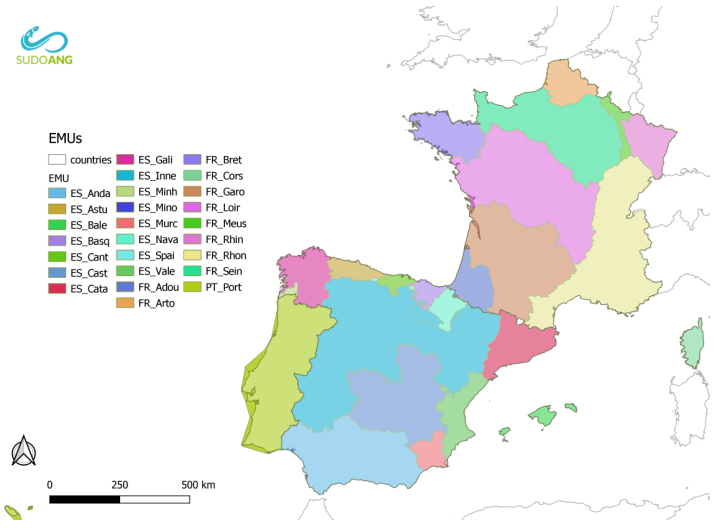

Figure 1.1: Eel Management Units (EMU) in the SUDOE area.

The construction of the EDA model started by the data collection in GT1 on the eel stock and river characteristics in the SUDOE area, thanks to the contribution of the SUDOE water managers and SUDOANG researchers. Data from GT6 (River basin network) for eels in the pilot basins has also fed the model. The estimate shall be based on a hydrographic network available at the scale of the SUDOE area. The potential users

of the results, many of whom are associate partners of SUDOANG, have participated in the implementation of EDA through three specific workshops (in Coruña, Bordeaux and Sukarrieta) and through mail exchanges. Specifically, they have detected data inconsistencies and have given their opinion regarding the variables to be considered and the way in which the results are presented.

This report provides a detailed overview of the model calibration and results. The results are included in the INTERACTIVE WEB APPLICATION (VISUANG) of GT5, one of the two main products of the project that hosts all the tools that have been generated in the different GTs. The results are discussed and detailed in summary table per country or EMUs.

2 Material and methods

Building the EDA model can be summarized as three major steps. The first step is the data collection and its compilation in a database, the second step consists in data validation and screening before modelling, and the third process is the model building.

2.1 Building the dataset

The dataset used to implement EDA consists of electrofishing data. These data include site locations, fishing operations which can be done several times at one site, and fish data collected during each operation. The operations are attached to stretches of river or river segments whose characteristics describe the conditions for presence, density, size structure, or silvering rate of the eels. In particular, the topology of the river network is used to extract important attributes such as the distance to the sea, or the path of river flowing downstream to the sea.

2.1.1 Rivers

The most time demanding aspect of building the EDA model is to build a consistent database of rivers. These rivers are connected from separate datasets in three countries to build a spatial topology. These datasets correspond to the most suited to operational management available at the time of the project. A previous implementation of the model, the EDA2.0 model (Jouanin et al., 2012b; Walker et al., 2011) was built on the CCMv2.1 (Catchment Characterisation and Modelling) (Vogt et al., 2003, 2007), a European hydrographical database. This network includes a hierarchical set of river stretches and catchments based on the Strahler order, a lake layer and structured hydrological feature codes based on the Pfafstetter system. Catchments are divided into unit catchments and unit river stretches. However, the building of EDA in France, or Ireland (de Eyto et al., 2016) using several river networks has shown that the main problem of the CCM is the lack of detail of rivers, in particular the water surface was underestimated, and this could lead to a large under evaluation of the eel production.

In France, the Theoretical River Network RHT has been used to build the EDA 2.1 model (Pella et al., 2012). This network was designed to analyse hydro-morphological characteristics of streams at the national level. It is a simplified representation of

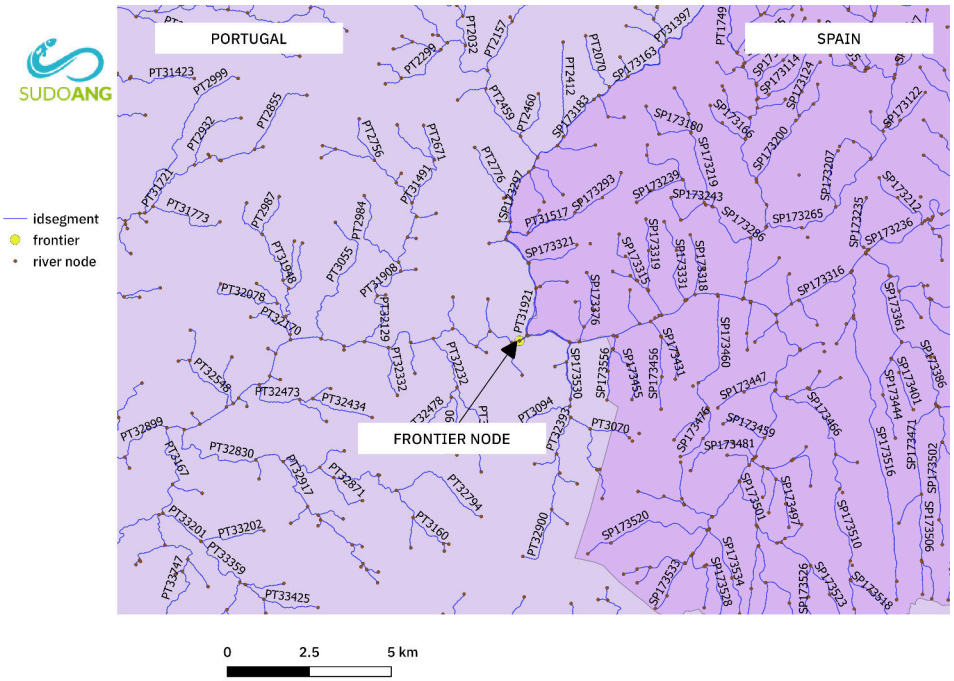

Figure 2.1: Map showing a detail of the river segments and their idenfication at the frontier between Spain and Portugal.

streams based on the BD CARTHAGE but excluding features such as river division into river branch in the downstream alluvial plains. It has been updated recently with a modelling of flow and river stretch characteristics (width, depth, and quantile flow) (Morel et al., 2019). This river network has been used to predict yellow and silver eel productions in the previous version of EDA (EDA2.1) (Briand et al., 2018), to explore the diffusion of eels within the river system (Domange et al., 2018). In Spain and Portugal, the river networks developed for the EU Directive 2007/2/EC establishing an Infrastructure for Spatial Information in the European Community (INSPIRE) are used (Figure 2.1). Both have been implemented following the Guidance document to implement the GIS elements of the Water Framework Directive (European Commission and Directorate-General for the Environment, 2003). The rivers present a tree structure similar to RHT, where branches cannot merge again once they have been divided (*e.g.* the river only forks when going upstream).

2.1.1.1 River dataset

The precision of the river network differs between countries. The RHT is the less detailed network, the Portuguese river network has an intermediate level of details, while the Spanish river network provides the most detailed river course. In the first part of the project, data was split at the frontier using the frontier location as a rough cutting edge. This raised problems particularly in border basins like the Guadiana (in Spain), where the river flows back and forth between segments of the Spanish and Portuguese river datasets. A large GIS amount of work was devoted to snapping all orphan river segments to the main river, remove duplicated segments and build a topologically consistent river network between the different countries. In some case, for instance in the Pyreneans, this required to extend river segments downstream beyond the fron-

tier to connect the Adour River basin for instance. This was done using the CCM as a validation in the background to retrack the true missing river course. The rivers corresponding to Andorra [1] are not integrated, as this river network is of minor importance regarding the eel. All frontier segments are identified including those flowing from or to countries other than those from the SUDOE area (Belgium, Luxemburg, Germany, Switzerland and Italy) (Figure 2.2).

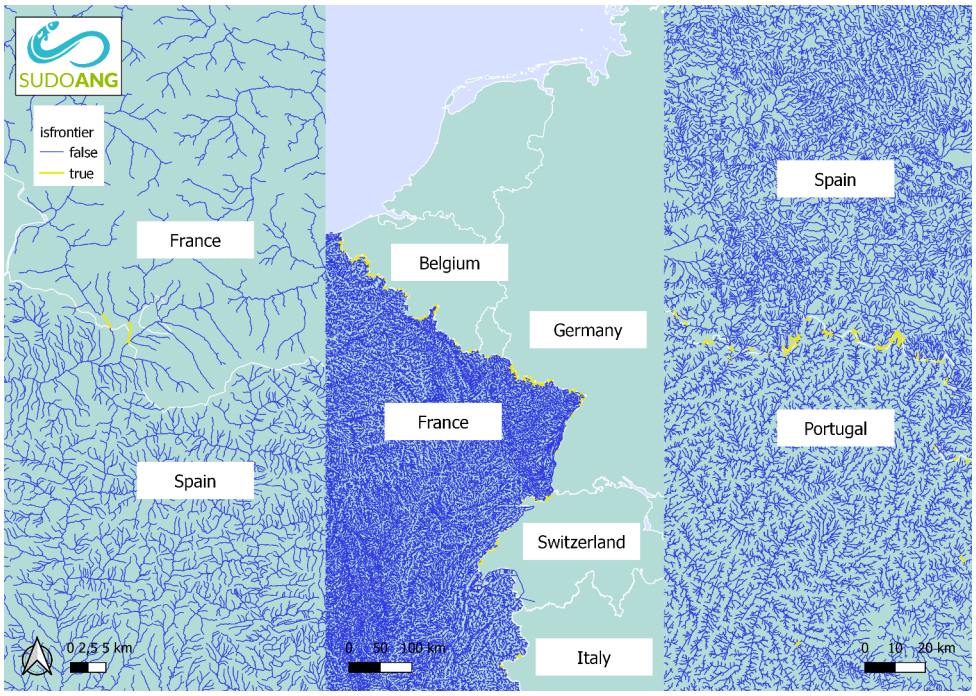

Figure 2.2: Identification of the frontier segments in the SUDOANG river Atlas.

All river segments flowing to the sea. Some work was required to differentiate between endoreic segments and those outlet located far from the coastline. The full qualification of frontier river segment, and sea river segments allowed to qualify and fully describe the endorheic river segments, as those were the remaining segments without downstream attributes.

2.1.1.2 Chaining streams

A chaining method was applied in R to calculate cumulated drainage areas and flow. The paths from the sea are also stored as a ltree object in PostGIS that allow to store hierarchical structures in spatial databases (link to R code).

Based on this river topology, the Shreve (Shreve, 1966) and the Strahler (Strahler, 1952) ranks and the cumulated surface of drainage basin upstream are calculated on the international river network including the transboundary catchments. Currently the surface of basins from Switzerland, Italy that are upstream from French basins are ignored.

Other variables such as the cumulated distance and the path to the sea, have been calculated by using routing algorithms starting from the sea. These have been used to store in the database the topological relationship within the river network (use of

[1] At the frontier between Spain and France.

PostgreSQL ltree paths). These paths are later used to build functions that quickly calculate which river segments are flowing at a particular point, *i.e.* that extract the whole basin upstream.

2.1.1.3 Discharge

Discharge data is collected from the RHT (Morel et al., 2019) in France. In Spain and Portugal, the discharge from the RiverATLAS (Linke et al., 2019) is added to the database. It corresponds to natural discharge average from the WaterGAP v2.2 (data of 2014) (Döll et al., 2003). Discharge from the WaterGAP model are close to the discharge calculated from RHT. As the SUDOANG river network is more detailed than the RiverATLAS, the joining is performed by selecting only segments with Shreve index larger than 2. When several segments can be joined, the closest in term of Strahler rank is selected[2].

Flow data are used to calculate the risk for a stream to be temporal. Most headwater reported in the Spanish database (under Shreve rank 6) have no visible riverbed. Built from thalwegs (altitude data) and slope using GIS tools, they often do not have any riverbed when looking at digital orthophotography and satellite imagery. Further downstream many streams are dry and the situation worsen when looking at satellite images from the South of Spain. Using the data from INSPIRE layer as a true river dataset would have been wrong. However, at the time of predictions building, only a partial dataset describing the temporal status of rivers was available, and mostly for the South of Spain. This dataset corresponds to the splitting of data along 5 classes: 1 Permanent, 2 Temporal, 3 Intermittent, 4. Ephemerous, 5 Without data. Our checks in the South of Spain have shown that several stream classified as permanent were not flowing to the sea. So the dataset has been corrected using Google Maps satelite observations. The streams have then been classified as temporal when no flow could be projected from the RiverATLAS (NULL flow) and when the Shreve rank was lower than 6. Temporal streams (class 3) have been assigned to all rivers with minimum flow lower than 0.1 $m^3 s^{-1}$ in the North of Spain and Portugal, and 0.3 $m^3 s^{-1}$ in the South of Spain and Portugal. All streams upstream from a stream categorized as temporal have been assigned a temporal status. Finally, for the Spanish Mediterranean, the temporal character was validated using local expertise and satellite imagery. Some of the rivers upstream might be flowing but it is likely that eel on the way to the upper river course would have died in the summer as the colonisation is a slow process (Ibbotson et al., 2002).

2.1.1.4 River width

In France, the river width is collected from Morel et al. (2019) model predictions. This model is built on reaches whose morphology was not altered (e.g., by channelization, reshaping or embankment) so the width computed correspond to an estimation of the river "natural" width. In Spain and Portugal, the width is obtained when possible, by joining the MERIT Hydro (Yamazaki et al., 2019) database licence CC-BY-NC 4.0. The average of the raster width projected at 10 points along the segment is used. This projection excludes the segments with Strahler 1 to 3 in Spain, and Strahler 1 in Portugal

[2] SQL Script to join the RiverATLAS.

to only keep the width calculated in reservoirs in the main streams [3]. A manual verification of width collected using electrofishing sampling has confirmed the right order of magnitude of the MERIT Hydro dataset projection, except in places with islands in the middle of the stream. For other segments, the width has been calculated using a model based on drainage area, basins grouped by runoff categories, and calibrated on data comprising both randomly collected width and electrofishing data [4].

2.1.1.5 Water surface

A particular attention is brought to water surface. Indeed, the final production of silver eel estimated in the EDA model corresponds to the multiplication of the density by the water surface. The riverine water surface has been calculated as the river width multiplied by the river length. Other types of waterbodies have been joined to the river dataset to build a consistent chained network of all water surface in the basin [5].

To summarize, as for the rivers, different layers have been used for the different countries to build the river network dataset. The data structure is detailed in the Atlas (Mateo et al., 2021). One of the problems is that two overlapping datasets might describe the same waterbody. For instance, a river crossing a lake is still identified as a river in the river dataset and it has its own water surface. We used GIS tools to split the dataset per unit basins surrounding all river segments, and then we removed from the additional waterbodies the surface corresponding to rivers within the unit basin. After this correction, the sum of river water and waterbodies surface, does correspond to the true water surface (figure 2.3).

Finally, the waterbodies have been classified according to the following types: estuary, lagoon, reservoirs, lakes, temporary lakes and large rivers. The downstream part of some estuaries in France are still not included in the EDA2.3 dataset and the estuaries have still to be separated in the downstream part of rivers. For Spain and Portugal, estuaries correspond to the WISE transitional waters. The lagoons have been included in Spain, Portugal and France. In France the main lagoons are identified by management units from the IFREMER source layer.

2.1.1.6 Topological variables

Topological variables have been extracted from the dataset. Eels migrating upstream in a river corridor might stop when they encounter a large water body in which they can settle. So, the largest the surface area below, the larger the chance that the eel might settle. Following this idea, we calculated the downstream cumulated water surface for the river and/or associated waterbodies, and the downstream drainage wetted surface corresponding to the sum of river water surface and associated waterbodies water surface in the basin downstream. The water surfaces are cumulated in the main drain and tributaries on all river segments that have the same or a lesser distance to the sea to calculate the downstream drainage area $downstdrainagewettedsurface$ in m^2. This metric corresponds to the habitat that can be accessed by eels in the basin downstream from the current drain. The same variable is calculated including the surface of the additional waterbodies $downstdrainagewettedsurfaceboth$.

[3] When joining the polygon of a reservoir and a stream, the downstream part of the tributaries connected to the river network may be attributed the width of the reservoir.

[4] Script to join the MERIT Hydro.

[5] html report and code.

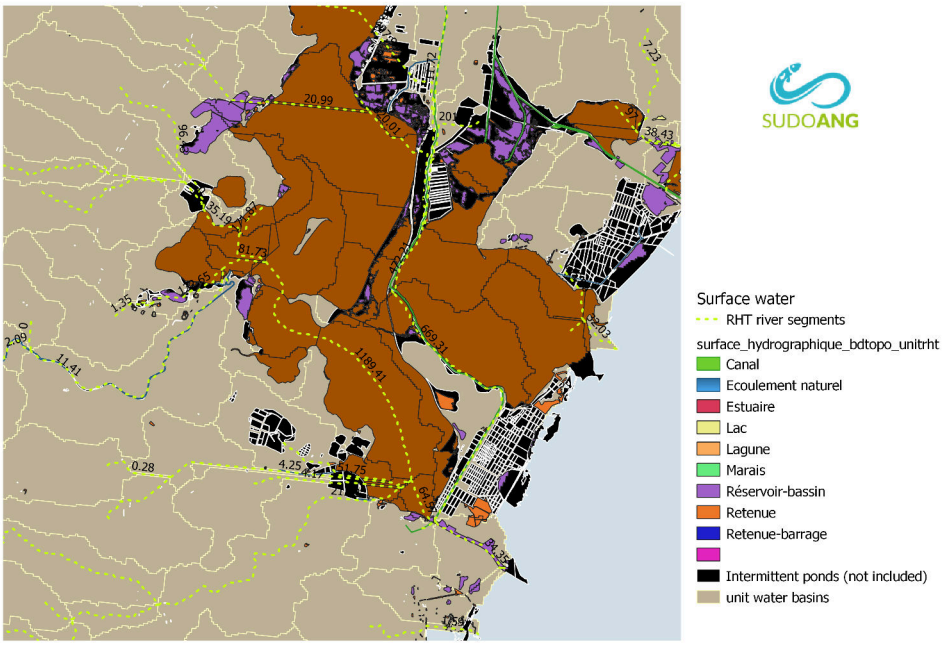

Figure 2.3: Other water surface per type and RHT river segments illustrated in the Bages–Sigean lagoon (France). The type of water and their geometry are those of the BD TOPAGE. Intermittent ponds are not included in the water surface, and the unit basins from RHT are used to connect the different waterbodies. A waterbody connected to the river network will have the same characteristics as the river segment in the model.

The shape of a river has also an impact on the colonisation, the eel migrating upstream will split up more in wide basins with a lot of river branches than in narrow basins with a single river corridor. The hydraulic density *hydraulicdensityperm* (in m^{-1}) corresponds to the cumulated length of river divided by cumulated land surface for river segments with a similar or lesser distance to the sea. The transformed downstream drainage wetted surface (*lddws*) corresponds to all types of water surface -so it corresponds to the surface of both the river drainage and additional water bodies wetted area (lakes, reservoir, ...)- divided by the surface of the basin, for river segments with a similar or lesser distance to the sea (Domange et al., 2018). It's an indices of "wetness" of the basin downstream (without unit).

2.1.1.7 Large geographical variables

Models are run with large geographical categorical variables. The largest level is country. The SUDOE area corresponds to grouping into several zones for recruitment (Mediterranean *MED*, Atlantic Coast of Portugal and Spain ATL_{IB}, Cantabria *CANT*, Atlantic France ATL_F, Channel *CHAN* and Rhin Meuse *RhinMeu*) (Drouineau et al., 2021). The next level is the eel management unit EMUs which correspond to regions of management for eel in the eel regulation. Basin level have also considered in calculations. The distance to Gibraltar is calculated along the coast excluding the circumvolutions of estuaries or bays with the starting point in Gibraltar. This distance is negative in the Mediterranean and positive on the Atlantic coast.

2.1.2 Electrofishing data

Electrofishing data collection was performed by GT1 Task Group. Using templates created by this task group, the SUDOE water managers, the SUDOANG researchers and pilot basins from GT6 submitted their electrofishing data. In the end most data came in their own various formats and scripts are adapted to each of the source format. The data providers are listed in Table 2.1.

For Spain and Portugal, data are imported in the SUDOANG database, whose structure is inherited from the DBEEL database. This data import process is described in deliverable 1.2.1. Electrofishing data is mainly based on fishing stations, operations and eel biometry (Figure 2.4).

The station level corresponds to a location, identified by a point geometry. These points are later projected on the river network to collect the attributes of the river network used in the model (e.g. distance to the sea, altitude).

The operation level corresponds to an event occurring at a specific date. The electrofishing table inherits from the operation table and adds a few more details such as the method or the material used, the wetted area, and electrofished length and width.

The batch level corresponds either to the whole fishing, in that case the total number of fishes or the density may be reported as a batch, but it also corresponds to numbers collected at each pass. The batch also corresponds to individual data. So, a batch of one fish is reported in the fish batch table.

Finally biological characteristics, such as length, weight, ocular diameter, pectoral fin length, and contrast are entered in the biological characteristics table. The identification of sex and stage (silver and yellow) is done after a data analysis using (Durif et al., 2009).

Table 2.1: Data providers

Data provider	Place	Years	Biometry	Silvering
Gipuzkoa Provincial Council, I. Azpiroz	Gipuzkoa	1996 - 2018	YES	YES
FCUL MARE	Portugal	2014 - 2018	YES	YES
The Government Agency of Asturias	Asturias	2011 - 2018	YES	YES
Catalan Water Agency	Catalonia	2016 - 2017	YES	NO
The Xunta of Galicia	Galicia	1988 - 2017	YES	NO
URA	Basque Country	2012 - 2018	YES	YES
Environmental Management in Navarra	Navarra	2016 - 2018	YES	YES
UCO	Andalucia	2002 - 2009, 2012	YES	NO
CIIMAR	Minho river	1988 - 2018	YES	NO
Ministry for Ecological Transition	Spain	2006 - 2015	YES	NO
Vaersa Generalitat Valenciana	Valencia	2013 - 2018	YES	YES

Data integration scripts were adapted to each of the data provider, starting from the SIBIC database [6], and continuing with all data providers from (Table 2.1) [7].

2.1.3 Type of sampling

A sampling protocol variable (ω) describes the various type of electrofishing protocols used in France: ω_{ful} full (two pass) electrofishing, ω_{bf} bank fishing, and ω_{dhf} deep habitat fishing (partial point surveys) (Briand et al., 2015). In addition, eel specific survey data (RSA database) are collected on index rivers in France (Somme, Vilaine, Soustons, Parc Marais Poitevin), during regional eel specific surveys. These are reported as eel specific point sampling (eel specific abundance index ω_{eai}) (Germis, 2009b,a; Laffaille et al., 2005b) or eel specific complete fishing ω_{fue} (Feunteun, 1994). These methods differ from the standard methods by keeping the electrode for a longer duration, at least 30 seconds at a specific location (Figure 2.5). In Spain and Portugal, the type of fishing used could not be specified but it is mostly single or several pass surveys. In absence of information, the type was set to an unknown type of fishing ω_{oth}. All electrofishing reporting eels in the second pass are considered as full electrofishing (Figure 2.6).

2.1.3.1 Water surface of electrofishing stations

Densities are calculated according to the type of sampling as following:

[6] When integrating data from the SIBIC, data without date or interpretable date format have been discarded, when no numbers was reported or the number of eels reported was null but a positive density was provided, this density has been used.

[7] More information is available in the import tool report E121 import tool, and the sql source are available.

Figure 2.4: Eel data diagram. The database works by inheritance, which means that all data withing the SUDOANG schema (on the right) are also available at higher level in the international diagram designed during the POSE report (on the left) (Walker et al., 2011). Reference tables used to constrain the different attributes are not shown in this diagram.

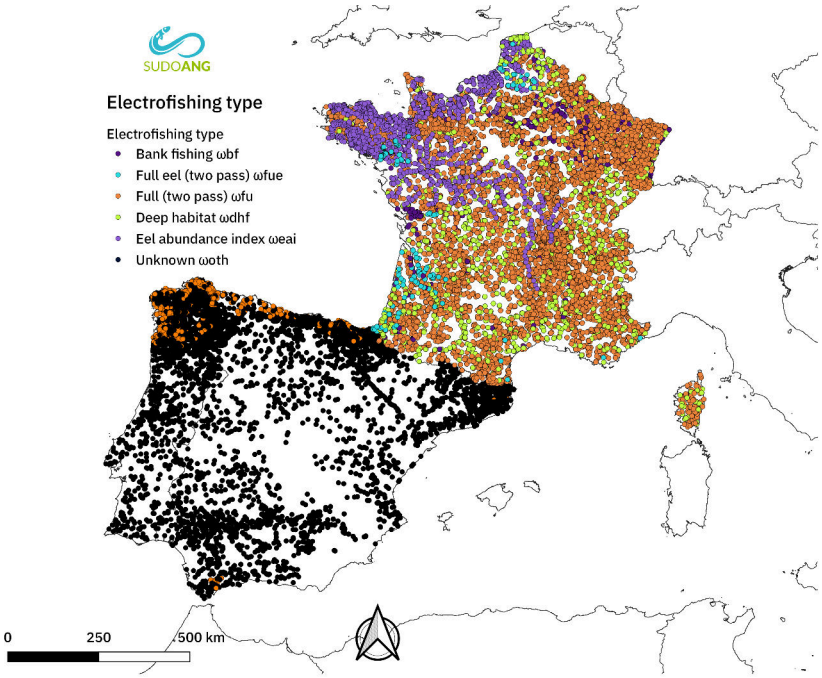

Figure 2.5: Location of electrofishing stations used in the model, categorized per type, source BDMAP, BD Agglo, DBEEL and RSA database.

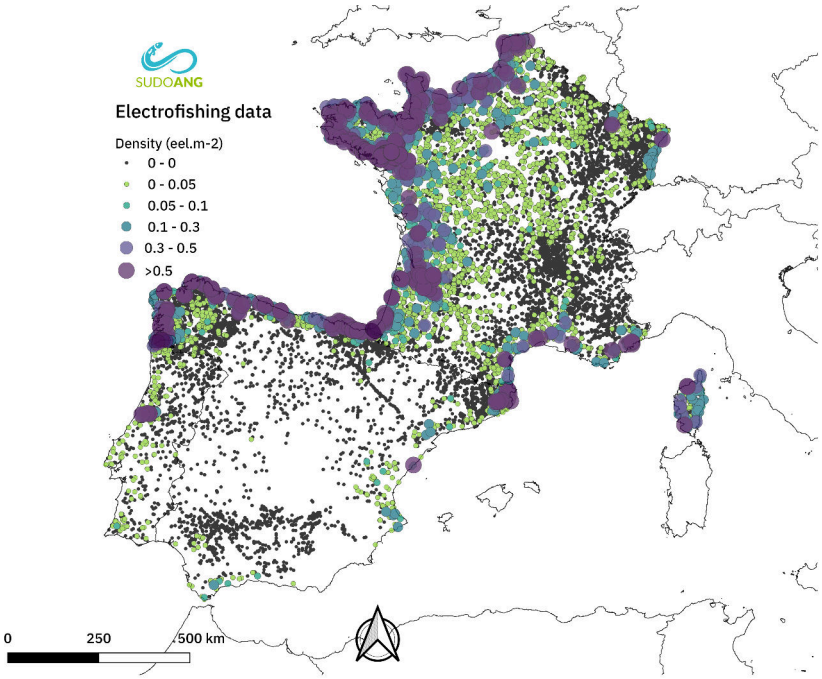

Figure 2.6: Location of electrofishing stations classified by electrofishing type, source BDMAP, BD Agglo, DBEEL and RSA database.

Full fishing & other For either eel specific surveys ω_{fue}, standard electrofishing ω_{ful} and other fishing ω_{oth}, the water surface corresponds to the water surface of the station. In France, stations where water surface is reported as larger than 3000 m^2 are removed from the dataset, while stations where the surface is too small are manually corrected using the same station at other dates. In Spain and Portugal, stations from the SIBIC with a water surface larger than 3000 m^2 are not included [8]. In addition, in Spain and Portugal, all electrofishing reporting a second pass are considered as full electrofishing.

Bank fishing ω_{bf} It was considered that the water surface corresponds to 4 times the length of the station: we consider that an anode placed in the water 0.5 m from the bank will reach an additional distance of 1.5 m from the centre of the anode, and that bank fishing is done on the two banks. This kind of electrofishing is only reported in France.

Deep habitat fishing ω_{dhf} Deep habitat fishing is done by point sampling, a surface of 12.5 m^2 (1.5 m of action radius and 0.5 m of electrode move) is used as a reference in the calculation (Belliard et al., 2008). This surface is correctly reported in the database with 75 or 100 points for one station. The more standard value of 100 points has been used as a replacement in the rare cases when both the surface and the number of points were missing in the database. This kind of electrofishing is only reported in France.

Eel specific sampling ω_{eai} For eel specific abundance index, a surface of 12.5 m^2 has been used, as in the deep habitat sampling. This kind of electrofishing is only reported in France.

Other sampling ω_{oth} In Spain and Portugal, data which is not reported as full fishing is qualified as "other".

Station surface allows to convert the numbers to density, in the case of point sampling density is not really known and the use of "standard surface" per point allows to get an indices of density that is probably not of the right order of magnitude in absolute terms but that can be integrated in the model alongside full survey densities. In the model, the predictions are made on complete fishing and the other data are used to produce standardized estimates, whose variations are used to provide information on eel abundance in the downstream part of large rivers where complete fishing is not possible. In Spain and Portugal, surface water <100 m^2 and corresponding to width of more than 10 m (N = 8(FR), 39(SP), 1(PT)) are removed from the dataset.

2.1.3.2 Estimation of total number in an operation

Densities have been calculated using Carle and Strub (1978) (FSA package, Ogle et al., 2020) for fishing events with two passes or more. A separate treatment has been applied to French data –which had already been collated from 2018 report and for which no new database was available at the time of the report– and Spanish and Portuguese data.

In Spain and Portugal, the average efficiency has been calculated by data provider, as they are expected to use different methods. When too few data were available –for

[8] When electrofishing stations larger than 3000 m^2 are reported, then probably the whole surface of the river is reported, not the surface of the station. Or the sampling is done extremely rapidly and eel would not be collected efficiently there

data providers with less than 10 fishing events with two passes allowing to calculate efficiency– the overall average efficiency has been used [9].

2.1.3.3 Size structured data

Eel lengths are collected from the DBEEL with an initial screening removing size data outside the range 50–1400 mm.

For France, values kept for size analysis correspond to:

a Operations where total count is less than 10 eels and all eels have been measured.

b Operations where total count is larger than or equal to 10 eels and at least 80% of eels have been measured.

c Values where total number is larger than 50 eels and the number of eels measured is larger than 30.

These checks were part of 2018 development of EDA in France (Briand et al., 2018).

For Spain and Portugal, no further checks were made on the representativity of size structure as this would require accessing the subsample size which are not available in the data reported in SUDOANG.

2.1.4 Dam data

The effect of dam is assessed within Task Groups GT1 and GT2, with first the compilation within the DBEEL of dam data collected from data providers and the AMBER project. The import process is described in the E221 data collection storage SUDOANG project deliverable. The work includes a separate model for France and the Iberian Peninsula (Spain + Portugal) for the prediction of missing heights. Two different models are applied in France and the Iberian Peninsula to predict the height of dams when missing.

In France dam height are log transformed linear model of dam height is fitted according to dam type, dam height, log(terrain slope+1), log(river median flow +1) and the BD CARTHAGE basin. The dam type is modelled as an interaction with basins as defined in the BD CARTHAGE.

In Spain and Portugal, dams of type bridge and culvert are excluded from the prediction dataset. This is different from France, where the dam datatype is nearly always associated always with an obstacle to migration. Those bridge with a null height or height zero are excluded from the dataset. Log transformed dam height are fitted according to dam category (*dam*, *weir* and *unknown* type) and log(slope). Missing values from flow, due to incomplete projection from the HydroATLAS database prevent from using it in the model.

The cumulated impact of dams is assessed by creating a table joining each river segment with all the dams located in the downstream course. Using this, various metrics are computed using different assumptions concerning the effect of dams. The heights are power transformed to test for a different effect of dam's height (the cumulated effect of 2 dams of 1m might be different than the cumulated effect of a single dam of 2 m), and functions are developed to calculate cumulated dam transformed variables. The presence of eel passes of various type, additional expertise for passability using

[9] contr.helmert contrast matrix (R Core Team, 2020).

the ICE protocol, or separate counts of dam heights according to the country to account for a different level of detail within each national dataset collected for dams are also tested (Briand, Mateo and Drouineau in prep, 2021).

2.2 Data validation

2.2.1 Electrofishing data

Electrofishing data systematically checked for spatial duplicates, for consistent water surface, date format, consistency between the number of eels reported in the fish table and those reported in operations. In addition, a Shiny application is developed to allow data providers to screen the data and check for possible errors for electrofishing operations where residuals from the first version of the EDA model are large, e.g. in places far upstream or above large dams where eels are reported in large density. These screening allow to remove spatial positioning problems, or misidentification of the species, but also allow to single out places where eel have been transported, thereby disrupting the natural repartition of eels along the river course.

2.2.2 Validation of dam data

Dams are projected to the closest river. This projection does not always correspond to the reality as small dams located on tributaries may have been projected on the main river body. This might create a real problem especially in large rivers where the access might be free, the dam type might be a *dam*, the dam height might have been missing and a value has been predicted for this dam. In cases where this structure is of type *weir* or *dam*, and it is located far downstream in a large river, the height predicted at that location may be high. For example, the Rhône has canals connected to the estuary that are not integrated in the RHT dataset. So, the weir acting as disconnection between the canal and the main course of the Rhône has to be identified and their heights set to zero (Figure 2.7)

The dam locations in Spain and Portugal have been evaluated for the GT6 pilot basins and their surrounding regions by the use of a Shiny application. Dams with very large height have been evaluated individually to check if the height was not an error and find out if it might be a penstock pipe. Complex dam systems might include several dams in branches of the same river. It is then necessary to only keep the dam in the main course and use a hierarchical relationship between the dams and only calculate cumulated height from the sea on the *ancestor* dam. In France, the ROE database hierarchical structure has been used, and recursive queries have been used to catch all dams or structure related to the main one. This hierarchical structure has then been reported in the SUDOANG database. Both types have been systematically selected and screened out also using the Shiny application. Both errors have led to calculate cumulated height for dams higher than the terrain elevation, a systematic examination of the sectors where this kind of errors occurs has been conducted.

Dams might still be in parallel in the lowest course of the rivers where the river network is more often braided, but these kinds of errors are thought to be rare and will only be related to smaller height.

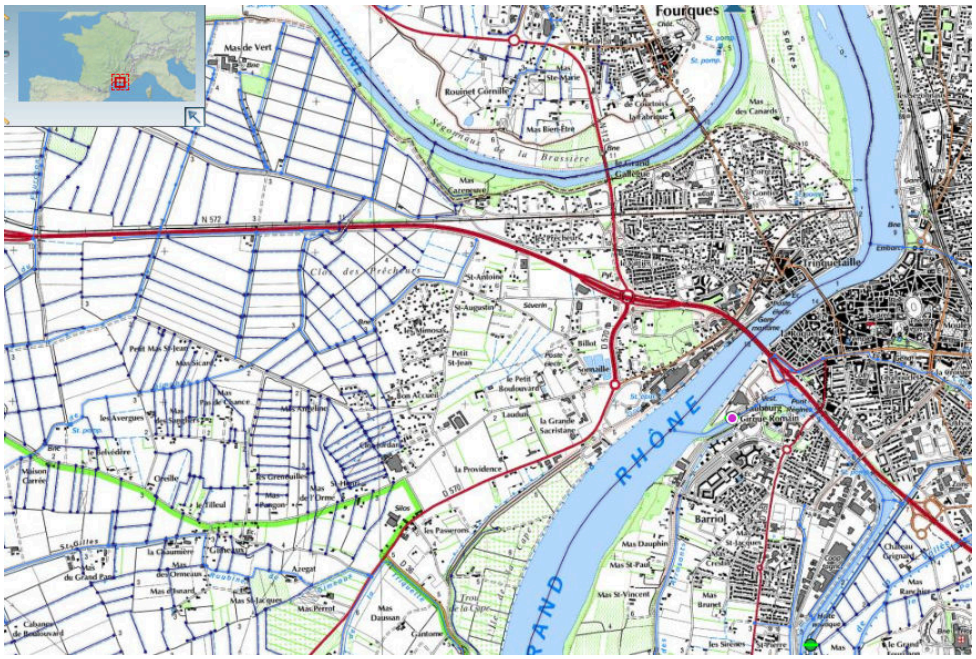

Figure 2.7: Map showing the location of a weir (red point), wrongly attributed to the main course of the Rhône as the artificial lateral canal is not part of the RHT river network. These dams have been set a zero height in the database. Image Source: geobs.

2.2.3 Screening for transport operations

The model is quite sensitive to having eels located far upstream into basins as the result of transport operations. In the first version of the model, some stations were described as having very large residuals and corresponded to eel collected far upstream from what can be described as fully impassable dams. The transport of eels is a common practise in many Spanish and French catchments. Eels found in the Rhine, Meuse, and Artois-Picardie basins located near the frontier with Belgium have a large chance to have been translocated as the result of past or current restocking operations in Germany or Belgium. In the Rhône upper basin (the Saône basin), such transport operations used to be also a standard practise. The transport of eels is also a routine operation in the Minho, in Andalusia, and Basque Country. For this reason, the basins where transport is deemed possible or sure are identified and those basins have been excluded from the calibration dataset (Figure 2.8).

In France batches of illegally caught glass eel seized during enforcement operations or glass eel used for experiments have been transported, quite often nearby electrofishing locations. They were characterized by a sharp increase in small size class numbers followed by an ageing of the eels and have been removed from the modelling dataset (Briand et al., 2018). Some fishing operations containing unexpectedly high small eel densities, at several hundred kilometres from the sea have also been discarded. In some cases, these correspond to a single river segment which will be further used as a single transport area.

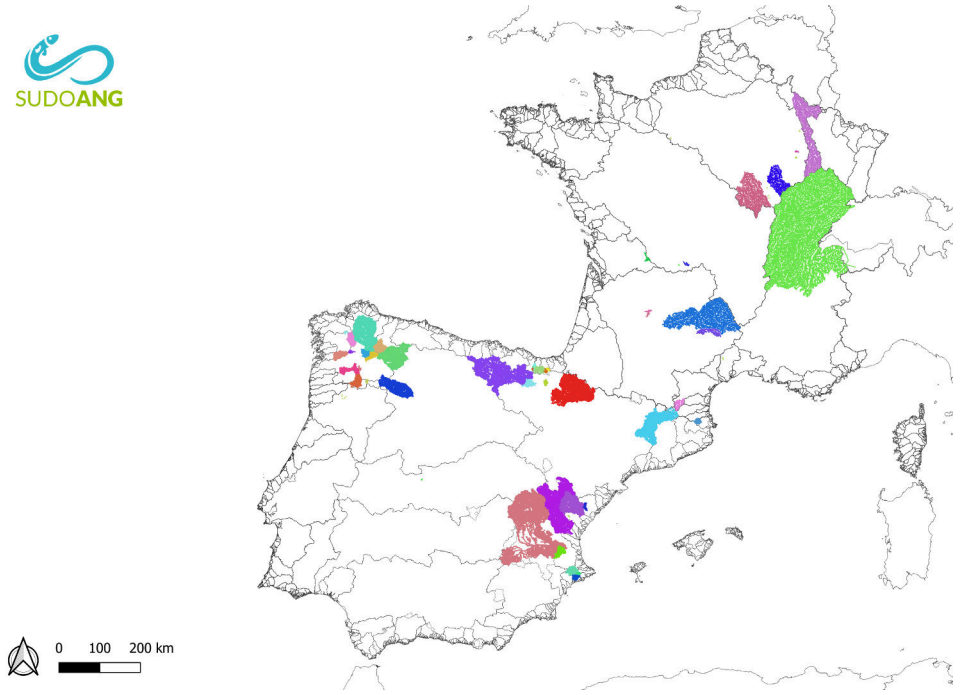

Figure 2.8: Identification of basins or subbasins with transport operations in France, Spain and Portugal.

2.2.4 Silver eel dataset screening

Individual measures of eel larger than 250 mm are extracted. These are examined for size structure, weight, size weight relationship, ocular diameter, size of the pectoral fin with several quality checks including the shape of the eye and the relation between eye diameter and the body size. Individual body measurements are used to calculate the silvering stage according to Durif et al. (2009) using data having passed all quality checks. Stages MII, FIV and FV are considered as silver, while pre-migrant stage FII is considered as immature.

2.3 Model selection

Four different models are applied to predict the production of silver eels. The two first models, Delta model (Δ) and Gamma model (Γ) are Generalized Additive Models (GAM) (Hastie and Tibshirani, 1990), models depicting the presence of eels, and the densities per surface of water electrofished (eel.m^{-2}) respectively. The two last models are GAM Multinomial used to predict the size class structure or the proportion of silver male, silver female and yellow eel (not yet silver eels) (Figure 2.9). All the models are GAM models which allow for a non-linear response of the variable response using tin plate regression spline (Wood, 2003).

For all models the response variable (presence/ absence (Δ), density (Γ), size class ($\mu\tau$) and silver proportion (μS)) is modelled using explanatory variables, which correspond to anthropogenic stressors (*e.g.* the cumulated number of dams), attributes (*e.g.* distance to the sea, altitude, river width), or attributes related to the electrofishing operation (*e.g.* type of fishing used, month, year, surface electrofished, ...). The ex-

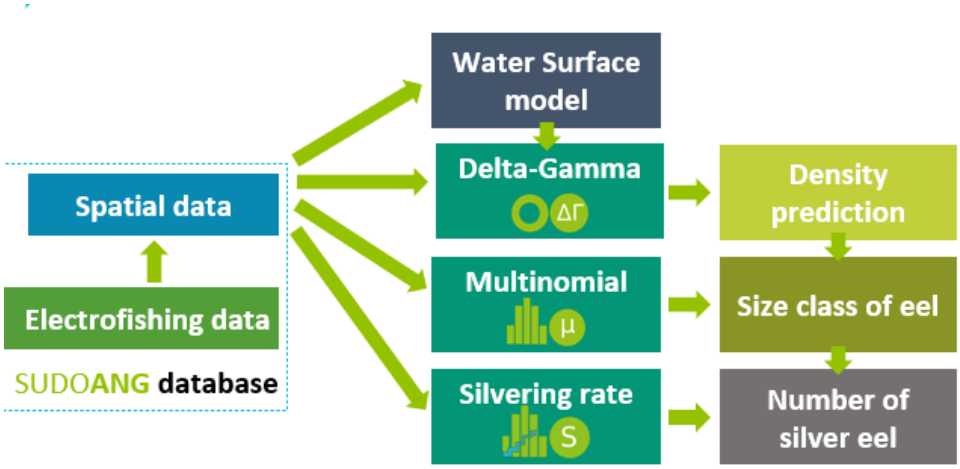

Figure 2.9: Graphical summary of the modelling process in EDA2.3 (SUDOANG). The final number of silver eel are the result of the combination of four models and GIS calculation of the surface of water.

planatory variables are checked for collinearity before entering the model using Pearson correlation coefficient (<0.6) and the GAM collinearity is tested in the model using concurvity (Wood, 2017).

Post calibration procedures (*i.e.* gam.check) are used to assess the response of the model and whether the number of degrees of freedom for the tin plate are sufficient. In some cases, a lower number of degrees of freedom is selected even it that comes at the cost of a less accurate calibration (Lower AIC, and lower predicted deviance percentage). The reason for choosing simpler model is to avoid overparametrization and to select a more generalist model considered as probably more accurate when trying to predict the response on new data.

The model calibration also involves checking regional variable response such as grouping per EMU or SUDOE areas. SUDOE areas correspond to grouping of river outlet along the coast using expert knowledge and four different areas (Vanacker et al., 2020) (Figure 2.10).

Again, after careful checks of the model predictions and responses, this selection which carried out a better fit of the model was discarded as it provided unrealistic responses in places where a more reduced calibration dataset is available.

Variables *distance to the sea* and *altitude* are truncated to 500 km and 800 m after examining the variable distribution, and the same truncation procedure is applied to topological variables such as *drainage_density*, *hydraulic_density* and *lwdds* (Table 2.2).

All endorheic streams are excluded from the analysis, missing data for altitude, distance sea, and some of the topological variables are imputed from their average values.

2.3.1 Delta model

The modelling of density is based on the Delta-Gamma approach (Stefánsson, 1996) which allows to explain a large part of the variance of abundance data when null values are overrepresented. The Delta model (Δ) estimates eel presence. The Δ model uses a

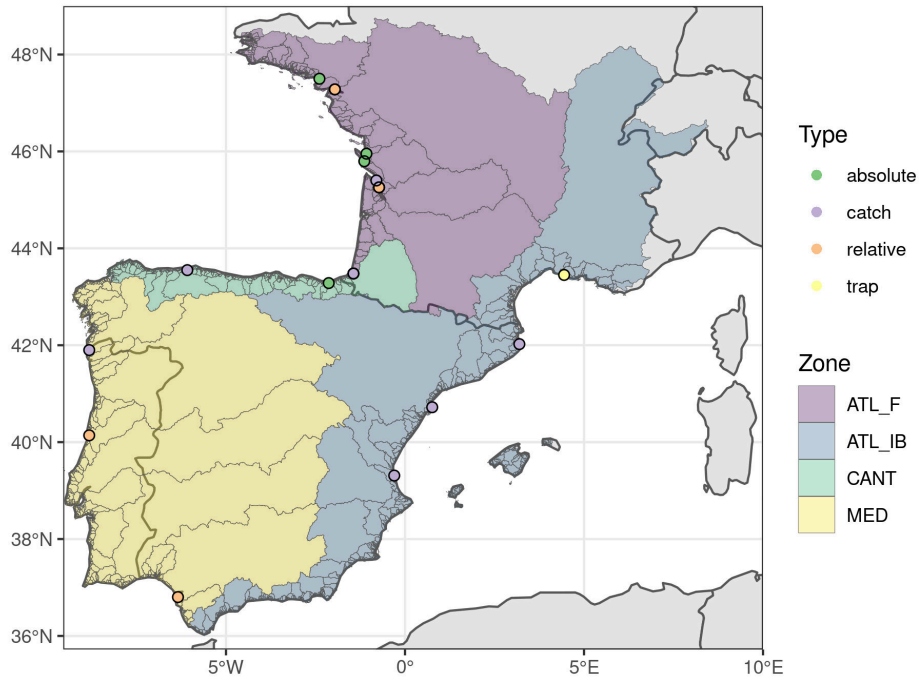

Figure 2.10: Areas chosen for recruitment calculations in the GEREM model. These areas are used to fit the EDA model.

boolean variable, which corresponds to zero when eels are absent from the dataset and one when eel are present. A binomial model is used to predict the presence/absence. The Δ model is quite sensitive to the presence of outliers, especially points with presence of eels very far upstream or above very high dams. An extensive screening of transport operation was thus led (see paragraph 2.2.3). The Δ model uses a binomial distribution and a logit link function to use in model fitting.

2.3.2 Gamma model

The Gamma model (Γ) estimates the non-null densities. The distribution of eel densities is lognormal: there are many sites with low densities and few sites with high density. The Γ model uses a SUDOE areas distribution and a logit link function. The dataset used to model the gamma prediction is much smaller as it excludes zero values.

2.3.3 Density

The multiplication of Delta and Gamma models (ΔΓ model) allows to predict the density of eel on a river segment. The number of eels N is predicted from the model on each river segment i, from the characteristics of each segment, and assuming that the electrofishing station would cover a surface of 600 m^2 and would be prospected with a full two pass method. The eel density ($\widehat{d_i}$) corresponds to the product of Δ and Γ models. The number of eels ($\widehat{N_i}$) estimated per river segment corresponds to the product of density, river water surface Ψ_i and temporal status of the rivers T_i ($T_i = 0$ for temporal rivers). (Equation 2.1):

$$\widehat{N_i} = \Delta_i \Gamma_i \Psi_i T_i = \widehat{d_i} \Psi_i T_i \tag{2.1}$$

with τ size class of eels, i the river segment.

2.3.4 Multinomial model

The 2.1 version of the EDA model used densities as dependent variable. In the 2.2 version, eels have been separated into size classes τ for each electrofishing operation. Size classes used in the model correspond to <150, 150-300, 300-450, 450-600, 600-750 and >750 mm. The data were stacked and considered independent for each size class, and a model allowing a different response for some variables per size class was considered. In particular, a different response of river width, time trend, was selected for each size class. This choice was made on the whole French dataset for which a large historical data treatment allowed to consider a density per size class for most electrofishing operations.

In the current version 2.3 developed for SUDOANG, data allowing to describe a size structure is much more reduced than that allowing to predict density. For this reason it was decided to apply a Multinomial model ($\mu\tau$) to the size structure data and use this model to predict the proportion of eel per size class. The proportion of eels per size class P_τ is predicted from the model on each i, from the characteristics of each segment. Variables tested in the model include geographical predictors, pressure predictors (dams) and month of fishing. The model uses the density predicted by the ΔΓ model as a predictor for size structure. When the predicted density was 0, a density values of 0.0001 was used.

The density predicted by the ΔΓ model $\widehat{d_i}$ is multiplied by the proportion of eels per size class P_τ to calculate the density of eel corresponding to each size class τ. The sum of the proportion of eel per size class for one segment is one (Equation 2.2)

$$\begin{aligned} \widehat{d_{\tau,i}} =& \widehat{d_i}\widehat{P_\tau} \\ & \sum_{\tau=150}^{\tau=750} \widehat{P_\tau} = 1 \end{aligned} \tag{2.2}$$

The number of eels per size class are calculated similarly to numbers of eels, using the product of density, river water surface Ψ_i and temporal status of the rivers T_i.

$$\begin{aligned} \widehat{N_{\tau,i}} =& \widehat{d_i}\widehat{P_\tau}\Psi_i T_i \\ & \sum_{\tau=150}^{\tau=750} \widehat{P_\tau} = 1 \end{aligned} \tag{2.3}$$

2.3.5 Silvering model

In previous versions of the model, EDA2.0 and 2.1, the silvering rate, which is the proportion of eel that become silver and start their seaward migration, was considering a fixed rate Π of 5% (Jouanin et al., 2012a) or 2.5 % for Ireland (De Eyto et al., 2015). Later, in EDA 2.2 (Briand et al., 2015) the large dataset collected by the ONEMA Institute on silver eel allowed to predict a varying silvering probability $\Pi_{\tau,i}$ on each , and for the different size classes (τ). A model was fitted on 1583 electrofishing operations over 797 stations in France (Beaulaton et al., 2015).

More precisely, mean silvering percentage per size class τ was modelled using logistic regressions with the average numbers of yellow eels in the most abundance size class (300-450 mmm) $\widehat{N}_{i,\tau=300-450}$ as one of the predictors. The dataset used for calibration consisted of all silver eel and yellow eel collected (one line per individual) and their characteristics including the density per size class $\widehat{d_{\tau,i}}$ Beaulaton et al. (2015). The silvering model was only applied to size class larger than 300 mm. It was calculated as a probability to become silver during the year for each size class. silver eels lower than 450 mm were all considered as males, while silver eels larger than 450 mm were considered as female. The main problem of this model is that it has led to skewed silver eel sex distribution with an excess of males in the upper part of the basins.

In this report, EDA2.3, we consider the proportion of silver eel male, or female or eel as the response variable. In our data set, we have three categories ς instead of two (being silver or not), and eel is considered to be in one of the following: silver male, silver female or immature eel according to (Durif et al., 2006) classification. A GAM Multinomial model is calibrated on the dataset using the VGAM package (Yee, 2013) and predicts the probability to belong to one of the categories $\Pi_{\varsigma,\tau,i}$. The proportion is predicted from the model on each river segment i, from the characteristics of each segment. Variables tested in the model include geographical predictors, pressure predictors (dams) and month of fishing. Before being integrated in the model, Month <7 and >10 have been grouped in a single class. The model uses the density predicted by the ΔΓ model as a predictor for silvering. Zero values for predicted density have been transformed to 0.0001.

The model is then applied to the whole SUDOANG river network to predict a silvering structure $\widehat{\Pi_{\varsigma,\tau,i}}$ in each river segment and the number of silver eel obtained by multiplying the predictions from the four models (Equation 2.4). Three categories are predicted but the number of eel remaining in the stream can be rebuilt from the two other silver probabilities.

$$\widehat{Ns}_{\tau,\varsigma,i} = \widehat{\Pi_{\varsigma,\tau,i}}\widehat{d_{\tau,i}}\Psi_i T_i \tag{2.4}$$

The biomass of silver eel is calculated using the silver eel mean weight $\overline{ps_{\tau,i}}$ (Formule 2.5):

$$\widehat{Bs}_{\tau,i} = \widehat{Ns}_{\tau,i} * \overline{ps}_{\tau,i} \tag{2.5}$$

The biomass of standing stock (yellow eel and silver eel) is calculated using the eel mean weight $\overline{p_{\tau,i}}$ (Equation 2.6):

$$\widehat{B}_{\tau,i} = \widehat{N}_{\tau,i} * \overline{p}_{\tau,i} \tag{2.6}$$

Size-fecundity relationships are rare for European eel, however MacNamara and McCarthy (2012) have recently proposed a relation for Irish silver eels (Formule 2.7):

$$\mathbb{F}_\tau(\tau > 450) = \widehat{Ns}_{\tau,i} * 10^{-2.992+3.293*log_{10}\bar{l_\tau}} \tag{2.7}$$

where $\bar{l_\tau}$ is the average length per size class.

2.3.6 Final calibration of waterbody productivity

Index rivers from France provide estimates of the number of silver eel produced. The analysis of the results of the alpha version of the model clearly showed that the numbers were overestimated in France. One of the major changes from EDA 2.2 is the inclusion of the waterbodies surface. However, when looking closely, some of the waterbody might not be contributing to the same extent as rivers to the total production. For instance, large rivers and reservoirs often have lower densities with eel concentrated in the border of the stream or the reservoir. In addition, some waterbodies, even if they are not connected to streams, and therefore do not have eels, are added to the total water surface. The water surface layers are classified into lagoons, large rivers, reservoirs, estuaries and lakes for the whole SUDOE area. The surface of the different type of waterbodies is used to fit the production per waterbody of the model. Each type of waterbody is assigned a coefficient of productivity Cw (Equation 2.8). For each Index river r the number of silver eel produced Ns_r is computed using river segments located upstream from the downstream migration control point in the basin. This number corresponds to a specific year y:

$$\widehat{Ns}_{r,\tau,y} = \sum_{i \in upstream(r),\tau} C_w \Psi_{i,w} \widehat{d_{y,i,\tau}} T_i \widehat{\Pi_{\varsigma,\tau,i,y}} \tag{2.8}$$

where w is the type of waterbody, C_w is the coefficient of productivity applied to each waterbody, $\Psi_{i,w}$ is the cumulated water surface per waterbody w in the unit basin of river segment i, $\widehat{d_{y,i,\tau}}$ is the density predicted for year y, river segment i and size class τ, $\widehat{\Pi_{\varsigma,\tau,i,y}}$ is the silvering predicted in year y, segment i, and size class τ, T_i is the temporal status of the river segment (zero or one).

The productivity per type of waterbody C_w has been fitted by minimising the difference between observed Nso and modelled $\widehat{Ns}$ numbers of silver eel. Each index river r might have numbers for multiple years y.

$$\sum_{y,r}(Nso_{r,y} - \widehat{Ns_{r,y}})^2 = f(C_w) \tag{2.9}$$

These productivities per waterbody type have been multiplied by the corresponding wetted area during the final run of the model in Spain, France and Portugal.

2.3.7 Transport operation

Some places have been excluded from the calibration dataset because eels were transported (see section 2.2.3, and Figure 2.8). For those places a simplified model has been fitted using the sector and testing a simplified set of variables. Geographical variables such as dam height, cumulated distance to sea, or altitude make no sense in the context of transporting. Other variables such as sampling protocol (ω) or electrofishing type were used in the model. The model was fitted using mixed models (glmer). For the final dataset building, models including transport are provided, and correspond for each segment to the maximum of densities or presence probabilities obtained from the Δ and Γ standard models on the one hand, and from the Δ and Γ transport model on the other hand. The reason for this calculation is that in places where density is expected to be high, *e.g.* near the sea, "natural" high densities would occur even it a low number of eel can be expected from the average density obtained in the transported sector. Further upstream, in places where migration is impaired, transport have a large impact on presence probabilities and densities and the natural density is superseded by the effect of transport.

2.3.8 Habitat loss

By running EDA 2.3. while setting the cumulated height of dams to zero, we can simulate the density of eel for various years without dam. This prediction is used to assess the effect of habitat loss due to dams on eel production. When predicting habitat loss, no change on the temporal status of rivers has been applied nor on the stream quality or productivity that would result from the removal of dams. In essence, this prediction gives the output of a theorical distribution if there were no dams, so for instance in places with high altitude or large distance to the sea, the effect of dam removal would be minimal on eel production, while the removal of a large barrier in the downstream course of a large basin would be expected to have a much larger effect. The gain in numbers cannot be compared to a mortality but more to a loss of potential productivity attributed to dams.

Table 2.2: Candidate variables used in the delta, gamma, multinomial size and multinomial silvering models.

Variable	Description (units)	Type, transformation, truncation
country	France, Spain or Portugal.	Categorical
sudoe area	SUDOE area, geographical area along the coast where identical recruitment is expected (Drouineau et al., 2021).	Categorical
EMU	EMU Eel management unit.	Categorical
dist_from_gibraltar_km	Coastal distance to Gibraltar (in km) computed along the coastline, >0 on the Atlantic coast and the channel and <0 in the Mediterranean.	Categorical
basin	Hydrographic basin	Categorical
distancesea_km	Distance to the sea (km)	Numeric, truncated at 500
electrofishing means	Type of electrofishing used: ω_{ful} ω_{eai} ω_{fue} ω_{bf} ω_{dhf} ω_{oth}	Categorical
altitude_m.	Altitude (m)	Numeric, truncated to 800 m (400 m for silvering model)
lriverwidthm	River width (m)	Numeric, log transformed
cs_height_10, cs_height_12, cs_height_15	Cumulated height of dams including prediction for missing values $\bar{h}$, $cs\_height\_10 = \sum \bar{h}$, $cs\_height\_12 = \sum \bar{h}^{1.2}$, $cs\_height\_15 = \sum \bar{h}^{1.5}$	Numeric, Truncated at 200, 500 and 800 for cs_height_10, cs_height_12 and cs_height_15 respectively
temperature	Average temperature from 1960-2000 from the CCM (Vogt et al., 2007)	Numeric
cumwettedsurfacekm2 cumwettedsurfaceotherkm2 cumwettedsurfacebothkm2 lddws	Surface of water downstream from the segment in the river. First corresponds to river, the second to other waterbodies, the third to both river and associated waterbodies and the fourth lddws is the log transformed value of cumwettedsurfacebothkm2. The area corresponds to all segments within the same basin with a similar or lesser distance to the sea (Domange et al., 2018)	Numeric, truncated at 15, 200 and 215 and 0.01
drainagedensityperm	River length / surface of basin in the basin downstream (m-1)	Numeric, multiplied by 10^4, truncated to 20
hydraulicdensityperm2	Number of riversegments per surface of basin (m-2)	Numeric Multiplied by 10^6, truncated to 1.5
year	Year of electrofishing	Numeric
month	Month of electrofishing	Categorical Month <7 and >10 have been regrouped, so month 7 ,8, 9 and 10.

3.1 River network dataset

The construction of the river network dataset and associated variables is described in the eel Atlas[1].

3.2 Dam dataset

The number of dams collected in the database is 85 036, 20 463 and 861 for France, Spain and Portugal respectively (Figure 3.1 and Table 3.1).

Two different models are applied in France and the Iberian Peninsula to predict the height of dams when missing.

In France log transformed dam height log(h) (N = 51 741) are calculated with a linear model according to dam type, dam height, log(terrain slope+1), log(river median flow +1) and the BD CARTHAGE basin. The dam type is modelled as an interaction with BD CARTHAGE basin. The model explains 30% of the deviance and all factors are highly significant in the model. The model is applied to 33.3% of missing values for height, the average height predicted by the model is 1.10 m.

In Spain and Portugal dams of type bridge and culvert are excluded from the prediction dataset. This is different from France, where the dam datatype is nearly always associated with an obstacle to migration. Those bridge with a null height or height zero are excluded from the dataset. Log transformed dam height 17 764 are fitted according to dam category (*dam*, *weir* and *unknown* type) and log(slope). The model with slope is better than the model without slope. Missing values from flow, due to incomplete projection from the HydroATLAS database prevent from using it in the model. Average height predicted are between 4 and 8 m for the *dam* and *weir* datatype and around 1-1.5 m for the *unknown* type of dam. The model is applied to predict missing values of height, representing 12.9% and 20.3% for Spain and Portugal respectively. The average height for missing dams is 5.5 m in Spain and 4.3 m in Portugal [2].

[1] The eel Atlas can be downloaded at trac EDA2.3 download page, SUDOANG task group page and eel Atlas download page

[2] For more details see link

Table 3.1: Number of dams per type. FR = France, SP =Spain, PT=Portugal.

code	name	FR	PT	SP
WE	Weir	45596	32	8583
DA	Dam	8211	364	4981
BR	Bridge	7485		2650
CU	Culvert	7303		21
RR	Rock ramp	6349		
PU	Physical obst. unknown	4773	465	4128
OT	Other	4749		
FO	Ford	570		35
PP	Penstock Pipe			65

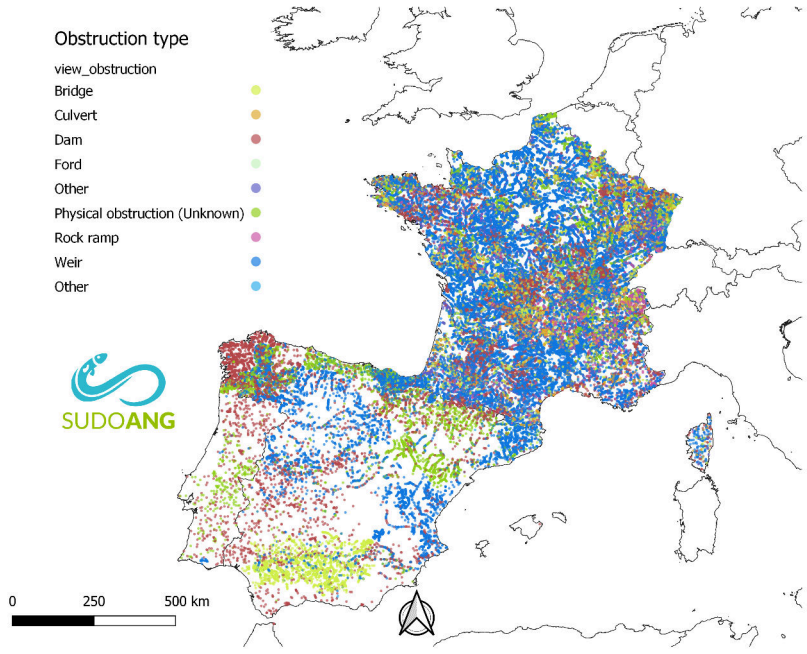

Figure 3.1: Dams according to their type in the SUDOANG database. Source of data: OFB, AMBER, Ministry for Ecological Transition, URA, UCO, The Xunta of Galicia, Catalan Water Agency, Portuguese Ministry. Link to technical report)

.

3.3 Eel dataset

3.3.1 Electrofishing stations

The number of electrofishing station is 777 (PT) 1.3026×10^4 (SP) and 13473 (FR) for the three countries. One of the step of data integration is to try to snap the electrofishing station to the river network. This is done within a limit of distance of 300 m, which means that electrofishing stations located too far from the river are not projected. When coming from different sources, the coordinates of the station might differ slightly, so stations within 50 m of an existing electrofishing station have been considered as duplicates. The number of projected stations is 760 (PT), 8931 (SP) and 13473(FR) [3]. A detail of the number of snapped stations per EMU is provided in Figure 3.2.

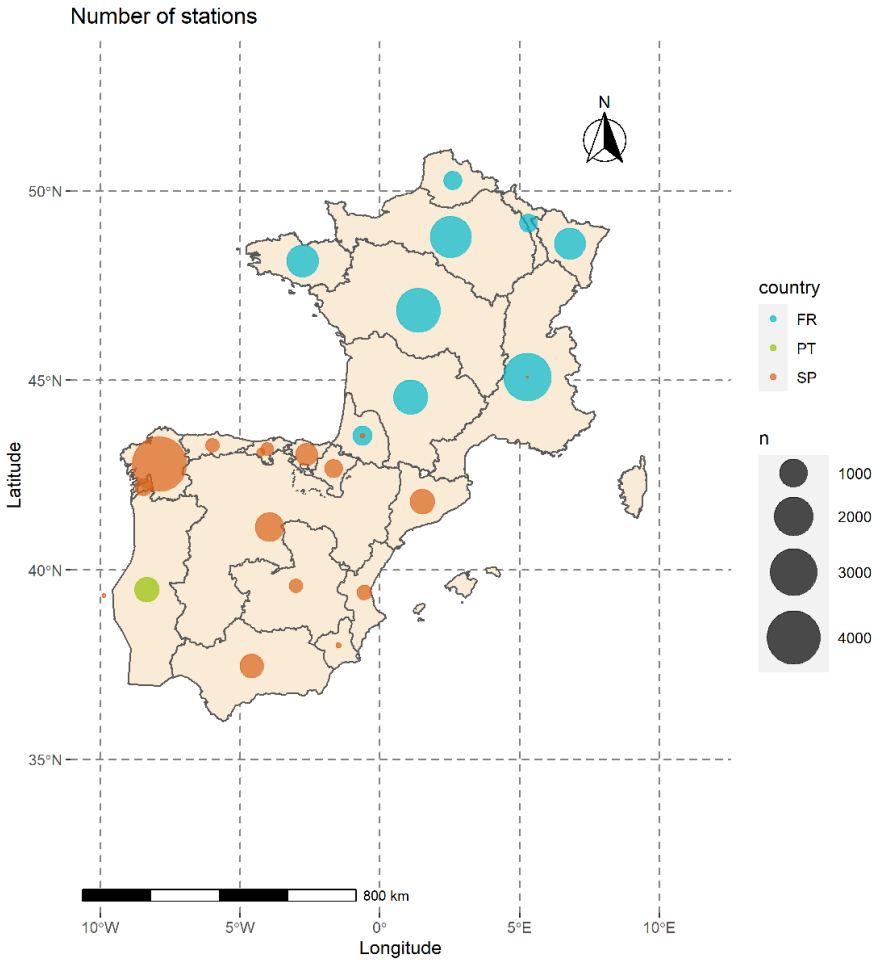

Figure 3.2: Number of electrofishing station per EMU after duplicate removal and projection on the SUDOANG river network.

[3]The French dataset has been compiled from the earlier version of EDA where only the snapped stations were present.

3.3.2 Operations

A station may be fished several times so the number of operations is larger than the number of station. The number of operation (corresponding only to the projected stations) is 970 (PT), (SP) and 32819(FR). Details of operation per EMU are provided in figure 3.3.

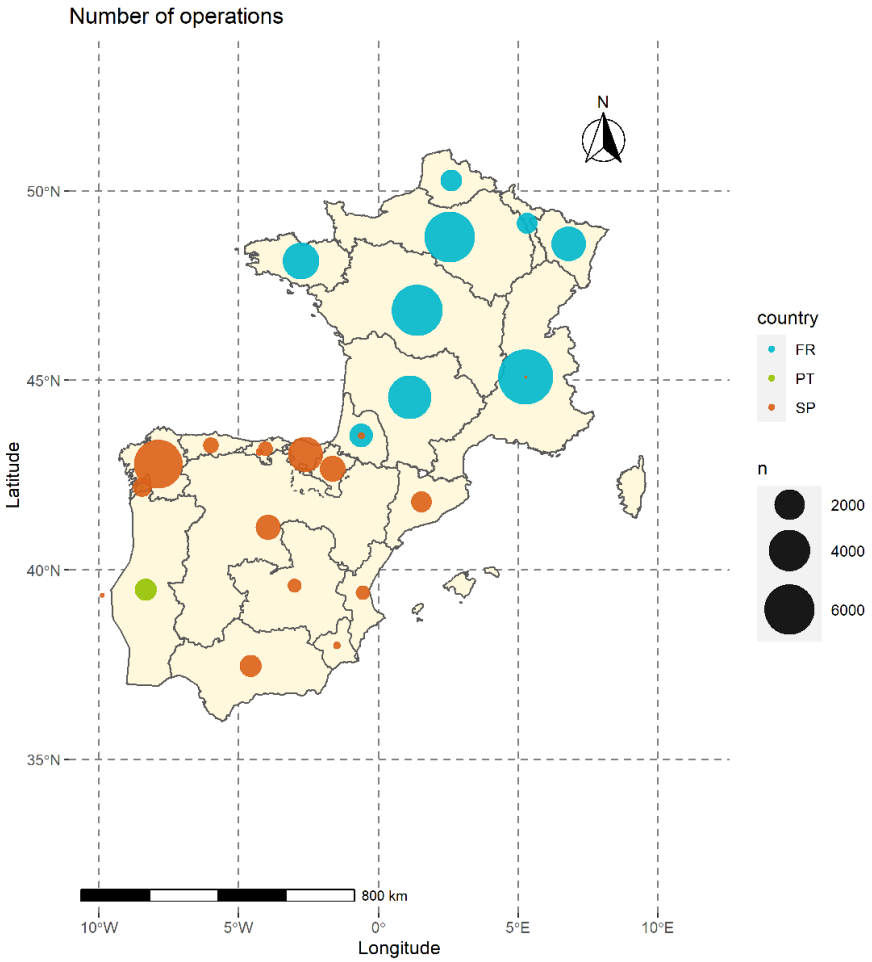

Figure 3.3: Number of operations per EMU, after duplicate removal.

3.3.3 Individual measurements and silvering

After screening and analysis, the size dataset used for model calibration comprises 494163 lines (each line corresponds to one individual). In France, data have been extracted from the EDA2.2 database and merged with the SUDOANG dataset. The number of stations with size structure data is 228 (PT), 3006 (SP) and 13473 (FR). Similarly, the number of operations with size structure data is 417 (PT), 5656 (SP) and 32819 (FR).

Data for silver eel are extracted from an initial database containing 151 403 eels with individual measures (Table 5.7 in annex provides details per year and per country). This initial silvering dataset comprises 4139 stations, 7894 operations on 298 basins. Data are processed for size, weight, pectoral fin length, eye diameter and shape

and filtered at each step (Annex 5.4). After selection, the final dataset contains 20101 eels, corresponding to 894 stations, 1690 operations on 153 basins. The steps of data selection are summarized in Table 3.2 (Table 5.8 in annex).

Table 3.2: Data selection for silvering criteria

criteria	missing	rejected	selected
size	1	254	151148
weight	25218	718	125467
pectoral	126946	320	24137
horizontal eye diameter	125814	981	24608
vertical eye diameter	124407	2484	24512
eccentricity	126926	64	24413
total	127934	3368	20101

.

3.3.4 Mean weight per size class

Average weight of eels per country are calculated in Annex in Table 5.2. The value of mean weight by 50 cm length class is shown in Table 5.6 in Annex. These results correspond to the quantile regression of $log(weight)$ $log(length)$, which is more robust to the presence of outliers (Beaulaton et al., 2015). The mean weight for the 150, 150-3000, ..., >750 mm size classes is reported in Table 5.2 in Annex for standing stock of eels and Table 5.5 in Annex for silver eels. The Table for silver eels is further split per sex in Table 5.4 in Annex.

3.3.5 Density and efficiency

In France, for electrofishing operations with a single pass, data are extrapolated using the average fishing efficiency ($\overline{ef}$). Fishing efficiency, defined as $ef = 100 * Nb_{p1}/N_{CS}$ is calculated as $\overline{ef} = 65.6$ for complete fishing (N=15 856), $\overline{ef} = 64.5$ for eel specific fishing (N=445) and $\overline{ef} = 39.2$ for bank fishing (N=2 805). Fishing with only one event are the most frequent (94%) for bank fishing, and correspond to 75% of complete fishing operations and 3% of eel specific complete fishing. A lower efficiency (40%) is chosen for bank fishing and a common value rounded to 65% for complete fishing and eel specific fishing methods.

In Spain and Portugal, the average electrofishing efficiency per data provider is 0.71 (Figure 3.6).

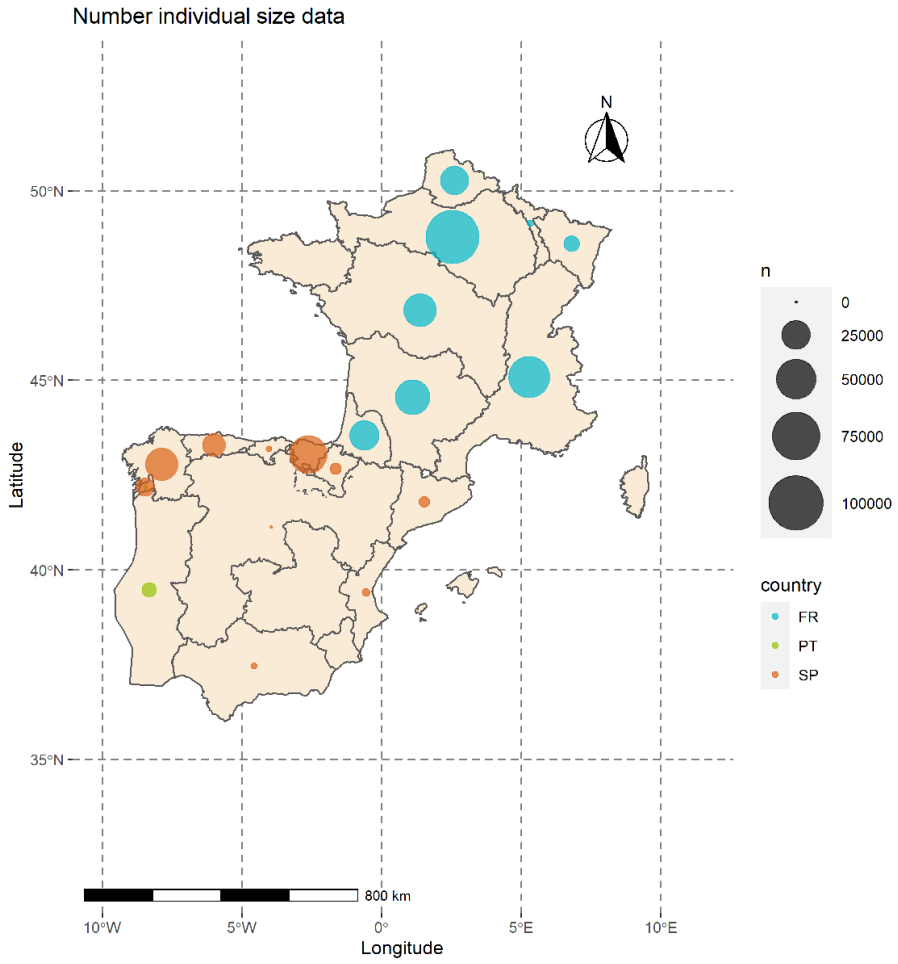

Figure 3.4: Number of operation where quality checks allow the use of a size structure.

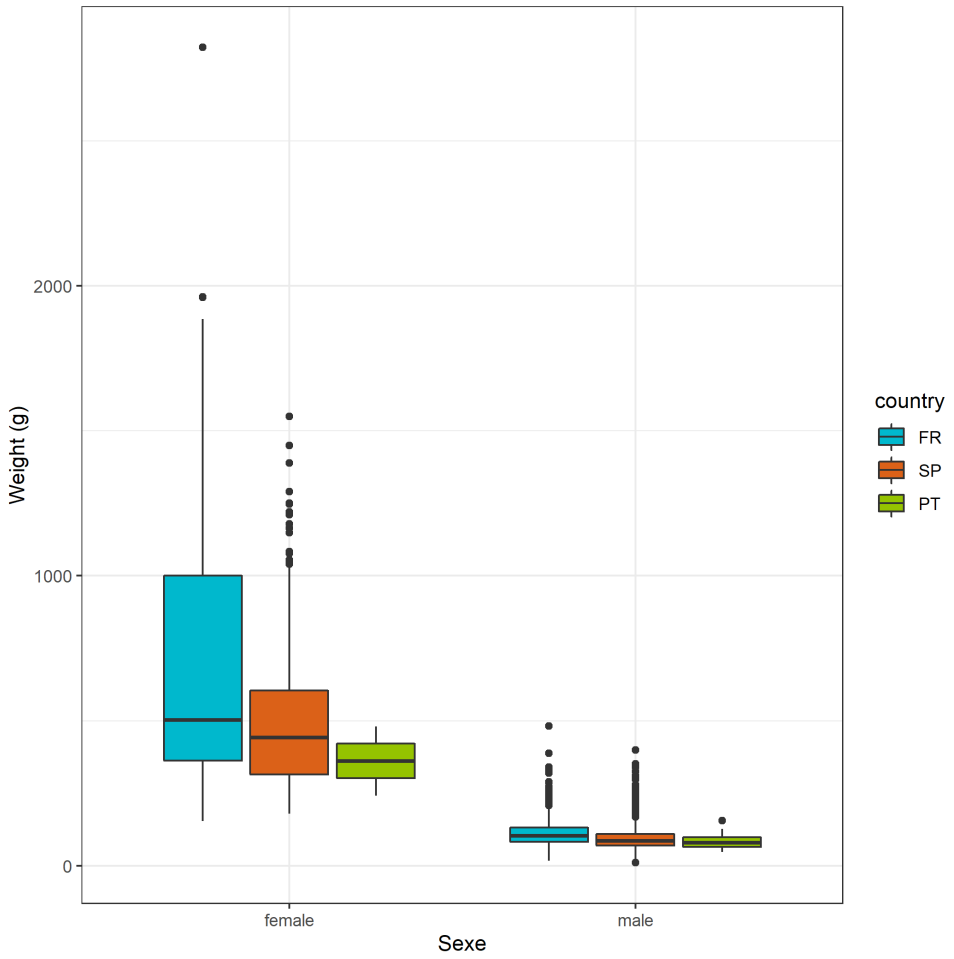

Figure 3.5: Box plots of silver eel weight distribution per sex and country.

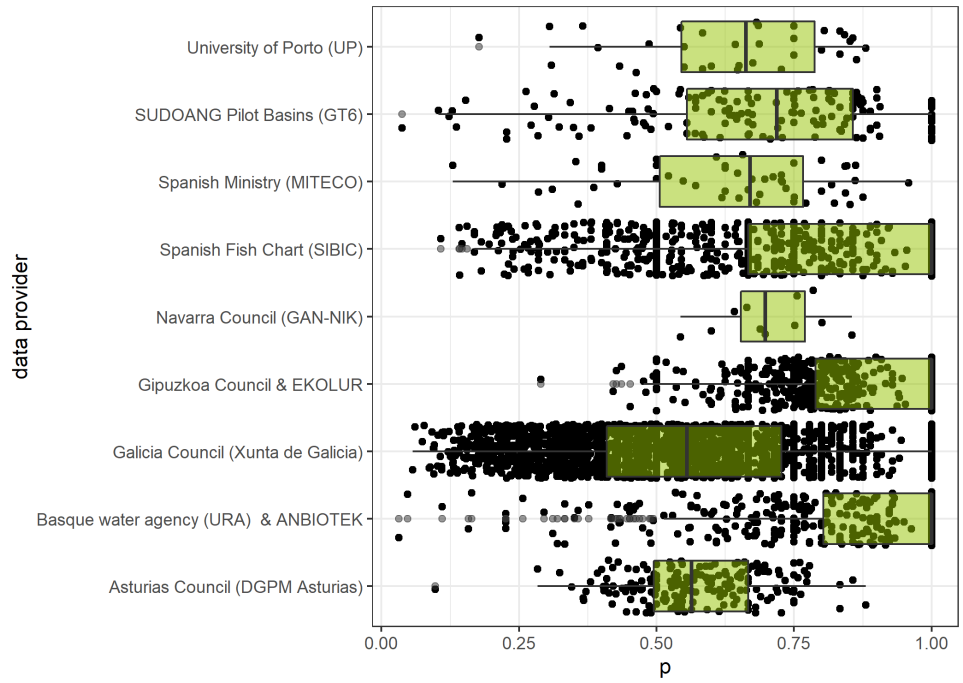

Figure 3.6: Efficiency of electrofishing calculated using Carle Strubb depending on the data provider in Spain and Portugal. Data providers with less than 10 electrofishing with a second pass are excluded from this graph.

3.4 Delta model

After screening, the final dataset for the Delta model (Δ) contains: 694 (PT), 8334 (SP), 12678 (FR) lines. Each line corresponds to the presence or absence of eel in the fishing operation.

The percentage of deviance explained by the model is 59.8%. In the calibration plot for presence/ absence, the Kappa is maximum (K=0.745, 0.003) for a presence probability of 40% (Figure 3.7). This means that at the 40% threshold, there will be a large number (91%) of stations where the actual presence is correctly predicted, without diminishing too much the number of stations where eels are absent, and the absence is indeed predicted by the model (85%). Finally, at a 40% presence probability, the model correctly predicts 87% of the operations in the calibration set.

The model with the best fit for presence absence includes smooth terms (with a s) and parametric terms (Table 3.3). The following parameters are ordered by decreasing importance in the model:

- **s(altitudem.)**: altitude of the river segment, in m,
- **s(cs_height_10_p.)**: cumulated height of dam from the sea $\sum \bar{h}$, no power transformation selected, missing values have been imputed [4] [5],
- **dist_from_gibraltar_km**: the coastal distance to Gibraltar in km,

[4]Note that different submodels with different response per area have been tested but not retained in the final model.

[5]This variable is integrated as a smooth factor in the model.

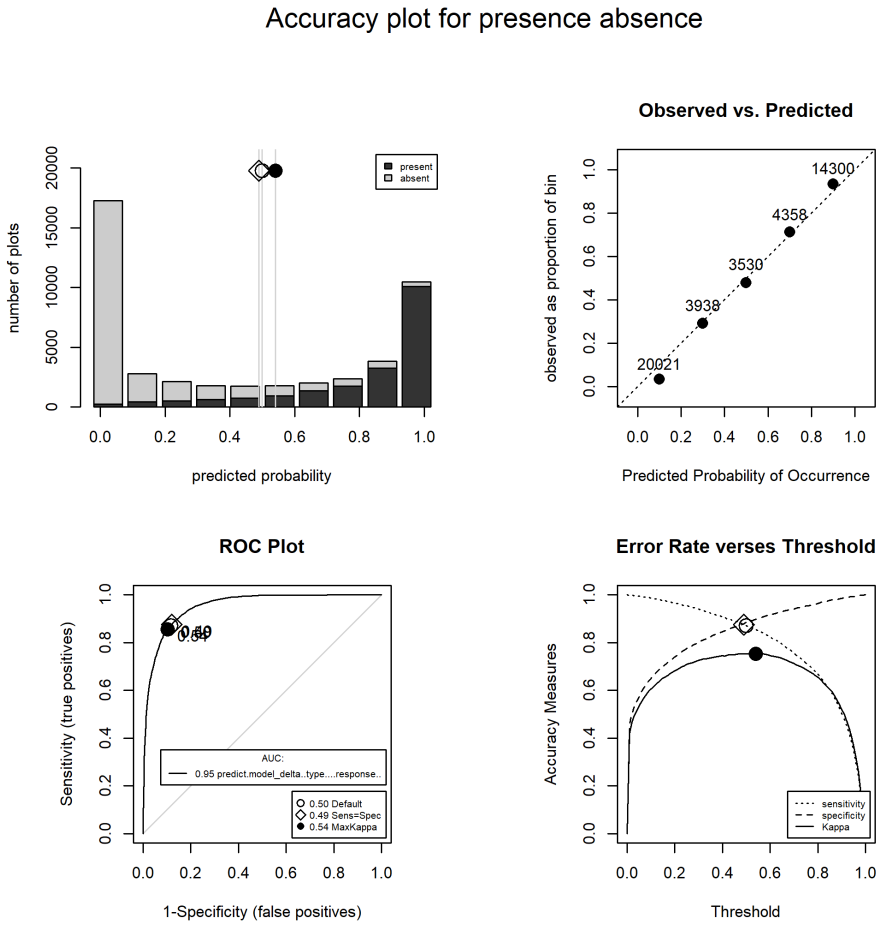

Figure 3.7: Presence absence Δ model diagnostics. From left to right and top to bottom, (1) predicted eel presence probabilities histogram, bars ordered according to observed values (2) Calibration graph allowing to evaluate the adjustment quality comparing predicted and observed values, (3) Receiver Operating Curve (ROC) (provides a method of evaluation of the model independent of the threshold, a good model must have a large number of true positive values while the number of false positive remains low) (4) Diagram of error rate versus threshold provides specificity, sensitivity and Kappa curves according to the threshold. The threshold has been set to 0.4.

- **s(ef_wetted_area)**: electrofishing station surface,
- **distanceseakm.**: distance to the sea in km,
- **s(year*area_sudo)**: year, discrete (factor) per SUDOE area.
- **s(lddw*country2)**: $log(downstream\ drainage\ wetted\ surface)$ The percentage of wetted area is the basin downstream [6],
- **area_sudo**: the SUDOE areas,
- **ef_fishingmethod**: fishing protocol ω,
- **s(hydraulicdensityperm2.):country2**: the hydraulic density in number of segment per surface area for the downstream basin. Different response expected between the Iberian Peninsula and France so different smooth used,
- **country2**: Iberian Peninsula (SPPT) and France (FR).

The response of the model for the different predictors used in calibration is shown in Figure 3.8.

Altitude is the best predictor in the Δ model (Table 3.3). Eel presence probability shows a decline in the first 400 m and a less important decline after (Figure 3.8d). A scatterplot examination of response shows that higher probabilities of presence are expected at high altitude in the Rhine Meuse zone [7] (Figure 5.5).

The cumulated height of dam is the second–best predictor of eel presence in the Δ model. Among the variables tested for the dam effect the best variable was the cumulated height of dam (without power transformation) and including the predicted values for missing height. Eel presence probability decreases linearly with cumulated height and drops after a cumulated value of 150 m (Figures 3.8a, 3.8b). The response per SUDOE area shows quite clearly the higher values observed in Rhine Meuse, otherwise the responses are quite close between EMUs and nearly identical between the model and average observations as the result of the importance of the dam variable in the model (Figure 5.3 in Annex). Note that the large drop beyond 150 m is the consequence of removing sites where transport operations were suspected. Without this correction it was more difficult to obtain a good fit for the dams as eels can be present at very large cumulated height when transported.

The distance to Gibraltar cannot be interpreted alone as the response of the model also depends on SUDOE area and country. For instance, the response on the Atlantic coast of France will always be linked with country = France and SUDOE area = ATL_F Atlantic France. Predictions are made using pre-defined values [8]. According to the

[6] Wetted surface including both stream area and additional waterbodies water surface divided by the surface of basin, for river segments located at a similar or lesser distance to the sea (Domange et al., 2018). Given the different river network between WISE layer (Spain and Portugal) and France, a different response is tested. There were too few calibration data in Portugal to treat it as a separate component.

[7] Rhine Meuse is located in the North East of France, with streams flowing to the Channel, through Belgium, Germany and the Netherlands. Transport operations have been routinely conducted in both Spain and Belgium and also in France in the past, and as a consequence the eel is present at large distance from the sea and above large dams.

[8] wetted area=600, altitudem=50, cumulated height of dams=50, distanceseakm = 50, lddws=-4 (0.018 without log transformation), ω_{ful}, hydraulicdensityperm2. = 0.2, and consistent values along the coastline. (Figure 3.8j)

Table 3.3: Summary of model (Δ) delta

A. parametric coefficients	Estimate	Std. Error	t-value	p-value
(Intercept)	-1.0966	0.2624	-4.1782	< 0.0001
area_sudoATL_IB	-2.5941	0.3176	-8.1690	< 0.0001
area_sudoCANT	-0.3548	0.1937	-1.8317	0.0670
area_sudoCHAN	0.2944	0.4448	0.6618	0.5081
area_sudoMED	-2.0951	0.6286	-3.3329	0.0009
area_sudoRhinMeu	2.7333	0.4974	5.4950	< 0.0001
country2SPPT	-1.4297	0.2246	-6.3649	< 0.0001
ef_fishingmethodcoa	0.8966	0.1878	4.7750	< 0.0001
ef_fishingmethodiaa	-0.1109	0.1022	-1.0846	0.2781
ef_fishingmethodber	0.3241	0.0717	4.5188	< 0.0001
ef_fishingmethodgm	0.7878	0.0656	12.0149	< 0.0001
ef_fishingmethodoth	-0.1044	0.1051	-0.9936	0.3204
B. smooth terms	edf	Ref.df	F-value	p-value
s(year):area_sudoATL_F	6.1178	7.1232	87.7701	< 0.0001
s(year):area_sudoATL_IB	8.5281	8.8732	79.4923	< 0.0001
s(year):area_sudoCANT	8.0459	8.7240	134.4372	< 0.0001
s(year):area_sudoCHAN	6.5227	7.4645	64.3601	< 0.0001
s(year):area_sudoMED	8.7241	8.9754	131.8527	< 0.0001
s(year):area_sudoRhinMeu	4.1639	5.0946	105.5642	< 0.0001
s(ef_wetted_area)	3.9212	3.9957	983.8974	< 0.0001
s(altitudem.)	3.8126	3.9768	1689.2409	< 0.0001
s(dist_from_gibraltar_km)	13.2102	13.8807	1003.3332	< 0.0001
s(hydraulicdensityperm2.):country2FR	1.9491	2.3779	8.9411	0.0123
s(hydraulicdensityperm2.):country2SPPT	4.4244	4.8397	45.5959	< 0.0001
s(lddws):country2FR	4.9348	4.9973	133.3241	< 0.0001
s(lddws):country2SPPT	3.4462	4.1267	134.6306	< 0.0001
s(cs_height_10_p.)	4.9409	4.9978	1120.7320	< 0.0001
s(distanceseakm.)	4.8131	4.9810	832.1135	< 0.0001

Δ model, the eel presence probability shows an important decrease from the North along the Atlantic Iberian coast and from the French Mediterranean coast to Gibraltar. Presence probabilities are lower in the Mediterranean area than on the Atlantic coast. Probability of presence are similar in the Bay of Biscay (Atlantic Iberian, Atlantic France) and in the Channel. They diminish further north along the Channel (Figure 3.8j).

Electrofishing station size increase the probability of finding an eel, first linearly from 0 to 500 m^2, and then with a less important slope from 1000 to 2000 m^2. Beyond that surface, the probability does not increase but the stations are very large (Figure 3.8f).

The **year effect** for the model only represents 8% of the total Chi square. The responses were allowed large degree of liberties and different response per SUDOE area have been built. Atlantic France ATL_F and $RhinMeu$ show an initial increase in the 1990's followed by a decrease. The Channel $CHAN$ shows an overall increasing trend. In Atlantic Iberia ATL_{IB}, the dataset covers the period 2015-2018 and shows an increasing trend around 2014, time of the recruitment peak. The increases after 2016

in zones with common data between Spain and France [9] and are to be treated with caution as the dataset after 2015 in France only contains eel specific survey, and thus is biased (Figure 3.9).

The **downstream drainage wetted area** is also a good predictor of eel presence according to the model. The downstream drainage area $lwdds$ is the indices of "wetness" of the basin downstream (without dimension). Very contrasted responses have been obtained in Spain and Portugal on the one hand and France on the other hand. In Spain and Portugal ($SPPT$) the probability of presence of eel will first increase between 0.2% (-6) and 1% (-5) of wetted surface. Beyond 1% the probability of presence diminishes. In France a different trend is observed with an overall diminution. The diminution is sharper beyond 1%. The F value is quite high for this variable which indicates a large contribution to the model (Table 3.3).

The response between **SUDOE areas** is contrasted with the lowest response in the MED and ATL_{IB}, and going further North, a smaller increase from $CANT$ to ATL_F, then $CHAN$ and finally the largest value in $RhinMeu$.

Fishing method is significant in the model but contribute to less than 3% of the total Chi square. Largest eel presence probabilities are obtained for deep habitat fishing (gm) ω_{dhf} and eel specific fishing using two pass eel specific surveys (coa) ω_{fue}. Low responses are obtained for other sampling ω_{oth}, eel specific sampling (iaa) ω_{eai} and standard electrofishing (com) ω_{ful}. Bank fishing (ber) ω_{bf} shows an intermediate response (Figure 3.8i).

Distance to the sea shows a rapid decline of the presence probability in the first 200 km with a levelling of the response after 200 km (Figure 3.8c). The response according to average sea distance illustrates the large penetration of eels inland in France in the first 400 km and their scarcity in both the Mediterranean (SPFR-Mediterr) and Atlantic Iberia (SPPT-Atlantic) (Figure 5.4).

Hydraulic density computes the number of river segments for the downstream basin divided by the surface of the basin. It depends highly on the structure of the river network, and this explains different results obtained in France and the Iberian Peninsula (Figure 3.8g). The response is not significant for France, and one of the lowest for the Iberian Peninsula but still significant. The response for the Iberian Peninsula shows mostly a decrease to a local minimum from 0.610^{-4} $segment.m^{-2}$ to 1.010^{-4} $segment.m^{-2}$.

The eel presence probabilities according to the Δ model are shown in Figure 3.10. The eel presence probability is low in the central part of Spain while it can be large in upstream sectors along the large river corridors in France. The map also shows a contrasted response between the Mediterranean and the Atlantic, with low probabilities of presence in the Mediterranean and in the Rhône basin.

The residuals of the Δ model show no spatial patterns. Larger residuals at a larger distance to the sea are the result of the model predicting lower probabilities of presence upstream (Figure 3.11).

[9] Areas ATL_{IB} and MED have a common dataset between France and Spain

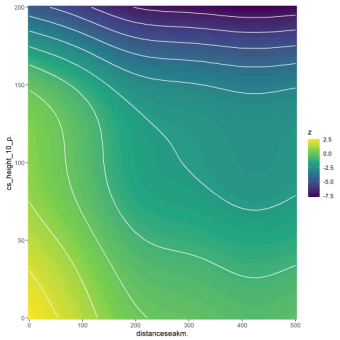

(a) $\Delta \sum \bar{h}$(m) - *Dsea* (km)

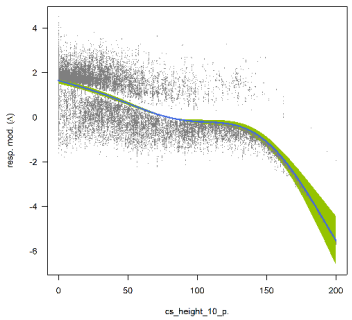

(b) $\Delta \sum \bar{h}$(m)

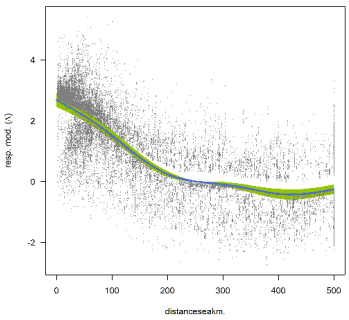

(c) Δ d_{sea} distance sea(km)

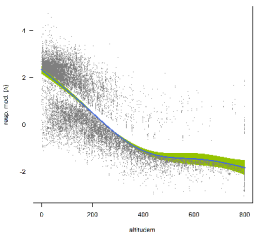

(d) Δ altitude (m)

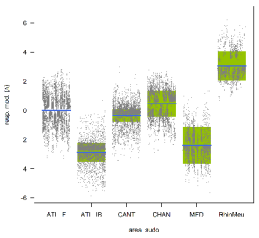

(e) Δ Sudoe Zone

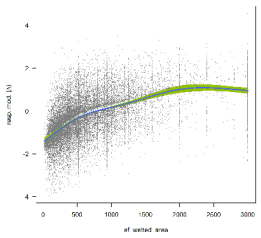

(f) Δ S_p Electrofished wetted area (m2)

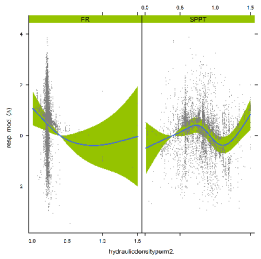

(g) Δ Hydraulic density

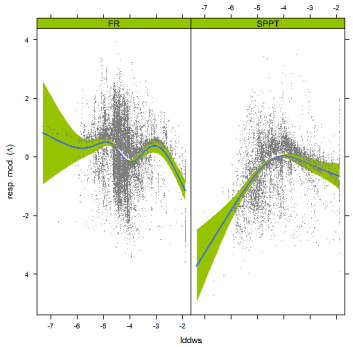

(h) Δ log(ddws)

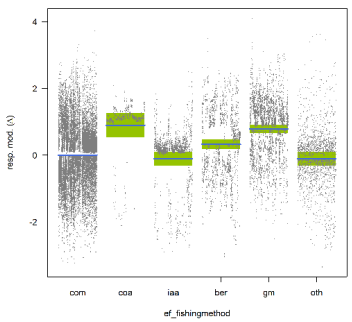

(i) Δ Fishing method ω

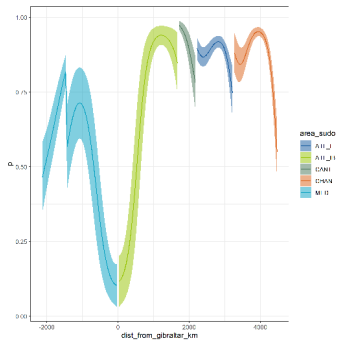

(j) Δ Distance to Gibraltar (km)

Figure 3.8: Predictors of the Δ model. (a) two dimensional contour plot to show the interaction, $\Delta \sum \bar{h}(m)$= sum of height of dams including the prediction of height when missing, Dsea (km)= distance , (b)-(j) Response plot, the values in the Y-axis correspond to probability of presence for the Δ model, ddws downstream drainage wetted surface ratio.

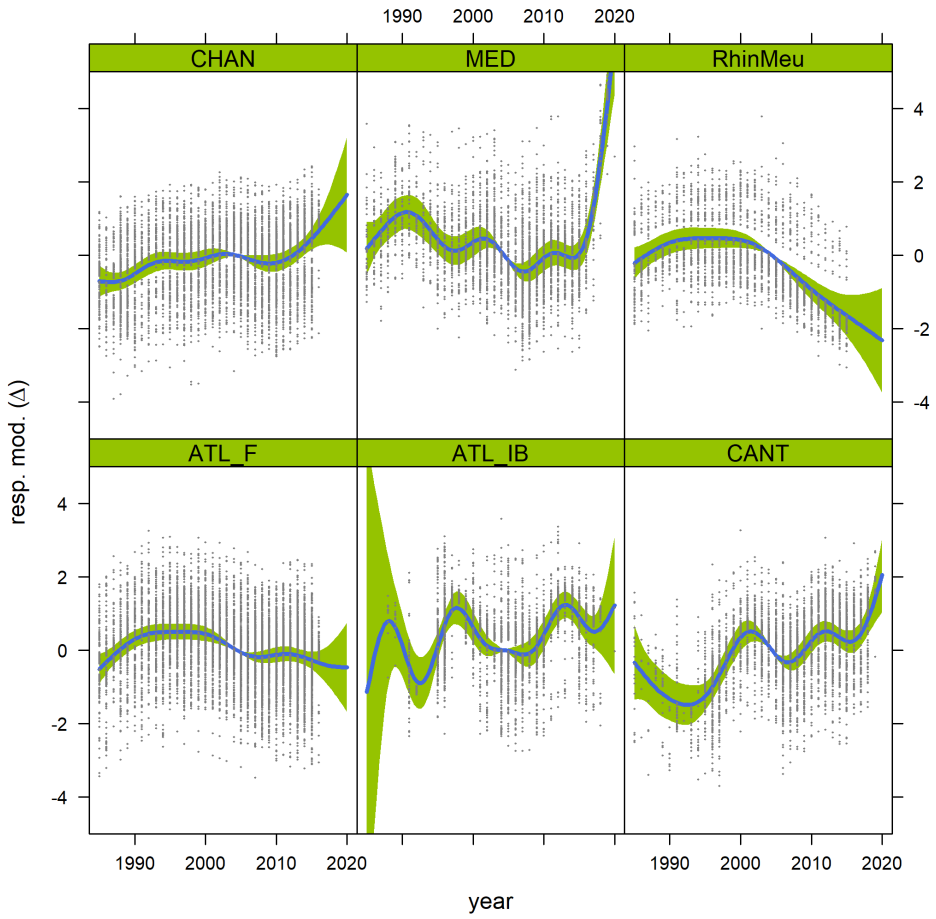

Figure 3.9: Response of the Δ model for year. A different response has been obtained for the different SUDOE areas. Data are missing after 2018 in France so the trends of common areas (CANT and the MED) are probably biased after 2018. The level of the response per SUDOE area is provided in Figure 3.8e.

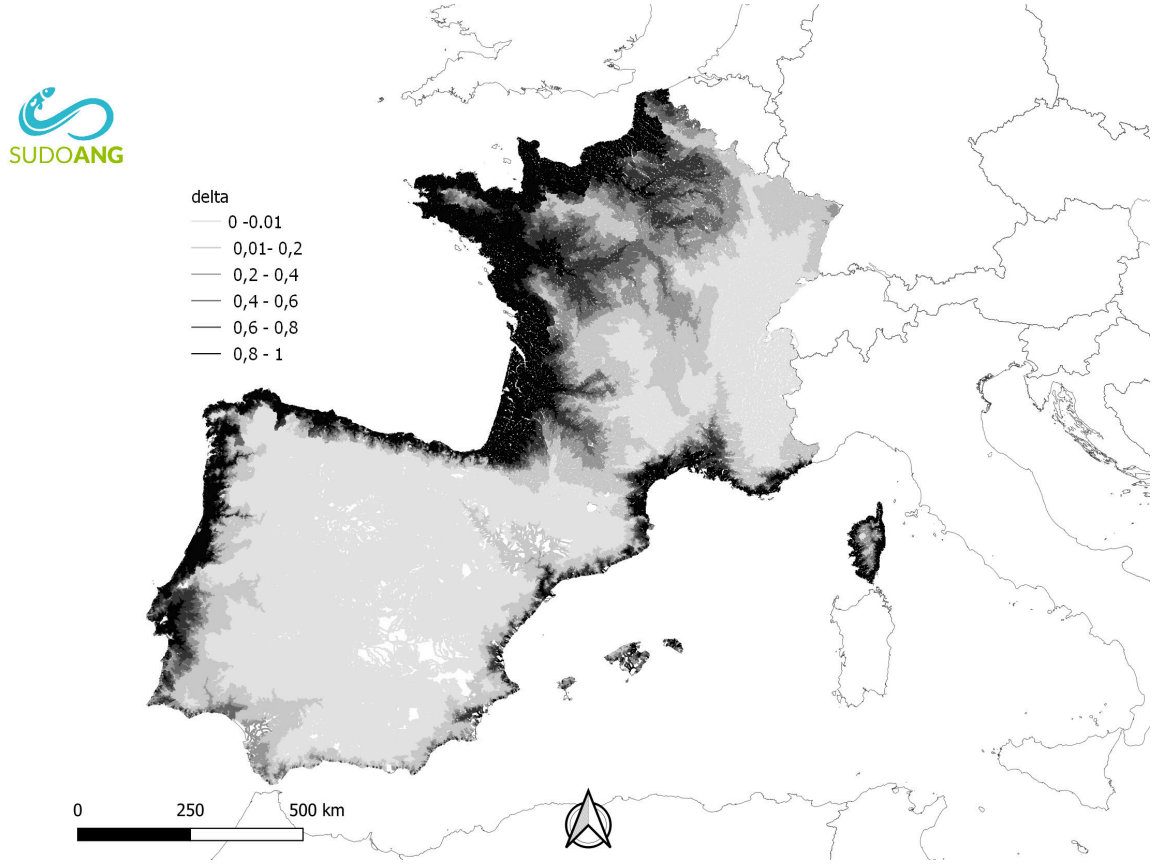

Figure 3.10: Eel presence probability in France, Spain and Portugal according to the Δ model predictions.

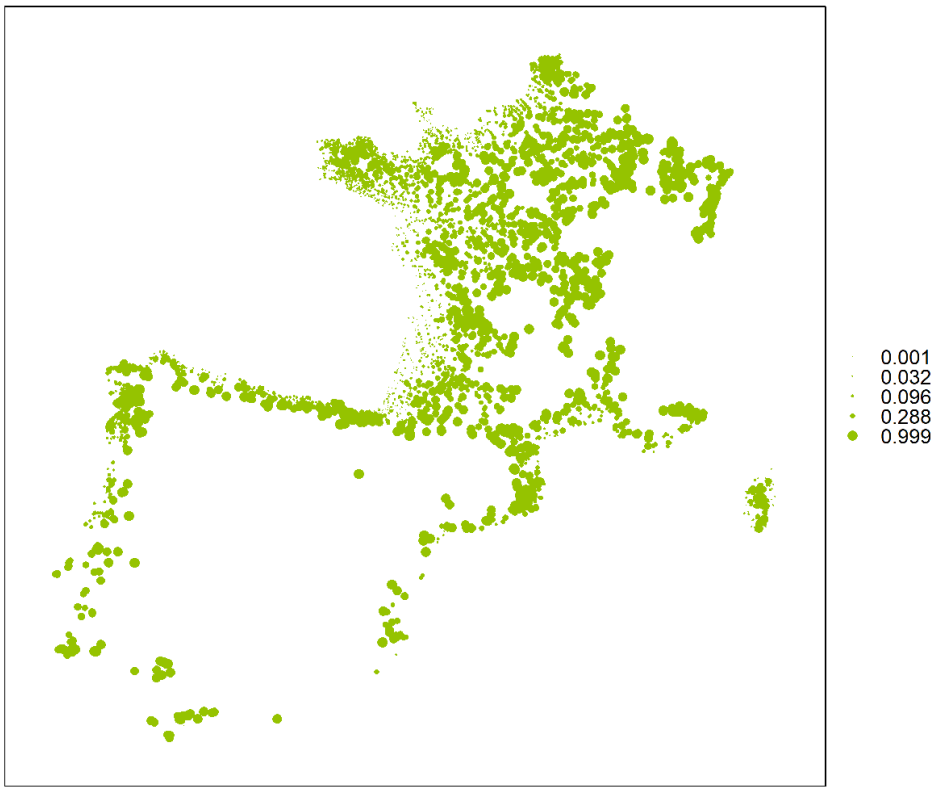

Figure 3.11: Residual of the Δ model, predicting eel probability of presence in France, Spain and Portugal. Green points indicate that the actual value observed was larger than prediction.

3.5 Gamma model

After screening, the final dataset for the Gamma model Γ predicting non null eel densities, contains 201 (PT), 2991 (SP), 5058 (FR) lines.

The model explains 42.2 % of the deviance on 19993 observations.

The model is summarized in Table 3.4, the best model includes the following explanatory variables:

- **s(distanceseakm.)**: distance to the sea, in km,
- **ef_fishingmethod**: fishing protocol ω,
- **s(altitudem.)**: altitude of the river segment, in m,
- **s(year):area**: year, discrete (factor) per SUDOE area,
- **s(dist_from_gibraltar_km)**: coastal distance from Gibraltar, in km,
- **ti(cs_height_10_p.,distanceseakm.)**: interaction between cumulated dam height and distance to the sea,
- **s(hydraulicdensityperm2.):country2**: hydraulic density in number of segment per surface area for the downstream basin. Different responses were expected between the Iberian Peninsula and France so different smooth have been used per area,
- **area_sudo**: the SUDOE areas,
- **s(cs_height_10_p.)**: cumulated height of dam from the sea $\sum \bar{h}$, this variable includes prediction of dam height when missing,
- **ti(altitudem.,distanceseakm.)**: interaction term between area and distance.

The Γ model corresponds to positive values of densities. The model includes tensor interaction for the distance to the sea and cumulated dam height, and for distance to the sea and Altitude.

The **distance to the sea** is the best predictor of eel density in the model. The eel density shows an initial sharp decrease between 0 and 120 km and then a smoother decline to 600 km (Figures 3.12e, 5.9 in Annex).

The **fishing method** ω is the second most important predictor in the model. As in the Δ model the largest densities are obtained for the eel specific fishing method using two passes (eel specific surveys - ω_{fue}). Bank fishing ω_{bf} shows an intermediate response. All other responses are low with in order standard electrofishing (com) ω_{ful}, eel specific sampling (iaa) ω_{eai}, other sampling ω_{oth}, and deep habitat fishing (gm) ω_{dhf}, which ranks among the highest in the Δ model. So, in general, eel specific fishing correspond to higher densities as they use methods and target habitats favourable to eels. The point sampling method has a high probability to find an eel, but overall, the number of eels collected remain very low (Figure 3.12g).

The **altitude** is the third most important predictor. It shows an increase from 200 to 400 m possibly a way to compensate for higher densities in the North-East of France (Seine Basin) due to unreferenced transport sectors (Figure3.12d).

Table 3.4: Summary of model (Γ) gamma

A. parametric coefficients	Estimate	Std. Error	t-value	p-value
(Intercept)	-3.4176	0.0800	-42.7410	< 0.0001
ef_fishingmethodcoa	1.7528	0.0696	25.1819	< 0.0001
ef_fishingmethodiaa	-0.0072	0.0609	-0.1187	0.9055
ef_fishingmethodber	0.6482	0.0573	11.3202	< 0.0001
ef_fishingmethodgm	-0.3558	0.0434	-8.1997	< 0.0001
ef_fishingmethodoth	-0.4772	0.0624	-7.6484	< 0.0001
area_sudoATL_IB	-0.4998	0.1272	-3.9307	0.0001
area_sudoCANT	0.0071	0.0795	0.0890	0.9291
area_sudoCHAN	0.2147	0.1064	2.0173	0.0437
area_sudoMED	-3.1572	0.4432	-7.1233	< 0.0001
area_sudoRhinMeu	0.8172	0.1703	4.7997	< 0.0001
B. smooth terms	edf	Ref.df	F-value	p-value
s(year):area_sudoATL_F	4.9394	4.9980	21.0083	< 0.0001
s(year):area_sudoATL_IB	2.6402	3.2320	7.1343	0.0001
s(year):area_sudoCANT	4.7939	4.9736	12.1780	< 0.0001
s(year):area_sudoCHAN	4.9553	4.9989	38.8338	< 0.0001
s(year):area_sudoMED	4.3534	4.8050	3.9740	0.0028
s(year):area_sudoRhinMeu	1.4870	1.8260	13.0367	< 0.0001
s(distanceseakm.)	2.8982	2.9901	348.1053	< 0.0001
s(altitudem.)	2.9945	2.9998	130.0947	< 0.0001
ti(altitudem.,distanceseakm.)	8.7575	8.9814	11.8740	< 0.0001
ti(cs_height_10_p.,distanceseakm.)	7.9143	8.3714	26.0079	< 0.0001
s(dist_from_gibraltar_km)	4.9730	4.9995	27.0269	< 0.0001
s(hydraulicdensityperm2.):country2FR	1.0024	1.0048	0.0779	0.7817
s(hydraulicdensityperm2.):country2SPPT	2.9092	2.9940	23.3196	< 0.0001
s(cs_height_10_p.)	4.7862	4.9754	14.5164	< 0.0001

The interaction between **year and area_sudo** shows higher values in the 1990's in France for the $CHAN$ and ATL_F. The densities in the MED are overall very low. The sharp decrease in density in $RhinMeu$ is somewhat consistent with the Δ model, which was the only zone to show a decline in eel presence probability, even though it was limited to in the 2000's, while the Γ response here shows a sharp continuous decline. The response in $CANT$ shows again an increase in eel density in the Γ model after 2015. It is necessary to remain cautious about this result given the lack of data after 2015 for electrofishing in France (Figure 3.13a).

The **distance from Gibraltar** response for the Γ model is overall not consistent with the Δ model. Eel densities show a sharp decline along the ATL_{IB} coast and then an increase from $CANT$ to the $CHAN$ (highest values around Britany) and then a decrease along the $CHAN$. For this coastal part, the decline is more consistent with the decline in eel presence probability observed in the Δ model (Figure 3.13b).

The tensor interaction between **cumulated dam height** and **distance to the sea** is illustrated in Figure 3.12a. The tensor interaction is included on top of the response of both distance and dam variables (Figures 3.12c and 3.12e). It shows that unlike the Δ model, the response in eel density is mostly driven by distance to sea and not by cumulated dam height. See also Figure 5.8 which illustrates the small effect of dam on

the density of eel within the gamma model dataset (positive values of densities).

The **hydraulicdensityperm2** shows a different response between the Iberian Peninsula and France. The eel presence predicted by the Δ model and eel densities predicted by the Γ model are quite consistent. Up to 0.6 10^{-4} segment per m^2 there is an increase in density and then the density declines for higher values.

The **area_sudo** show the highest densities for Rhine Meuse and the lowest densities in the Mediterranean. Predicted densities are low for Atlantic Iberia, quite high in Cantabria. They increase in France from South to North (Figure 3.12f).

The **interaction between altitude and distance to the sea** (Figure 3.12b and 5.10 Annex) illustrates again the importance of distance to the sea on eel density. High values of densities are found at 400 m altitude and small distance to the sea. Those altitudes of 400 m are mostly found in the *CHAN*, and correspond either to a good penetration inland of eels in the Seine Basin, or to unreferenced transport operations in the Seine Basin.

The map of eel densities (Γ model) shows that high densities are predicted in the coastal areas, large densities are expected in the south of Portugal and low densities are found in the coastal zone in the Mediterranean in the Southeast of Spain (Figure 3.15).

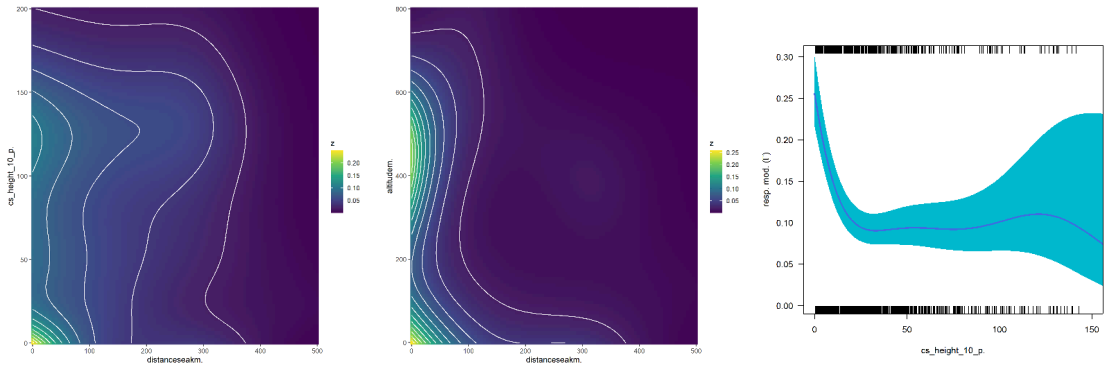

(a) Distance sea (km) - Cumulated height dam (m)

(b) Altitude (m) - Distance sea (km)

(c) Cumulated height dam (m)

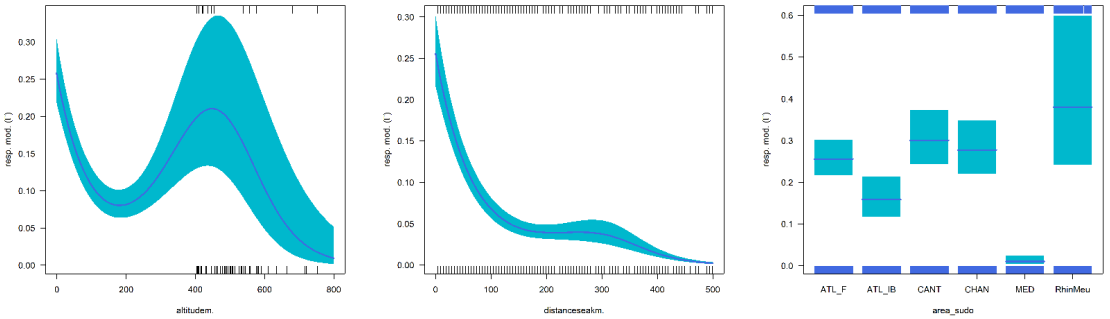

(d) Altitude (m)

(e) Distance to the sea (km)

(f) area_sudo

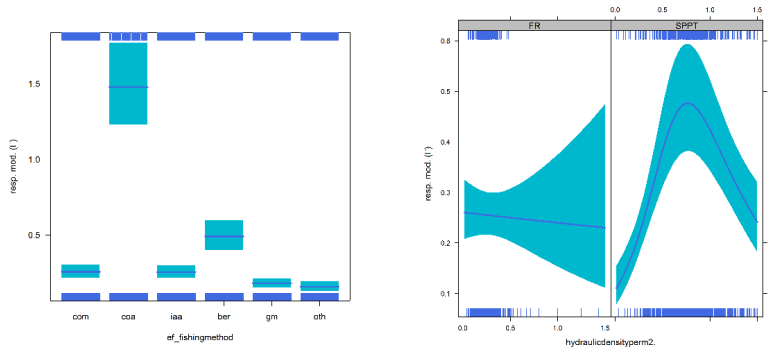

(g) Fishing method

(h) Hydraulic density (m^{-1})

Figure 3.12: Predictors of the Γ model. (a) (b) two dimensional contour plot to show the interaction, (c)-(h) Response plot, the values in the Y-axis correspond to densities (eel.m⁻2) for the Γ model (modelled on a subset of positive values). When not included in the plots, variables have been set to: cumulated height dam [10] = 0 m, altitude = 0 m, distance sea = 0 km, distance to Gibraltar = 3000 km, fishing method = full (two pass wadable electrofishing ω_{ful}), year=2015.

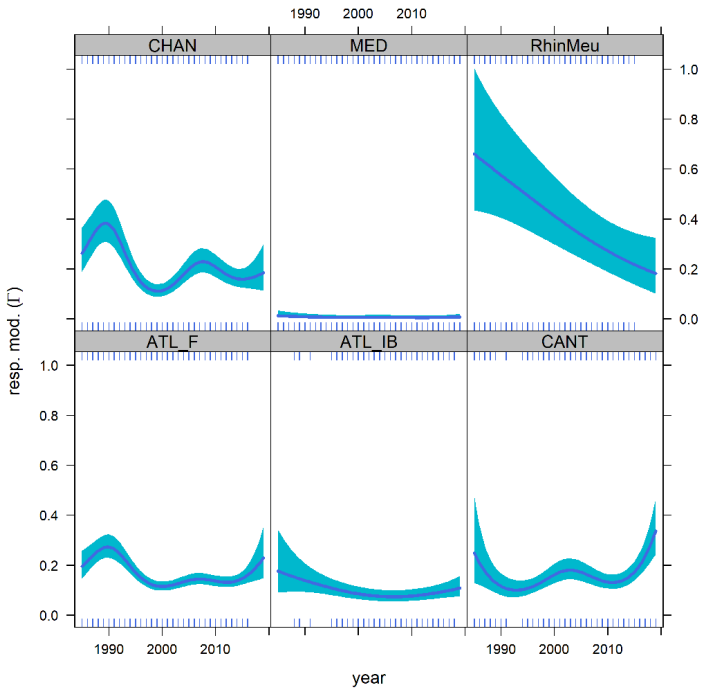

(a) Year:area_sudo

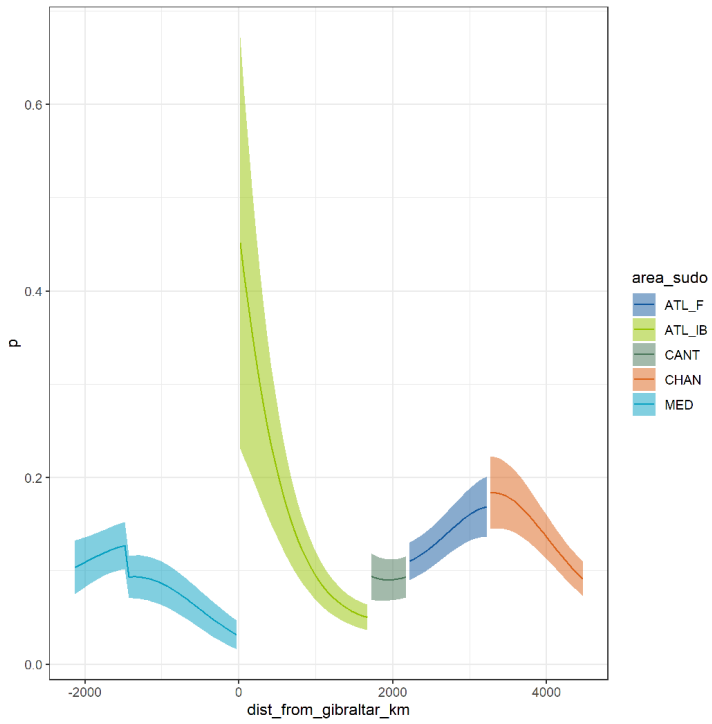

(b) Distance from Gibraltar (km)

Figure 3.13: Spatial predictors of the Γ model (continued). Effect of SUDOE area and distance to Gibraltar (km).

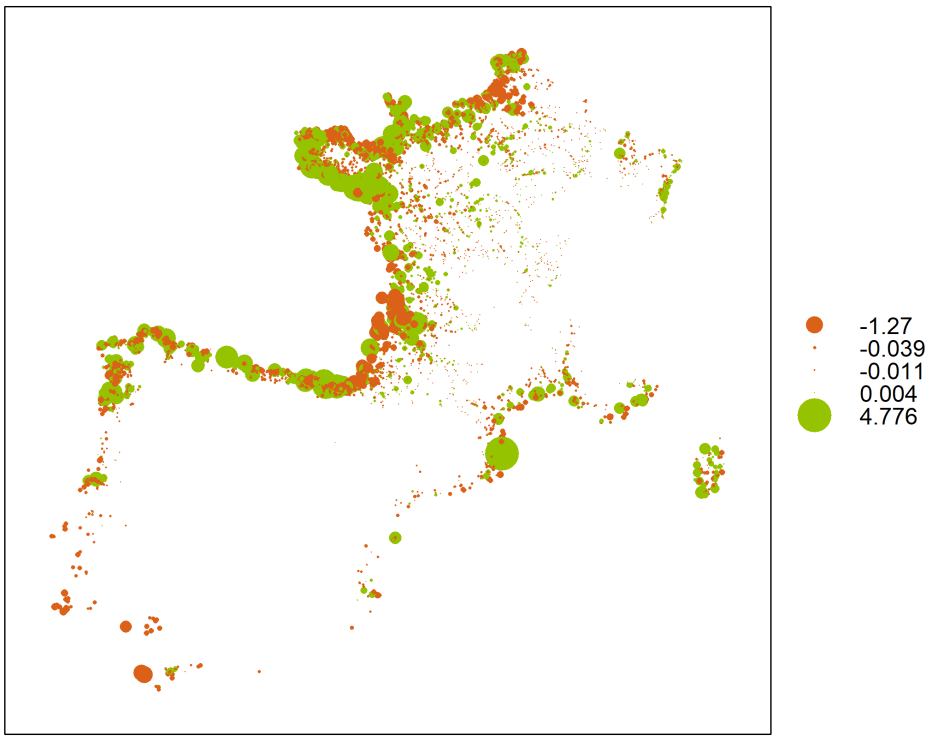

Figure 3.14: Residuals of the Γ model fitted on positive densities in France, Spain and Portugal. Positive values (in green) indicate that the actual value observed was larger than prediction, negative values (in orange) indicate a prediction larger than the number of eels observed.

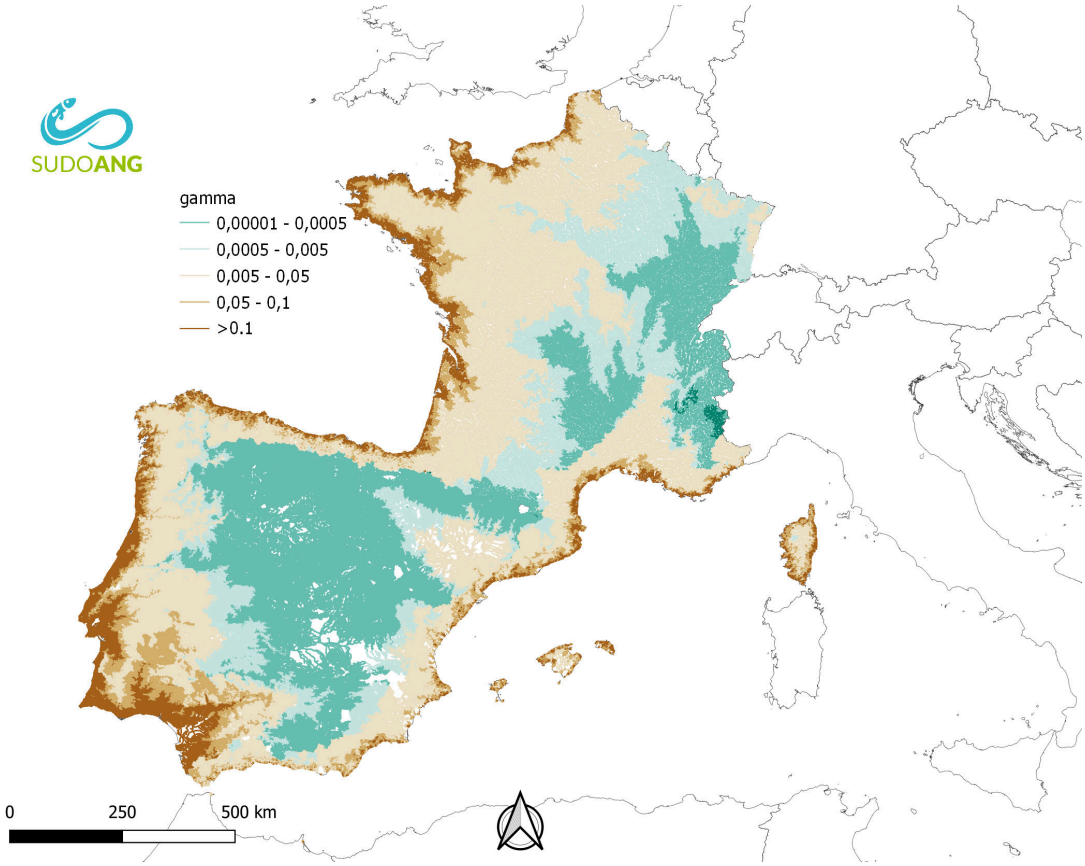

Figure 3.15: Map of eel density when present (Γ model) in France, Spain and Portugal.

3.6 Density

Density per river segment is calculated as the product of Delta (Δ) and Gamma (Γ) models. The patterns of densities reflect the results of the Γ (largest densities near the coast) and the Δ model (contrasted inland migration between France and the Iberian Peninsula) (Figure 3.16). Residuals are calculated as the product of Δ and Γ residuals (Figure 3.17).

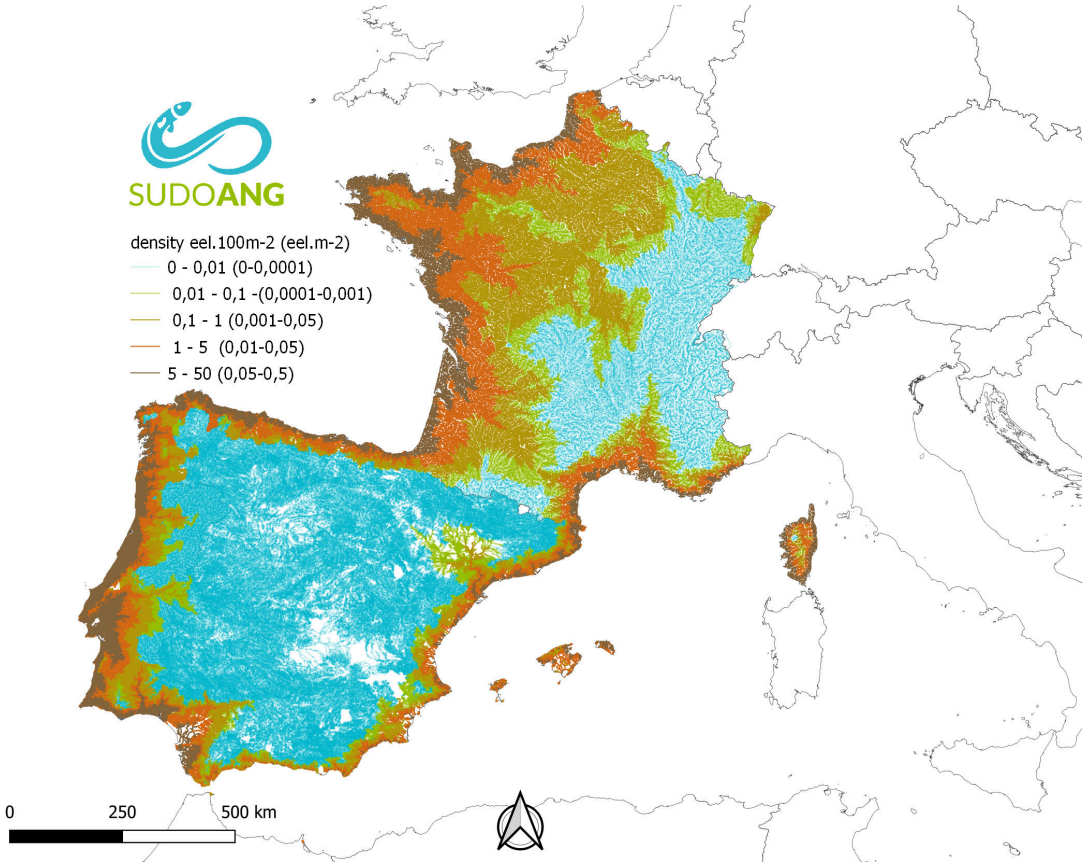

Figure 3.16: Eel density in France, Spain and Portugal according to the ΔΓ model responses.

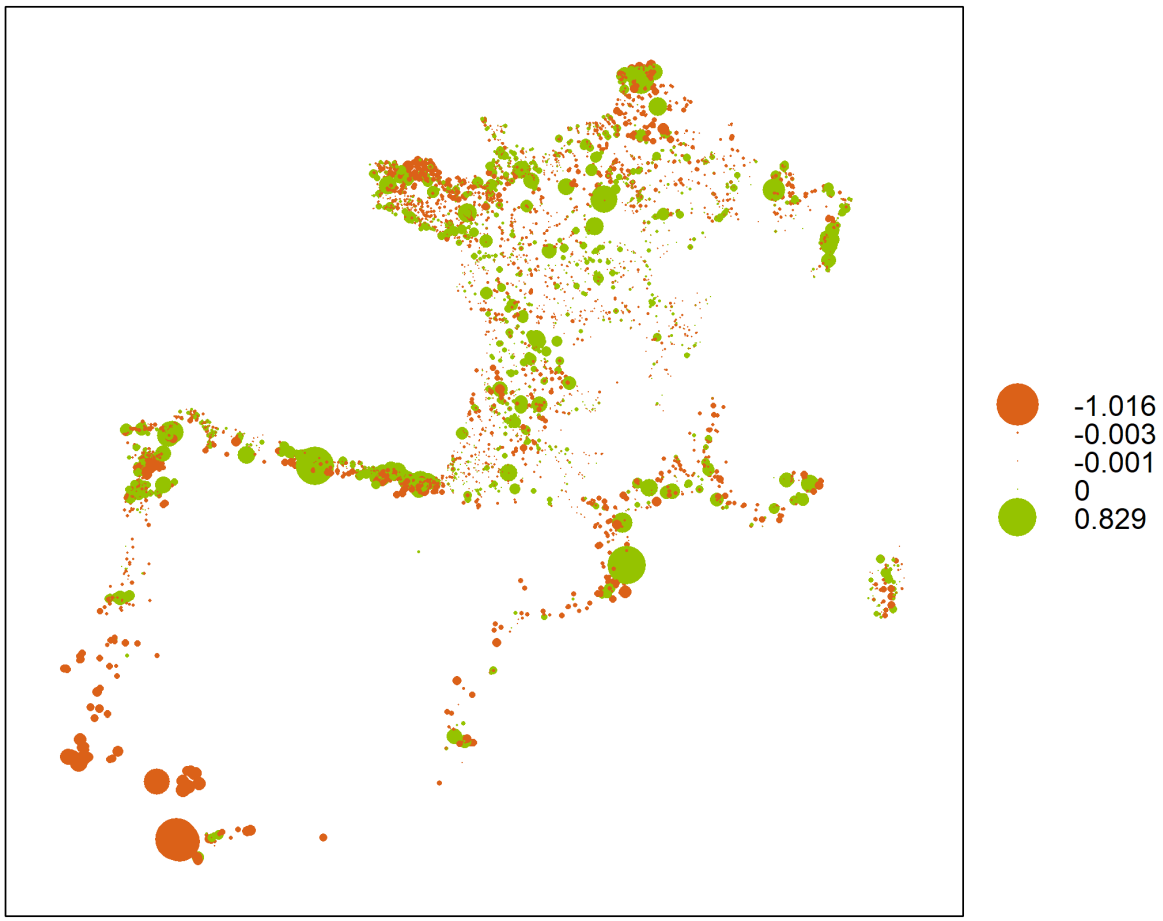

Figure 3.17: Map of $\Delta\Gamma$ model residuals. Positive values (in green) indicate that the actual value observed was larger than prediction, negative values (in orange) indicate a prediction larger than the number of eels observed

3.7 Multinomial model

The Multinomial model ($\mu\tau$) predicts the proportion of eel in each size class. The continuous model predictors: year, density and distance to the sea are fitted using smooth responses using three degrees of liberty. Densities are censored to 100 in eel/100m^2. The model is fitted on 494163 individual size values, with each line being the size of an eel. The best that best predicted eel proportion in each size class uses the following variables ordered by contribution:

- **Density** predicted by the $\Delta\Gamma$ model. When densities are high, the proportion of the smaller size class is higher. Eel densities are the most important predictor in the model in term of predictor contribution, the largest response in term of Chi Square is obtained for the 300-450 size class (Figure 3.18c).
- **Year**: The proportion of younger eels tends to increase in time while the proportion of large eels decrease (Figure 3.18a).
- **Distance to the sea**: the smaller eel class proportion < 150 mm decreases with distance to sea (Figure 3.18f).
- **Fishing method**: the proportion of small eels is larger in eel specific fishing and standard electrofishing while point sampling tends to collect larger eels (Figure 3.18b).
- **River width**: smaller streams tend to have a larger proportion of small sized eels, the best model was obtained with a linear response on the log transformed variable (Figure 3.18d).
- **Area_sudo**: the proportion of small eels is larger on the Atlantic coast of ATL_{IB} and ATL_F, and lower in the MED and the $RhinMeu$ (Figure 3.18e).

The percentage of deviance explained by the model is quite low (14%). The maps of model predictions are shown in Figure 3.19. Multiplying these proportions by densities we get the densities per size class (Figures 3.20).

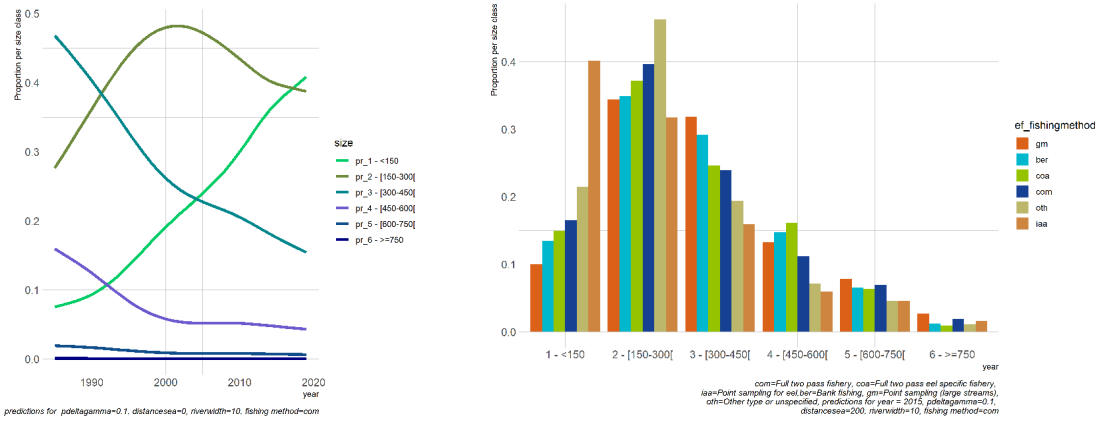

(a) Year (b) Fishing method

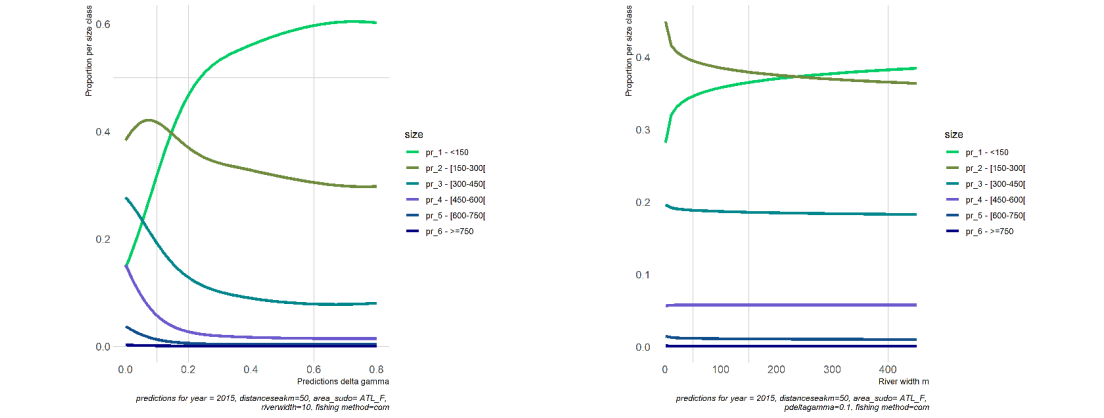

(c) Density (d) River width

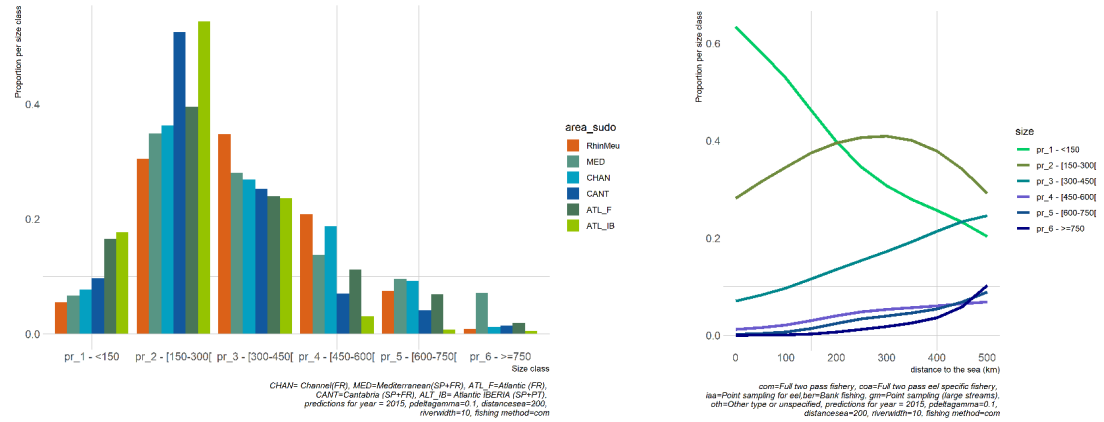

(e) area_sudo (f) Distance sea

Figure 3.18: Proportion of eels by size class as a function of different predictors ($\mu\tau$) model.

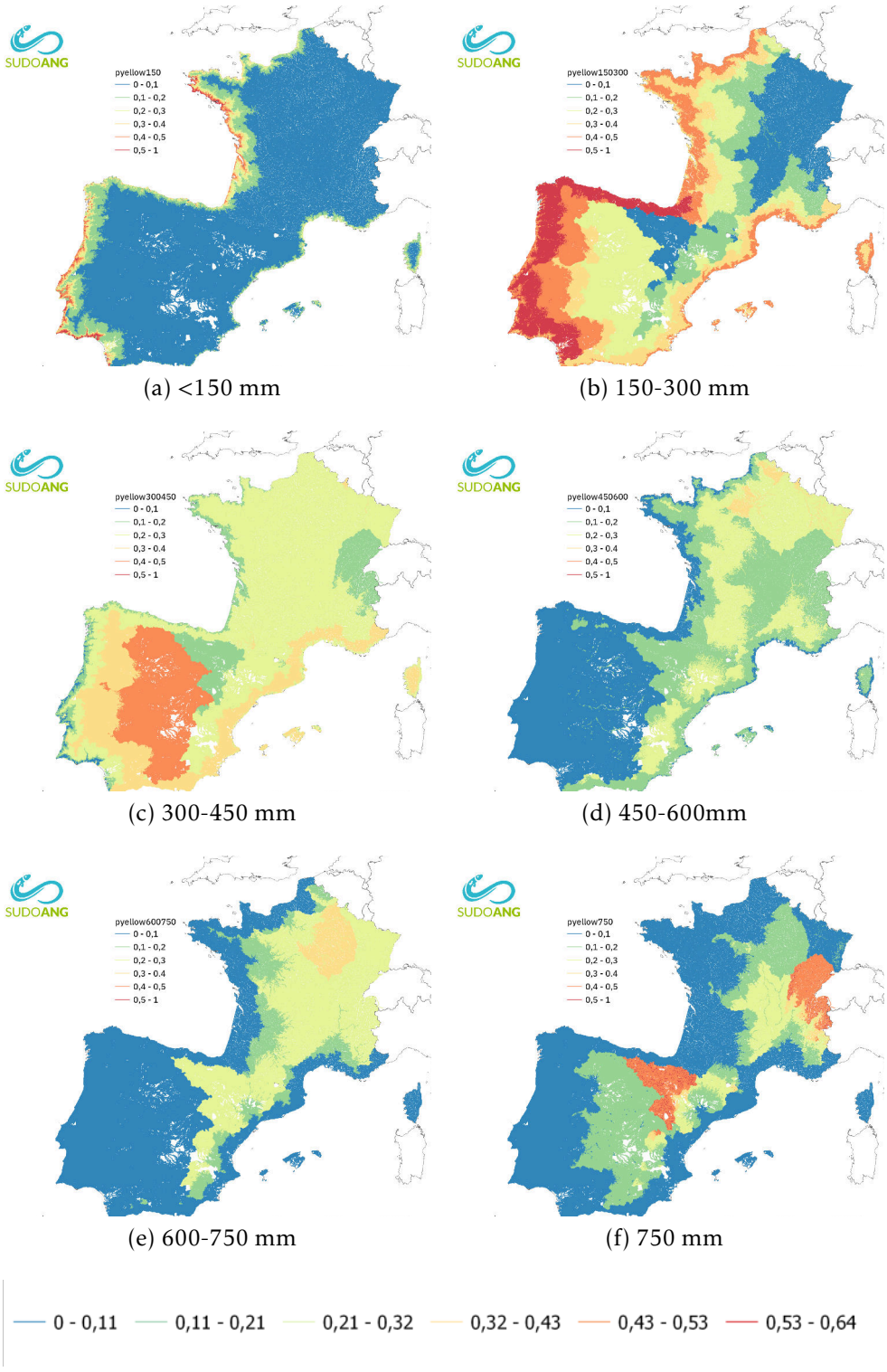

(a) <150 mm

(b) 150-300 mm

(c) 300-450 mm

(d) 450-600mm

(e) 600-750 mm

(f) 750 mm

(g)

Figure 3.19: Map showing the proportion of eels by size class for the Multinomial size structure model P_τ for the Multinomial ($\mu\tau$) model in 2015.

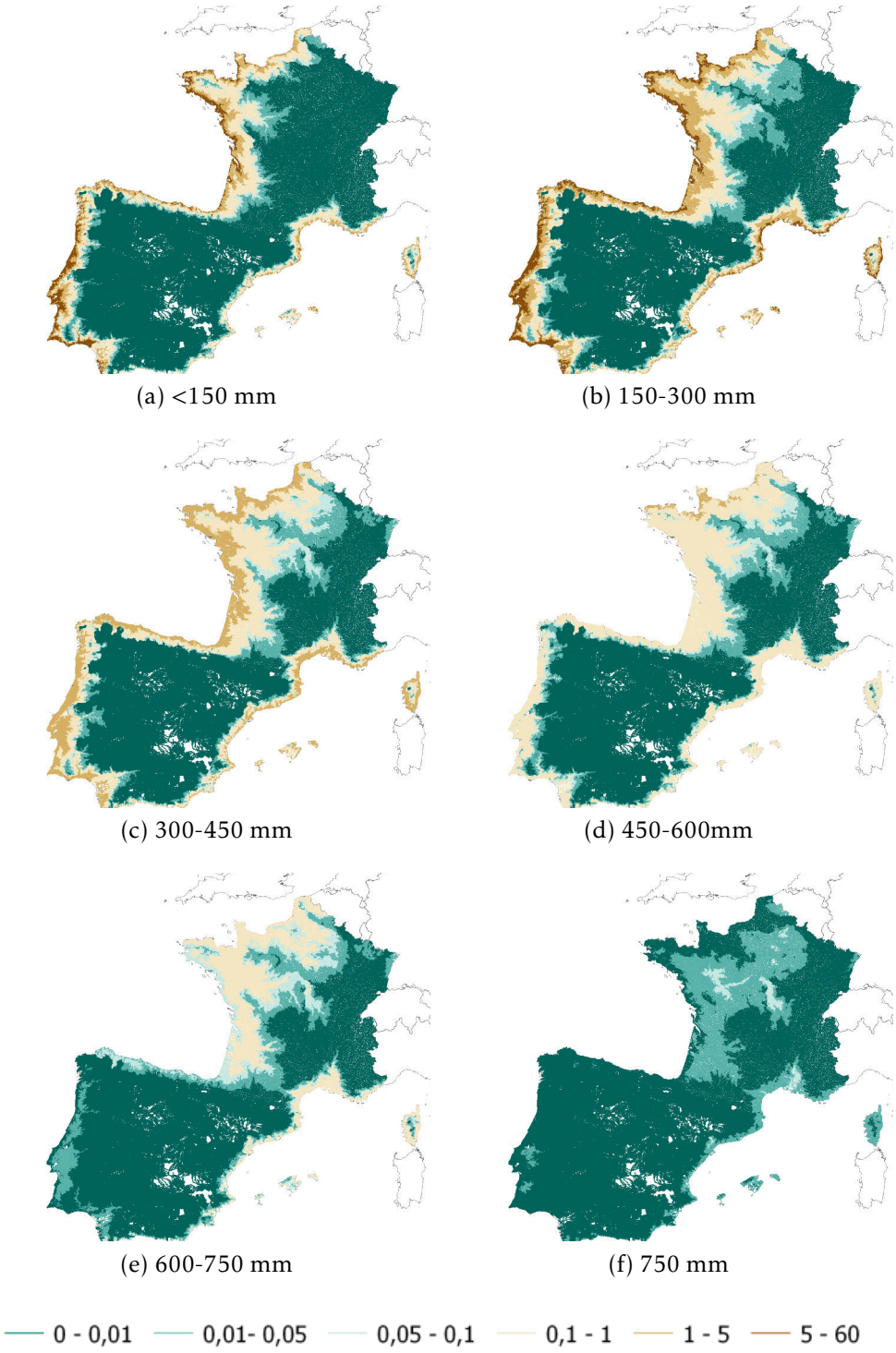

Figure 3.20: Map showing the prediction of density per size class $d_\tau = \widehat{d_i}\widehat{P_\tau}$ in eel.100m^{-2} predicted by multiplying the proportion per size class P_τ in each river segment i, with the density predicted by the $\Delta\Gamma$ model in 2015.

3.8 Silvering

To estimate the silvering class, the silvering model divides eels into three categories: immature, silver male and silver female. So before modelling the 20101 eels larger than 250mm of the SUDOANG dataset were classified according to the silvering status of eels using the Durif index (Durif et al., 2009) (Figure 3.21a and 3.21b).

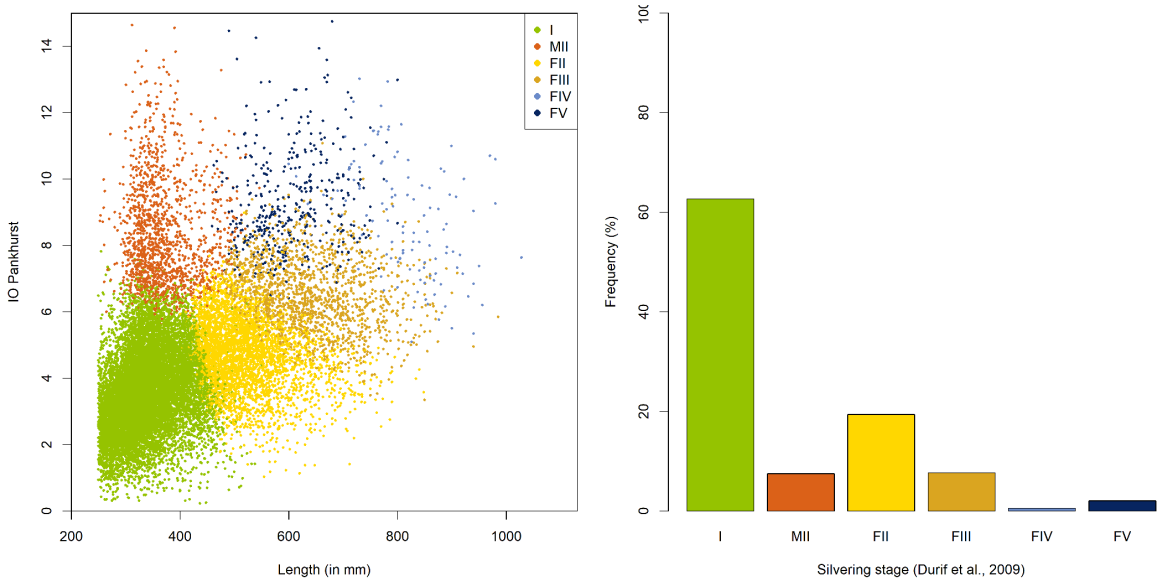

(a) Length-IO-Durif (b) Silvering stages

Figure 3.21: (a) The class of maturity for 20101 eels containing silvering information, according to Durif et al. (2009) relating length and eye size (Pankurst index). (b) Frequency of the class of maturity and sex obtained with Durif et al. (2009) (I: undifferentiated males and females (=immature in the model), MII silvers males (=male silver in the model), FII Resident females (=immature), FIII Pre migrant females (=immature), FIV & FV migrant females (=silver female)).

According to Durif stage classification Durif et al. (2009) the SUDOANG dataset contains 82.1% of immatures, 7.7% pre migrant and 10.2% silver eel. The sex ratio[11] is 2.8, which means that the proportion of females is 26.4%, and most eels 89.8% are immature. Another metric of maturity based solely on eye index is available using the Pankhurst index[12]. Using the latter index, the percentage of silver eel is a bit lower at 9.9% (instead of 10.2%).

The percentage of silver eels within this size class is quite low: 1.95%, all of them being males. Male silver eels are found at a smaller distance to the sea than females, and at higher density (Figure 3.22).

The best model incorporates density ($\Delta\Gamma$) prediction, distance to the sea, distance to Gibraltar, altitude, Strahler rank, month and size as predictor variables. The percentage of deviance explained by the model is 0.32 for the continuous model and 0.27 for the categorical model.

[11] male/female

[12] Limit for silvering: ocular diameter > 6.5 mm for males (<450 mm), 8 mm for females.

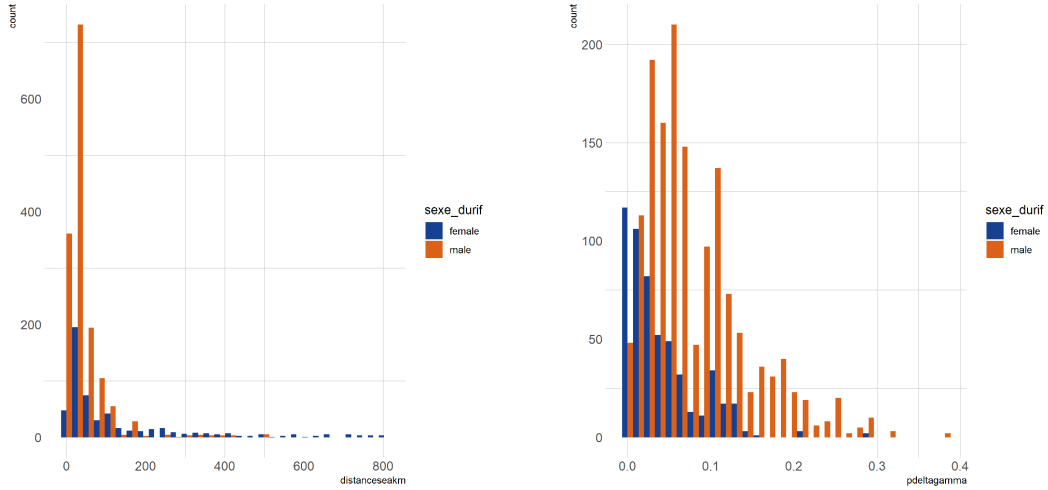

(a) Silver eel - Distance sea (km) (b) Silver eel - Density

Figure 3.22: Count of silver eel according to distance to the sea (a) and density (ΔΓ) eel/m^2(b)

The proportion of silver (both males and females) increases with size (Figures 3.23a, 3.23b). (Figure3.23a).

Depending on the size class considered, the effect of density is different. For small eels (300 mm) the proportion of silver eel increases with density up to the level of 0.2 eel/^{2}m, and then decreases for densities beyond 0.4 eel eel/^{2}m. For intermediate sized eels, the same trend is observed with a larger proportion of male silver eels produced than with the small eels. This trend is associated with a continuous increase in the proportion of females with density. For large eels, only females, the effect of density is much weaker, but an increase is still observed in the proportion of silver eel when density increases (Figure 3.24a).

The proportions of males and females decrease with distance from the sea; contrary to the immature class, whose proportion tends to increase with distance from the sea (Figure 3.24b). This is in opposition with the more common idea that the proportion of silver eel increases with distance to the sea. The proportion of silver eel increases from the Italian frontier in France to Spain up to Gibraltar [13]. This proportion is very large in Portugal and South of Spain, and then decreases along the ATL_{IB}, ATL_F coast and along the *CHAN* zone (Figure 3.24c).

Strahler increases the chance to be male, but it is not a large effect (Figure 3.25). There is an increased chance to be silver in August and a smaller chance in July and the month before.

Temperature has not been included in the model as it is correlated with size. The inclusion of the upstream catchment area does not improve the model.

The number of silver eel or sex ratio per river segment is obtained multiplying the Δ Γ Multinomial and silver eel models (Figures 3.26, 3.27). The percentage of eels becoming silver is calculated for Δ model probability >0.01. It shows that the percentage of silver is high in the Iberian Peninsula and in inland locations in France

[13] negative values of distance to Gibraltar correspond to the *MED* zone.

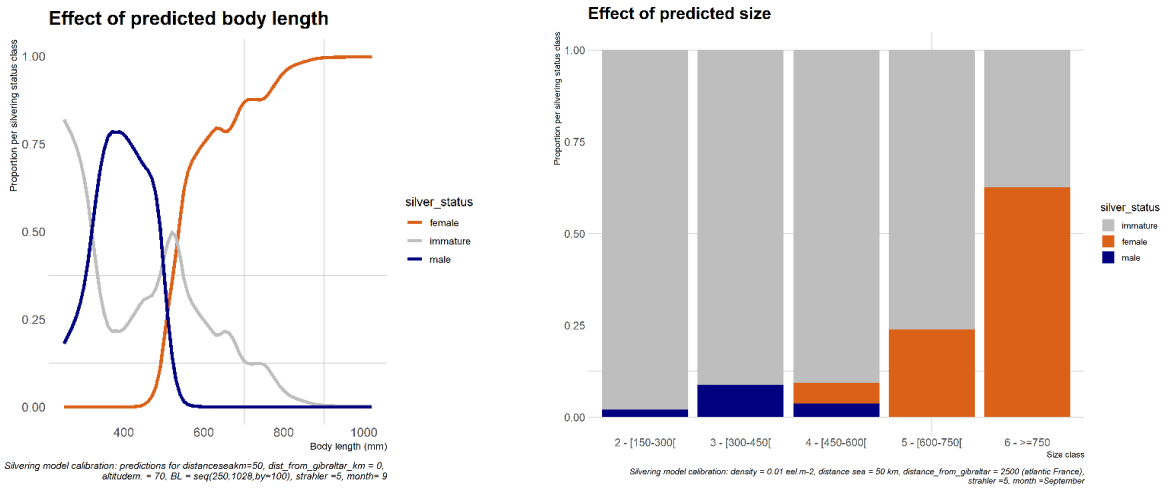

(a) Silver eel model - Body length

(b) Silver eel - length class

Figure 3.23: Proportions between undifferentiated, male and females predicted for body length class by the Multinomial silver model. Model response (a) using body length as a continous response variable. This results presents an additional model using continuous data for size. Note the shift from male to female around 500 mm. (b) Second model using size class, coming from the multinomial size model. This model is used for predictions in SUDOANG.

(where only large eels are found) (Figure 3.26). The percentage of males is higher in the downstream locations and in the Iberian Peninsula where female are rarely dominant except for those predicted in upper part of the Ebro basin (Figure 3.27).

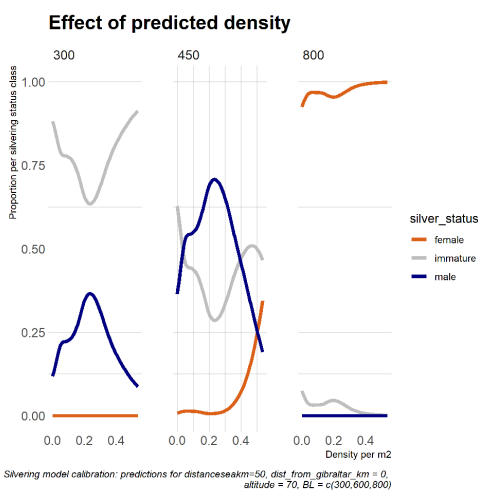

(a) Silver eel - Density

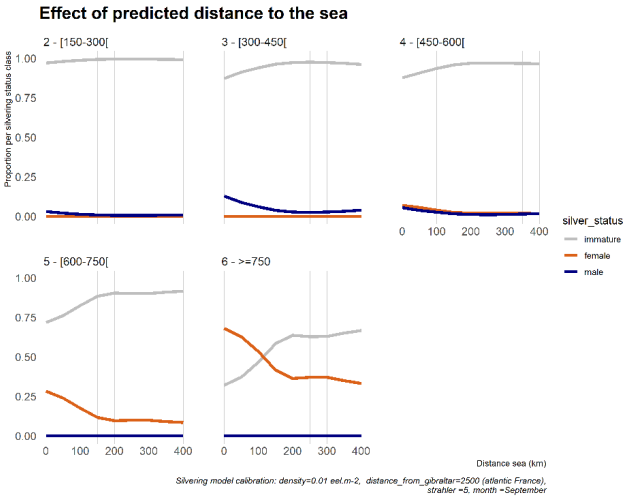

(b) Silver eel - Distance sea

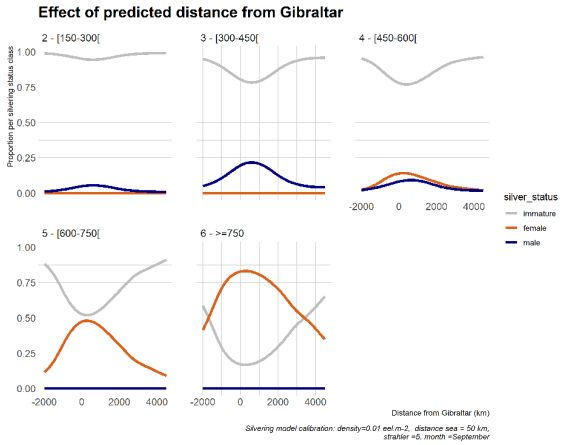

(c) Silver eel - Distance to Gibraltar

Figure 3.24: Proportions of undifferentiated, male and females predicted for 3 body length classes (300, 600 and 800 mm) by the Multinomial silver GAM model. (a) Response for density, (b) distance to the sea, (c) distance to Gibraltar.

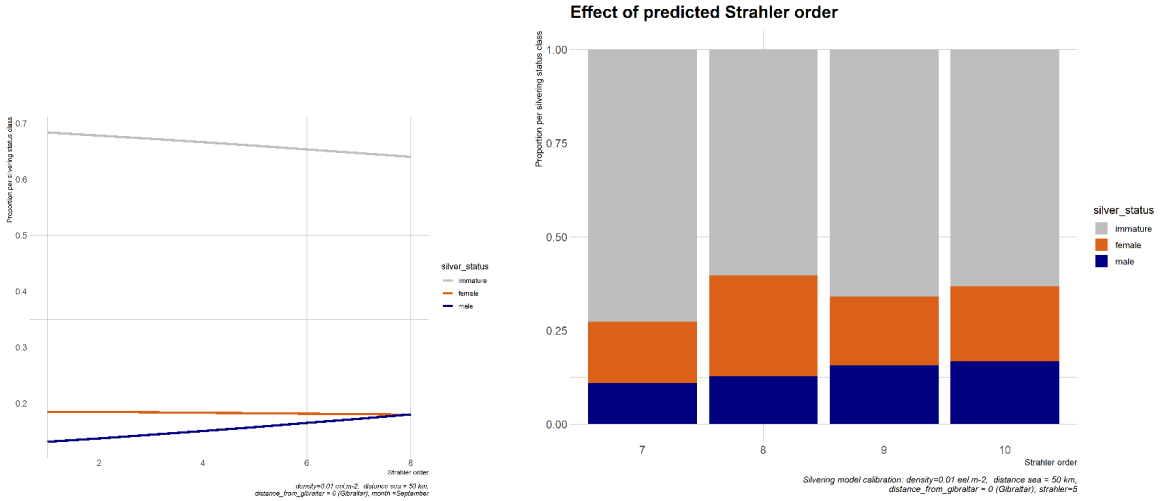

(a) Silver eel - Strahler

(b) Silver eel - Month

Figure 3.25: Proportions of undifferentiated, male and females predicted for 3 body length classes (300, 600 and 800 mm) by the Multinomial silver model. Response for (a) Strahler and (b) month.

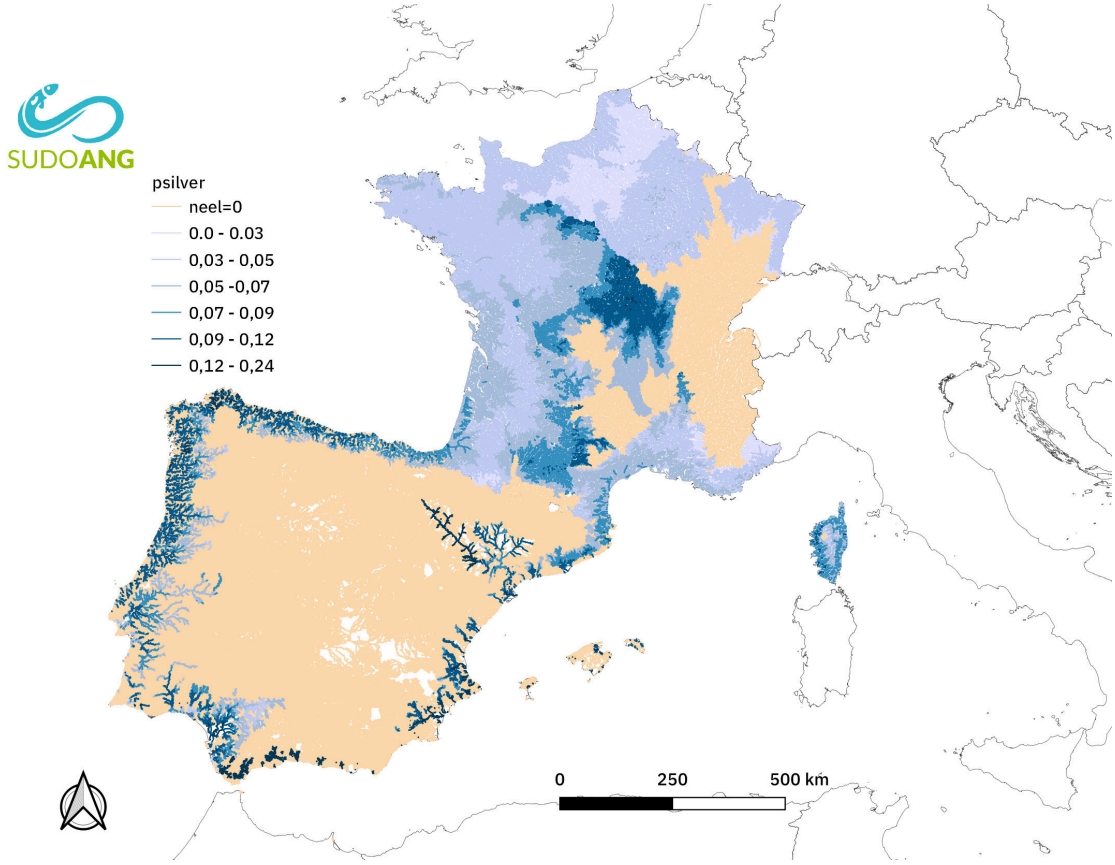

Figure 3.26: Map showing the percentage of eels becoming silver $\frac{Nsilvermale+Nsilverfemale}{Nimmature+Nsilvermale+Nsilverfemale}$.

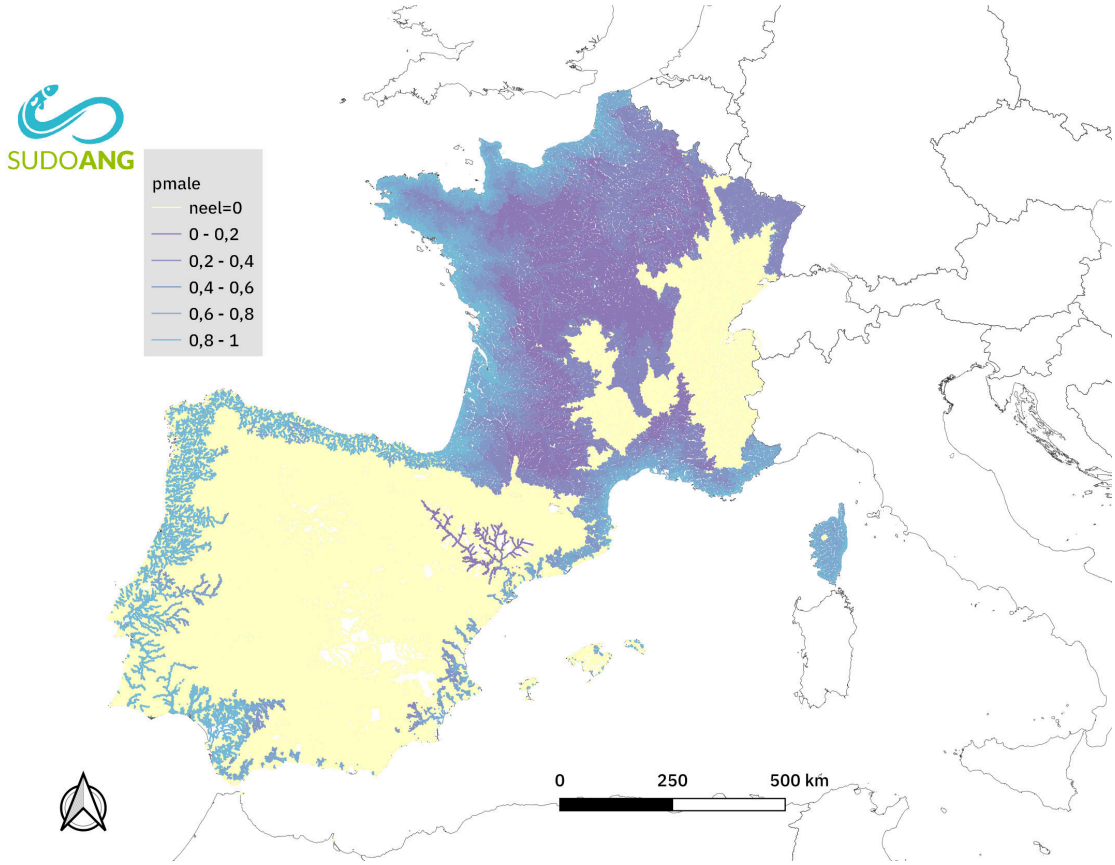

Figure 3.27: Map showing the percentage males. $\frac{Nsilvermale}{Nsilvermale+Nsilverfemale}$.

3.9 Transport model

The best model selected were

$$densCS \equiv ef\_wetted\_area + (1|sector)$$

for the Δ model and

$$densCS > 0 \equiv ef\_wetted\_area + \omega + (1|sector)$$

for the Γ model where ω corresponds to sampling protocol, ef_wetted_area is the surface of the station, and $sector$ is the sector identified in section 2.2.3 and Figure 2.8. The probabilities of presence for transport model and densities selected for the transport model are shown in Annex (Figure 5.21 and 5.22). The transport model results and prediction are shown in the Atlas.

3.10 Final calibration of waterbody productivity

A productivity value of 1 has been established for rivers, and by comparing the actual productivity of different French index rivers with the predictions from EDA and the surface of different waterbody type per in each index river, it has been estimated that the productivity of large rivers, lakes and reservoirs is 0.55, 0.18 and 0.05 lower respectively than the productivity of a river. Lagoons have been estimated to be 1.29 more productive than rivers. Thus, the total average productivity of each waterbody type was multiplied by these coefficients and the coefficient obtained was applied to the other areas of the basin

In practice the lake result is mostly driven by the results from the Soustons watershed in Southwest France, while the lagoons are fitted by the results of Etang de l'Or and Vaccares in the Mediterranean (Figure 3.28).

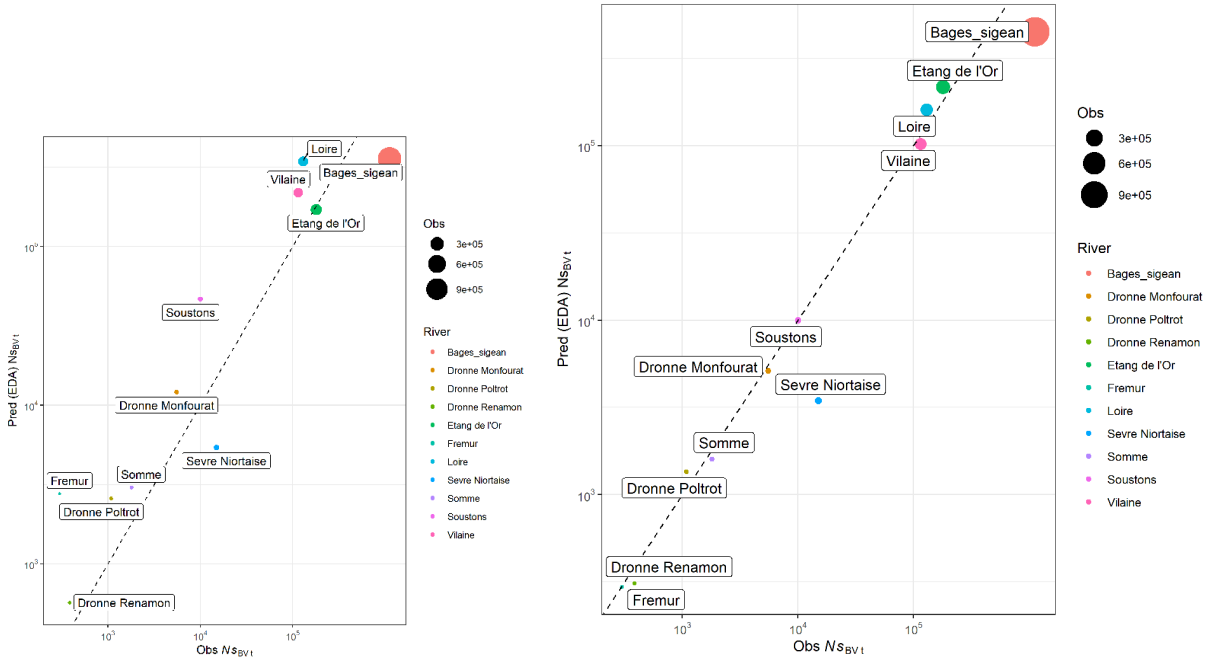

(a) Observed / predicted before optimisation

(b) Observed / predicted after optimisation

Figure 3.28: Post calibration of productivity for rivers, lakes, lagoons, large rivers, and reservoirs using 11 sites with known silver eel production.

3.11 Predictions on the SUDOANG water surfaces.

The total number of eels predicted is calculated both for the surface of rivers W_r: 1122.2 (FR), 222.9 (PT), 727.4 (SP), 2072.5 (total) km^2 and for additional waterbodies W_o: 6009.7 (FR), 1124.7 (PT), 2646.5 (SP), 9780.9 (total) km^2 (Table 3.5). The number of eels (in million) per country $\sum Ny$ is 125.3 (FR), 78.1 (PT), 170.9 (SP), and the total for the three countries is 374.3 million of eels. Most eels are produced in "other waterbodies" ($\sum Ny_o$=374.3), the rest are produced from river segments ($\sum Ny_r$=47.8).

Table 3.5: Eel number and wetted area per country in 2015, $\bar{d}$ density eel/^{2}m, $\sum N_r$ *number of eel in the rivers in millions,* $\sum W_r$ *wetted surface in* km, $\sum N_o$ *number of eel in additional waterbodies in millions,* $\sum W_o$ *surface of additional waterbodies* km, $\sum N$ *total number of eel in millions.*

country	$\bar{d}$	$\sum N_r$	$\sum W_r$	$\sum N_o$	$\sum W_o$	$\sum N$
FR	0.017	17.5	1 122.2	125.3	6 009.7	142.9
PT	0.047	22.1	222.9	78.1	1 124.7	100.2
SP	0.007	8.2	727.4	170.9	2 646.5	179.1
All	0.015	47.8	2 072.5	374.3	9 780.9	422.1

The number of silver eel (in million) per country is $\sum Ns$ 8.1 (FR), 6.7 (PT), 12.9 (SP), see Table 3.6).

Table 3.6: Silver eel number and wetted area per country in 2015, $\sum Ns_r$ (million) number of silver eel produced on the river network, $\sum Ns_o$ (million) number of silver eel produced on additional waterbodies, $\sum Ns$ (million) number of silver, $\sum Ns_{♂}$ (million) number of silver males, $\sum Ns_{♀}$ (million) number of silver females, $\sum Bs_{♂}$ (tonnes) biomass of silver males, $\sum Bs_{♀}$ (tonnes) biomass of silver females, $\sum Bs$ (tonnes) biomass of silver eel.

country	$\sum Ns_r$	$\sum Ns_o$	$\sum Ns$	$\sum Ns_{♂}$	$\sum Ns_{♀}$	$\sum Bs_{♂}$	$\sum Bs_{♀}$	$\sum Bs$
FR	0.85	7.28	8.13	6.59	1.54	587.37	934.99	1 522.36
PT	1.70	4.96	6.65	6.48	0.17	405.80	59.98	465.78
SP	0.76	12.15	12.92	12.06	0.85	856.91	372.63	1 229.54
All	3.31	24.39	27.70	25.13	2.57	1 850.08	1 367.60	3 217.68

3.12 Habitat loss for eel

Dry rivers (or non–existing rivers in the headwaters) removed from the dataset correspond to 0 (FR), 81% (PT), 60% (SP) of the number of river segments, 0 (FR), 56% (PT), 51% (SP) of the water surface of rivers and 0 (FR), 24% (PT), 42% (SP) of the water surface of other waterbodies (Table 3.7). In terms of silver eel production, the numbers that would have been produced in dry rivers is 35% of the total production (dry + wet) for both Portugal and Spain rivers and 5 and 13% for additional waterbodies silver eel production in Portugal and Spain respectively. When combining both productions (rivers and additional waterbodies) the loss in number of silver eels is estimated as 15% for both countries.

Table 3.7: Number of river segments N_r where an eel production is predicted (flowing rivers) or where the eel production is set to zero (temporal rivers) N_dry for the different countries. Water surface of rivers W_r and additional waterbodies W_o in km, *corresponding to flowing and temporal (dry) rivers. The associated waterbody eel production is set to zero if the corresponding river is dry.*

	FR	PT	SP
N_r	114384	14487	79637
$N_{r\ dry}$	0	60346	243857
W_r	1122	223	727
$W_{r\ dry}$	0	286	771
W_o	6009	1124	2646
$W_{o\ dry}$	0	361	1888

The model is run by setting the height of dams to zero to assess the effect of dam loss. The percentage of eels that would be gained by removing barriers (according to the model) $(Npristine - N)/N$ in 2015 ranges from 4% to 12% in the coastal EMUs. It is very important (100%) for inner Spain where eel has disappeared now in non–coastal EMUs, but the production in term of silver eels is quite low, so even with a large percentage, this would correspond to a small number of eels. The lowest habitat loss is found in Portugal (3.5%). By comparison, the habitat loss in France is much more important, and ranges from 9% in the Garonne, 11% in the Loire to 36% in Artois (*CHANN* SUDOE area). The lower habitat loss in the Loire (11%) is expected as the

Loire remains one of the few long Atlantic rivers where the low number of obstacles still allows a very long free migration to the upper course. A similar low value is found in the Rhône (11%) and linked with the accessibility of the Mediterranean lagoons. The Garonne would even have been much lower had the Gironde been taken into account (currently part of the Gironde is not accounted for in the basins derived from RHT database) (Figure 3.29).

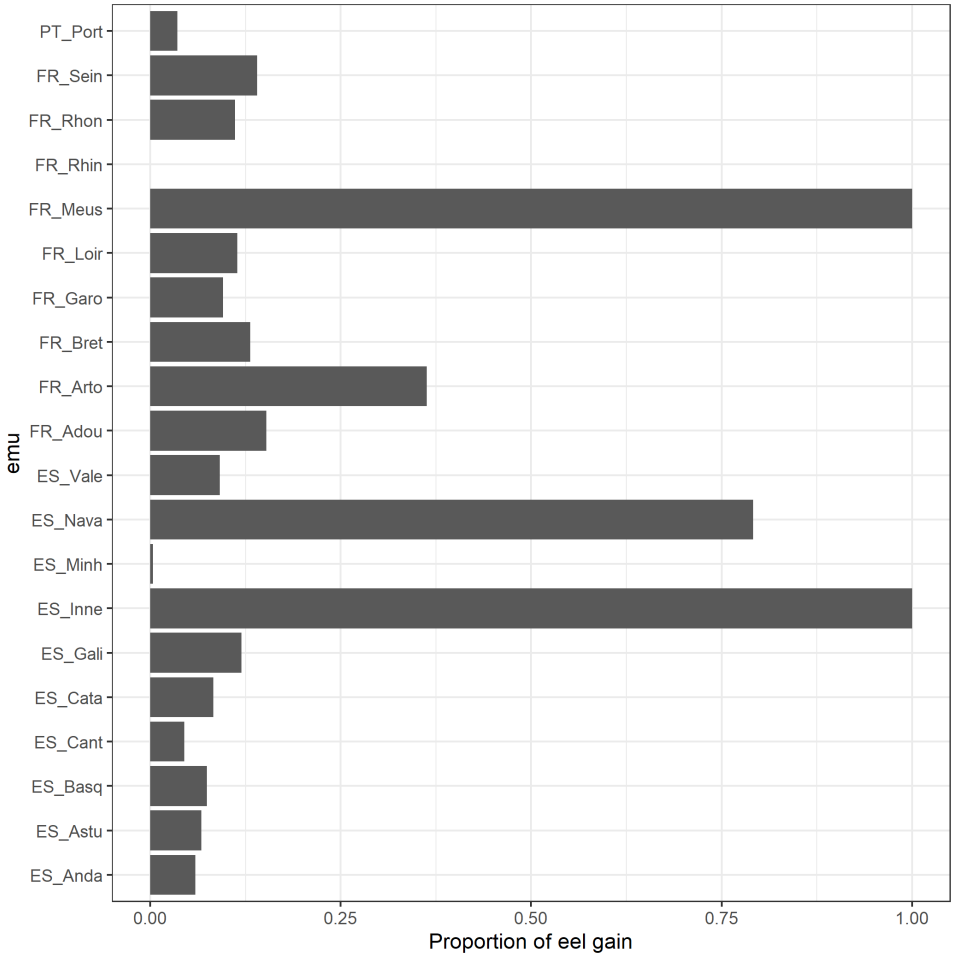

Figure 3.29: Habitat loss. Measure of the effect of dams in the model, the proportion of eel that would be gained by setting all dam heights to zero.

4 Discussion

4.1 River network

GIS models have the ability to rapidly and quantitatively assess geographical variables over varying temporal and spatial scales (Meixler et al., 2009). Model built from consistent geographical source including linked reaches, together with detailed information on climate, geology, land use, mean flows and gradients can be used to assess large-scale management scenarios for eel, e.g. the spawning escapement of large female longfin eels *Anguilla dieffenbachii* in New Zeeland (Graynoth et al., 2008). However, when working at the international level, as was the case for the SUDOANG project, the compilation of different types of GIS data remains a challenge as it is built from nationally distinct data sources, with different levels of details and attributes. Hence, the most time–consuming task in the implementation of the EDA model is the constitution of a consistent three-country dataset including the whole river network and its adjoining surfaces and the predictors of the EDA model. When predicting the number of eels from density model, a correct assessment of the available habitat is paramount to the assessment. The measure of correct water surface is the main driver of errors when comparing predictions of EDA and known silver eel productions. Examples in France and Ireland have shown that the use of the CCM (Jouanin et al., 2012a; Vogt et al., 2003; de Eyto et al., 2016) or the failure to include lakes (Briand et al., 2018) has led to a large underestimation of eel production.

Depending on the country, the information on water surface was either very detailed [1] (BD TOPAGE), or had to be calculated from models built from scratch with both river width models, and the projection on the river network of the rasters for the MERIT Hydro database (Yamazaki et al., 2019). The collection of information about lakes, reservoirs, ponds, lagoons and their chaining with the river network is a major achievement and allows to build spatially consistent predictions of the number of silver eels.

[1] Though not always accurate when dealing with GIS descriptors such as waterbody type or salinity.

4.2 Dry rivers

Within riverine geographical attributes used in the model, one of the most difficult to collect was the temporal / permanent status of rivers. In the Iberian Peninsula, this information was however crucial to determine whether a river was, or not, a habitat for eel. A geographical expert judgement based on exiting data on the temporal status of rivers, geographical attributes such as water temperature and precipitation, the presence of large reservoir upstream, discharge collected from the different source (Morel et al., 2019; Linke et al., 2019), further validated by local expertise (University of Cordoba) and satellite imagery have been used. The Spanish river network used as a basis for building the EDA river network is clearly a network of theoretical streams calculated from elevation data. Most first or second order streams are simply just thalwegs and do not correspond to any physical stream structure. In addition, most streams that do exist have no water. Our rationale in building the dataset has been that any stream located upstream from a dry section would be no habitat for eel, eels might be able to cross a dry section when the stream is flowing in rainy conditions, but the chance that it would be stuck and die in a dry section of the stream is probably very high. So as a first assessment of eel habitat, the model is probably the best large–scale expertise available, especially since migration barriers have been included in much detail in the assessment. However, when looking at detailed data at local scale it is probably wrong and should be further ameliorated especially in Portugal. The amount of eel habitat set as temporal (thus non eel habitat) was expertised as 60% of the total habitat in Portugal and 75% in Spain. When running a new version of the model without habitat, the magnitude in the decline of the number of eels predicted was only about 30% in Portugal and 16% in Spain.

The current Spanish hydrographic network represents more the thalwegs at the head of the basin than the watercourses and many of the waterways described by the model do not exist. We have therefore strived to correct this problem of absent watercourses, but this correction will not replace reliable data and so the numbers and biomass produced by the model may be biased, particularly in the upstream part of the rivers. In the Mediterranean area, local expertise has been conducted to improve the quality of temporary stream data. Improvements of the Spanish river model including a clear prediction of the temporal status of the river would help to improve the model. In Portugal, the information on the temporal status of the river was simply missing, so again, obtaining data would help to improve the model.

4.3 Electrofishing

The collection of electrofishing data used to calibrate the model also plays a very important role in the quality of the final product. All Spanish and Portuguese data have been integrated in a single database.

All electrofishing data have been integrated in the database developed during the POSE project. They are included on top of existing data from Ireland, Belgium or France and this demonstrates the functionality and suitability of this database to store information about eel. The integration of data from dozens of different formats into a single SQL database cannot however be automatised and will always require extended SQL squills and drills. The effort however resulted in a very large dataset of 15 500

electrofishing stations and nearly 50 000 electrofishing stations.

In France, the database developed by the French Biodiversity Office (OFB) and the ministry was not updated or available at the time of the implementation of the model so the data was not updated after 2015 except for data coming from eel specific surveys. This has created some problem in the inclusion of temporal trends for shared rivers between France and Spain. In Portugal the restriction to a dataset containing only eel has hampered the ability of the model to provide consistent results in the whole peninsula and some trends obtained for the Gamma model along the Atlantic coast of Portugal are probably overfitted and resulting from a lesser number of electrofishing collected. These problems will very probably be corrected in future implementation of the EDA model as more data could be collected.

As was the case for river network, the methodology used in electrofishing was country specific, and if standard electrofishing operations have been common in all three countries, some of the electrofishing method (single pass point sampling eel electrofishing, deep habitat sampling, ...) have remained localized in one country.

4.4 Obstacles

Building from many different sources in Spain and Portugal and from a centralized database in France, leads to different levels of details. This project has been built along with the AMBER project and both projects have provided the first comprehensive assessment of obstacles for fishes in the Iberian Peninsula. The added value of the SUDOANG project is chaining dams along the river course and allowing a calculation of cumulated impact across countries (From Portugal to Spain) and using a common database between the three countries to build up the metrics of impacts. The project has also collated specific data on hydropower dams that have been used to build up other models, like integrated mortality assessments at the catchment scale.

4.5 Structure of the model

The model calibration describing eel density, size structure and potential escapement was proven successful at the scale of three southern European countries as the fit of the model was better with a larger Kappa and larger percentage of deviance explained that in one country alone. The dataset used to predict the silver eel escapement comprised about 513 000 river segments with 26 spatial attributes. The Δ, Γ, $\mu\tau$ and silver models have been fitted on dataset of 46653, 20597, 494163 and 20101 lines. The drawback from this large-scale assessment is that it fails to capture small-scale variations such as difference in productivity of different Mediterranean lagoons. Estimations produced by EDA are fitted on electrofishing data collected in freshwater.

The model acts as a two-stages process. The most important part is the Δ because there are lots of zeros in the dataset. The use of Δ and Γ models (Stefánsson, 1996) allows to deal with situations where there are a lot of zero values and a log-normal distribution of positive values. The predicted number of eels is based on all variables used in either Δ or Γ model. This imbrication of both Δ and Γ models make it difficult to interpret the trend of density for a predicted variable as response are different for both models.

The Kappa of Δ model (K = 0.745) is larger than the previous models that were calibrated in France or in French and Spanish regions (EDA2.0 K = 0.56 - 0.67 Walker et al., 2011, Annex A2, EDA2.1 K = 0.71 Jouanin et al., 2012, EDA2.2 K = 0.58 Briand et al., 2018), which indicates that despite having a more heterogeneous source of data, and a much wider dataset and geographical range, the model provides a better prediction. When compared to other set of predictions in Sweden, a similar model (on a more reduced geographical range) explained variation in occurrence to 81.5% for small eel and 76.2% for large eel, while the EDA model only accounts for 59.8% of the deviance.

4.6 Overview of the main model predictors

The importance of different variables in the model is summarized in Table 4.6.

Table 4.1: Variables used by the models, Delta Δ, Gamma Γ, size P and silver eel model $\Pi_{\tau,\varsigma,i}$. +++ is the most important variable in the model, + + + >10% of total chi square, < 10 % of total chi square, - tested and not included in the model, ∅ cannot be part of the model structure, either for structural reasons (e.g. density is the result by ΔΓ) or missing in dataset. ♭ For the multinomial model, a categorical variable (sudoe zone) is used instead of distance to Gibraltar to describe spatial variation along the coastline.

	Δ	Γ	P	$\Pi_{\tau,\varsigma,i}$
distance sea	++	++++	++	+
dams	++	+	-	-
distance to Gibraltar	++	+	++♭	+++
year	+	++	++	-
altitude	++++	++	-	-
basin wettness	++	-		
fishing method	+	+++	-	-
hydraulic density	+	+		
station wetted area	+	-	-	-
river width	-	-	+	-
-				
month	∅	∅	∅	+
strahler	-	-	+	-
eel density	∅	∅	++++	+
body length	∅	∅	∅	+++

4.6.1 Effect of dams and habitat

Recent studies on the fragmentation of European rivers (Belletti et al., 2020) emphasise the role of small obstacles on river continuity. Dams disrupt the natural distribution of eels in rivers (White and Knights, 1997; Ibbotson et al., 2002; Halvorsen et al., 2020). The data collection performed in this study was relying on the French database ROE, ICE, and BDOE, whose aim is to collect the effect of obstacles. In this dataset, a lot of the very small obstacles in small streams are not reported, however, these would probably not have been projected on the RHT river network which does not cover

headwaters. When trying to correct for the extent of missing data (Belletti et al., 2020) showed that France had a comprehensive assessment of the number of dams. There was an extensive exchange between AMBER and SUDOANG projects but there were differences in both method and source of data used. Belletti et al. (2020) indicate that maybe 80% of obstacles are missing. While this is probably true for Portugal where the inventory of dams is currently on going, it is probably not true in Spain, or would only concern smaller barriers. As very large dams are present, their effect on eel distribution was probably well integrated and it is certainly more than the cumulated effect of missing small barriers. In addition, the problem of rivers drying out is probably much more important for eels than the presence of obstacles in the South of Spain and in Portugal, and as we considered that any temporal stream would bar the migration of eels upstream, large parts of the riverine habitat has effectively been wiped out from our predictions in Southern Spain and Portugal.

The indirect effect of dams on hydrological, geomorphic and ecological processes (Grill et al., 2019) in river networks have partly been assessed by EDA when accounting for habitats where rivers are no longer permanently flowing to the sea.

Clavero and Hermoso (2015), performed a pioneer work on the effect of river fragmentation on eel distribution in the Iberian Peninsula. However, in their modelling they only used major dams, which they considered blocking barriers for eel movement. The results of the delta model are consistent with their prediction of a distribution limited to the lower part of the main river basins.

The effect of dam comes as the second most important variable in the Δ model, it is also used as a tensor interaction in the Γ model, it is still significant but with low contribution. The positive tensor response of the model is probably used to fit high densities in sectors with free access near the sea. The effect of dams was not significant in the size structure Multinomial model nor in the silvering model. So the dam effect comes mostly as a predictor of the repartition of eels but does not describe their density or size structure or silvering. The correlation between distance and the cumulated height of dams was low (0.45) and less than 0.5 from the gamma model. The correlation between altitude and the number of dams is high in the delta model (0.68) but low (0.36) in the delta model. However, the concurvity estimated for altitude and dam height was less than 70 % in the Δ model.

The collection and validation of dam data has proved a huge task that remains incomplete. Comparisons between both sides of the frontier between Spain and Portugal shows that is higher in Spain, as the inventory of dams in Portugal needs to be updated. In fact, the Portuguese administration confirmed that the dam census was incomplete and that a new database would be released soon. However, we tested a variable with different cumulated count per country and it did not significantly improve the model.

The same can be said when testing spatialised response between different areas. Those led to local responses with increasing number of eels when dam height increased for the western part of the Iberian Peninsula, probably as a consequence of local overfitting occurring when too many missing data are present. A similar problem was encountered by Graynoth et al. (2008), in a model for longfin eel in New Zealand, could not use distance nor altitude because these caused problems in deviance residuals.

The French dataset was the most complete. For this reason, tests on the response of the model on dam were first made in France in an initial model calibration. The best model is obtained when calculating the cumulated height of dams including prediction for missing values. Power transformed values of dam height summed from the

downstream reaches were less performing than the simple sum of height. The idea would be that two 0.5 m dam might have a lower effect than a single 1 m structure. Our results didn't find any better performance for power transformed models. This is different from the previous calibration of the model in France for which a power 1.5 was used to transform dam heights (Briand et al., 2018). The selection of a larger power transformation would indicate that the effect of higher dams is more important than lower dams. Here our results show that the model selected the sum of height as the best descriptor of the dam effect, while larger power transformation, by 1.2 and 1.5 were less performing. The dataset in France was much more complete and included the effect of fish passes and a limited dataset on dams accessibility. Using those did not provide a clear improvement of the model probably because the assessment of dam passability did not cover enough dams. Also, the calibration of the previous version of the model used specific response per size class (Briand et al., 2018). The spatial distribution of the smallest size class, 150 mm, 150-300 mm is much more sensitive to the effect of dams, even if small eels might naturally be good climbers (Feunteun et al., 2000; Halvorsen et al., 2020; Legault, 1988). They are probably still retarded in their riverine penetration (Lasne and Laffaille, 2007; Kume et al., 2020) and are in an active phase of dispersal (Imbert et al., 2010) than larger eels, which have more time to achieve their inland penetration (Lasne and Laffaille, 2007) and might find ways to overcome apparently impassable dams during drought or flood events. It is possible that a model restricted to those size class only would have given a different response. In a study testing the effect of cumulated dam height on Japanese eel distribution Itakura et al. (2020) addressed the same question. They tested alternated models where the dams for which height was lower than 30 cm were removed from the cumulated counts. They found that all dams, even low height trans–river structure, were affecting the eel density. In an overall study of the distribution of fish in Japan, Han et al. (2008) didn't find any effect of dams on eel distribution, but the metric tested was the presence of dams upstream. The obstacle type (bridge, culvert, dam) has an incidence on the obstacle passability. Another way of testing the dam effect is to count the number of structures per type downstream from the sampling area (Halvorsen et al., 2020; Tamario et al., 2019). These models used a count of the number of dams per dams type downstream as predictor and not the obstacle height. In our case, there was large regional bias in the choice of dam type (dam, weir, culvert, other type...), and this means that there was not a simple way to test the dam type within the model. Whatever the type of obstacle, obstacle height is probably one of the best explanatory factors explaining dam passability (Baudoin et al., 2015), and this is what we confirm here with a model using more than 100000 dams, where height was a better fit than a simple count of the number of structures.

It was not possible to collect the timing of dam or fishway construction. When assessing the effect of dams this information can be important (Halvorsen et al., 2020; Tamario et al., 2019).

The construction of dams has caused a very large decline in the habitat available worldwide (Drouineau et al., 2015) and especially in the Iberian Peninsula where Clavero and Hermoso (2015) estimated that more than 80% of the habitat was lost to eels. The decline in male eel production has been proposed as a candidate scenario allowing to explain the decline in eel recruitment Kettle et al. (2011). Assessing the habitat loss on eel stocks is a complex task (ICES, 2020). Our assessment covers partial and total inaccessibility due to dam construction but not the change in water quality,

nor the effect of loss of permanent status for rivers due to water abstraction, pumping and drying out of rivers. In short it only considers the effect of loss of accessibility of rivers caused by dams.

In our models, the dam effect is not the most important when trying to explain eel distribution. Clearly, distance to the sea and altitude are also used to predict the inland eel distribution. Dam construction has not affected the estuaries which remain the major habitat for both future males and females. While the habitat lost to dams is huge, its effect on silver number is low (4 to 12% reduction of current production in coastal habitats.) Higher eel abundances in France and Portugal compared to Spain are interpreted as the consequence of the lower altitude of the rivers, compared to Spain, where altitudes below 150 m are limited to the coastal part. The model predicts a rapid decline of eel densities with altitude. Predictions of the current repartition without dams show that eels could have been present in the whole range of the riverine area, as has been further confirmed by historical studies (Clavero and Hermoso, 2015). In a similar modelling assessment, Graynoth et al. (2008) estimated that the loss of longfin eels was equivalent to about 36% of the original tonnage (habitat) of longfin eels in other waters in New Zealand. However, in this model, distance to the sea or altitude were not used.

Our findings contradict the assumptions of Kettle et al. (2011). The author hypothesized that habitat loss in Southern Europe could have caused a dramatic decline of the available habitat around the time of the first drop in recruitment and been one of the drivers of stock collapse. Most habitat currently used by the eel stock in Spain and Portugal is located below large barriers, and that while the currently available percentage of water surface, and especially reservoir is really small, this coastal confinement of eel population has retained a large part of the available eel stock. It should however not be stated that dams have no effect.

The effect of dams is also indirect as obstruction will increase densities below obstacles, increase competition, predation, it might affect sex ratio and act as a selecting process against individual more prone to migrate (Drouineau et al., 2015). The extent of this effect is less important than the loss of habitat to dry streams. The loss of riverine habitat due to drought affects also the lower part of rivers. According to our results, 40% of the surface of habitat is lost to temporal streams or inaccessible habitats due to temporal streams in the Iberian Peninsula. This translates to a loss of about 35% of silver eel produced. This result includes the overestimation of the number of streams due to the GIS system at least in Spain (some of the rivers in the GIS are not rivers in the headwaters). In France, the temporal status of rivers was not considered but this is more the consequence of a lack of data, that the field truth especially in the Mediterranean area. However, as the GIS network was less detailed than in Spain and Portugal, the error linked with overestimating the eel production in dry rivers would also have been less than in Spain. It is also not clear what historical trend there is in the temporal status of rivers, and more data should be collated to assess this effect and the effect of climate change in the future.

Another point that must be stressed out is that, although cumulated height is the factor that best explains the dam effect on eel distribution, its effect is low compared to other variables. Indeed, a cumulated height of 100 m is similar to an inland migration of 200 km. Probably this might be an effect of dam transparency improved by fishway equipment. Information on dam equipment was probably not accurate enough, especially in Spain and Portugal, and in France the absence of timing of construction

might have prevented its accounting in the model. Rivers with canal and navigation locks might also be partially transparent (Verdon and Desrochers, 2002).

Only a careful screening of the dataset and removal of eel transport sites prevented the model from going wrong. All eel presence above 250 m of cumulated height of dams were considered as transport area, and the surrounding basin was identified as transport sector. Some eels below 250 m might still have been transported and not identified as such.

Close examination of modelled and observed dataset do confirm the good fit of eel densities and both distances upstream and the number of dams. Smaller structures in France are clearly easier to cross than the huge dams in Spain and the model which fitted the same type of response for France, Spain and Portugal has probably given a good account of inland distribution of eels. The large response of *RhinMeu* SUDOE area variable is the consequence of transport operation at a very large distance from the sea and with a large number of dams, the model somehow compensates for the distance and dams (Figure 3.8e).

The effect on eel presence of the percentage of wetness in the basin downstream $log(wdds)$ seems to indicate that a larger habitat downstream will decrease the probability of presence upstream in France. This is probably because when a larger habitat is available, the eel will settle there and not have to migrate upstream. This result is different from Tamario et al. (2019) where presence of lakes downstream in the water course was not significant for eel presence. The response in the Iberian Peninsula was quite different from France, as the percentage of wetness downstream increases the probability of presence. This might be related to the stress of summer period. Regions with a lesser percentage of wetted surface are more dry and more subject to more hydric stress. It might be particularly true for small streams that will be more prone to dry out. This difference between France and the Iberian Peninsula might also be due to different data in France, Spain and Portugal with probably more water surface included in France in the BD TOPAGE.

The same interpretation can be done for hydraulic density (the number of streams per surface of water). In France, there is a global decrease in probability of presence where hydraulic density increases. In Spain and Portugal, the response is different, and there is also a low probability of presence where hydraulic density is the lowest and which probably corresponds to dry areas. In places where the density of rivers is the lowest, the eel would tend to disappear, and this is an indication of the stress related to lack of water.

4.6.2 Distance to the sea

Distance to the sea is significant in all models (Δ, Γ, size, and silver). In the Δ model this variable comes fifth with eel presence showing a rapid decline in the first 200 km. It is the best predictor in the Γ model. The model predicts that eel densities will decline rapidly in the first 100 km from the sea and that a levelling of the decline is expected beyond that distance to 500 km (upper limit of distance before truncation). It has been observed in other studies that eel densities or occurrence decrease with the distance to the sea for European eel (Ibbotson et al., 2002; Aprahamian et al., 2007; De Eyto et al., 2015; Imbert et al., 2008; Feunteun et al., 2003; Degerman et al., 2019; Halvorsen et al., 2020; Briand et al., 2018), American eel (Smogor et al., 1995; Velez-Espino and Koops, 2010) and Japanese eel (Kume et al., 2020; Kazuki Yokouchi, 2014)

but see (Matsushige et al., 2020) where the effect of distance to the sea is not significant [2]. This effect is the largest for the smallest size class < 300mm (Tamario et al., 2019; Imbert, 2008), and the proportion of female and large sized eel increase with distance to the sea (Velez-Espino and Koops, 2010; Tamario et al., 2019; Haro and Krueger, 1991). The progressive intrusion of eels of increasing size into water basins leaves only the largest eels in the upper reaches (Lasne and Laffaille, 2007; Naismith and Knights, 1993).

The Multinomial model confirms these observations since it predicts that the proportion of eels < 150 mm will decrease sharply with distance to the sea, and the proportion of 150-300 mm will start decreasing beyond 300 km from the sea. The proportion of eel classes 300-450 450-00 600-750 and >750 mm increase with distance to the sea. When combined with the $\Delta\Gamma$ model, these results are in adequation with (Briand et al., 2018) (EDA2.2), who also found that the decrease in abundance with distance to the sea was less sharp in large eel size classes.

4.6.3 Year effect

The annual trend has only a medium importance in Δ model and Γ model and eel presence and density show different trends. The variable plays the third role in the Multinomial model, with a clear increase of the 150 mm class over time. The year effect was not included (not significant) in the silver eel model. When comparing with Δ model results of EDA version 2.2.1, the trend for France is very similar and mimics the increase in probability of presence in the 80's early 90's followed by a steady decreasing trend. The decline was already demonstrated in earlier studies (Clavel et al., 2013; Poulet et al., 2011; Briand et al., 2018; Jouanin et al., 2012a). Some of the most recent trends in areas shared between Spain and France are probably biased due to incomplete data in France after 2015.

4.6.4 Altitude

Altitude is the best predictor of eel presence the Δ presence model, with a sharp decrease in the first 400 m, less important after. Although altitude was also selected in the Γ model to explain changes on eel density, it has less importance than when explaining presence. There is a strange and probably spurious increase between 200 and 400 m, which compensates higher densities found in the Seine and Meuse basins for which transport operations cannot be ruled out. Altitude has not been selected to explain size structure difference in the Multinomial size model nor to explain the silvering probability the silvering model. Higher grounds are found in the Alps, Pyrenean mountains and central mountain in France, and they form a large part of central Spain. As those grounds are also blocked by large dams, this might explain that altitude is used as the most explanatory variable in the Δ model. Historically, the species was not infrequent at elevations above 1000 m with a maximum found at 1360 m Clavero and Hermoso (2015).

[2] Though this effect is measured for stations located within a few kilometres from the sea

4.6.5 Distance to Gibraltar - latitude

Distance to Gibraltar was used because it allowed to describe a continuous variation in eel presence and density in different basins along the coastline. The alternative, using only geographical areas such as SUDOE area, gave a lesser fit. This variable is quite important in the Δ model, as it comes third with nearly the same importance as dams, and electrofishing station wetted surface. It is not important (fifth) in the Γ model, the response along the Portuguese coast is probably overfitted, and leads to very large densities predicted in the South of Portugal. The distance to Gibraltar is not retained in the Multinomial model where SUDOE area is used instead, but it is the most important variable in predicting the percentage of silver eel (especially male percentage). The distance to Gibraltar acts by decreasing the proportion of immature in favour of the proportion of males or females in the South of the Iberian Peninsula near Gibraltar. This proportion of immature increases away from Gibraltar both in the Mediterranean and further North along the Atlantic coast of Portugal, Spain and France.

The percentage of silver eel (both male and female) is larger in the coast of the Iberian Peninsula. A relationship between life history traits such as growth rates, size at silvering or the proportion of migrating females also varies with latitude in American eel (Oliveira and McCleave, 2000; ICES, 2010).

4.7 Silver model

The proportion of eels becoming silver varies among countries and within river basins, according to the results of the combined implementation of the Δ, Γ, Multinomial size models and silver eel models. The proportion of eels becoming silver is the highest 12-24% near the sea and is the lowest far from the sea. The number of silver eel tends to decrease with distance upstream (Figures 3.26, 3.27). The proportion of silvering is maximum at densities around 0.2 eel m^{-2}.

In the first versions of EDA, a constant silvering rate of 5% (Jouanin et al., 2012a) and 2.5% (De Eyto et al., 2015) was applied. Size as a continuous variable, and size class used for prediction are clearly the most important variable in the silver model. Collecting silver eel data is difficult. Systematic sampling was done for several years in France and forms the bulk of our data (72% of operations with silver eel) (Beaulaton et al., 2015). In this French protocol, all eels >250 mm were systematically measured even if visibly they were clearly not silver eels. In Spain and Portugal however, the silver eel measurement collected might have different, and any silver eel might have been measured even if it is a rare occurrence. In the absence of systematic sampling of yellow eel, the rare silver eel smaller than 300 mm, will have been systematically measured while yellow eels of more than 250 mm will have very rarely have been measured for silvering indices. This has probably led to increase and overestimate the proportion of very small eel in the samples and in our model.

Table 4.2: Proportion of silvering (%) and sample size (N) per emu

	pre-migrant	silver	yellow	N
ES_Anda	0	12	88	95
ES_Astu	1	20	79	1541
ES_Basq	8	25	67	2573
ES_Cast	60	20	20	5
ES_Cata	2	34	64	133
ES_Nava	5	13	82	506
ES_Vale	6	17	77	618
FR_Adou	4	8	87	676
FR_Arto	7	7	86	1186
FR_Bre	5	8	88	1489
FR_Gar	8	4	88	2601
FR_Loi	17	6	77	2182
FR_Meu	0	0	100	5
FR_Rhi	46	10	44	48
FR_Rho	6	7	86	3273
FR_Sei	9	4	87	3136
PT_Port	9	82	9	34

4.8 Post calibration of the model

EDA is built to predict densities in rivers in places where electrofishing can take place. The inclusion of other type of fishing can to a certain extent, allow to expand the model further downstream to try to predict densities. The initial version of the model (EDA2.3 before post calibration) overestimated the production for most inland basins, especially for those have a large amount of water surface corresponding to reservoirs. Waterbodies surface have been added to the river segment within each unit basin, without knowing if the reservoir was indeed in connexion with the stream. As such, a large part of waterbodies is probably not part of the surface. In addition, streams in the downstream part of the rivers might have less carrying capacity that small head streams where electrofishing take place. While those might still possess the largest part of the eel stock, the actual density in large deep stream is probably lower. On the other hand, coastal marshes and lagoons might have high productivity and the productiviy of lagoons was underestimated for the Bages Sigean lagoon in the first version of the model. The calculation of water surface differs between layers collected from the habitat directive (where the area covered at the highest tide is considered) and other source of data such as the RHT in France. While the inclusion (merging) of missing part of estuaries in France has been envisioned, it was not completed during the project, and it is felt that further work is necessary concerning the habitat surface of estuaries in Spain, Portugal and France, and on the productivity of lagoons and estuaries.

5.1 Eel weight tables

Table 5.1: Weight by size class after selection, min, median, max, and Ws specific weight issued from quantile (0.5) regression on the middle of the size class, and 80 mm for eels > 100mm.

length_class	n	min	Q50	max	Ws
(40,100]	4733	0.1	1.0	10.0	0.7
(100,150]	15536	0.3	3.0	36.2	1.4
(150,200]	22872	0.7	8.1	81.9	5.0
(200,250]	21013	2.0	18.0	150.0	12.5
(250,300]	19817	4.6	34.0	233.0	25.4
(300,350]	18921	6.9	59.6	408.0	45.3
(350,400]	8515	12.7	89.8	467.0	74.0
(400,450]	4256	20.2	131.5	582.0	113.0
(450,500]	3303	30.4	188.0	886.0	164.3
(500,550]	2405	42.3	260.0	773.0	229.5
(550,600]	1619	50.2	345.0	925.0	310.7
(600,650]	1053	76.0	454.8	900.0	409.5
(650,700]	636	211.0	579.0	1280.0	528.0
(700,750]	403	163.3	730.0	1389.0	668.1
(750,800]	200	300.3	893.5	1520.0	831.8
(800,850]	100	529.6	1104.5	1882.0	1020.9
(850,900]	57	793.0	1320.0	2000.0	1237.6
(900,950]	19	1266.0	1638.0	2000.0	1483.9
(950,1e+03]	6	1438.0	1739.0	1961.0	1761.9
(1e+03,1.05e+03]	2	1325.0	2074.0	2823.0	2073.5
(1.05e+03,1.1e+03]	1	2828.9	2828.9	2828.9	2421.0

sizecl	country	N	Mean	Min	Q3	Median	Q5	Max
w1	FR	10 250	2.5 (2.5 - 2.6)	1.0	1.0	2.0	3.0	30.0
w1	SPPT	23 488	2.9 (2.9 - 3.0)	0.3	1.3	2.6	4.0	36.2
w2	FR	17 872	19.4 (19.2-19.6)	1.0	10.0	16.0	27.0	215.0
w2	SPPT	63 216	19.6 (19.5-19.7)	0.7	9.0	16.0	27.3	265.7
w3	FR	8 707	84.9 (84.1-85.7)	15.0	58.0	76.0	104.0	667.0
w3	SPPT	24 302	75.7(75.3-76.1)	6.8	55.3	68.0	88.0	575.0
w4	FR	2 860	253.6(250.5-256.7)	40.0	191.0	237.0	304.0	929.0
w4	SPPT	3 852	247.0(244.4-249.6)	26.3	188.0	233.0	297.1	849.5
w5	FR	738	552.4(541.7-563.0)	146.0	447.2	519.5	631.0	1 288.0
w5	SPPT	753	547.1(536.1-558.0)	75.1	446.1	516.9	615.0	1 389.0
w6	FR	69	954.7(901.5-1 007.9)	245.0	827.0	948.0	1 054.0	1 761.0
w6	SPPT	84	1 061.2(998.9-1 123.5)	300.3	880.0	1 036.8	1 220.2	1 954.2

Table 5.2: Weight of yellow eel per size class, w1= <150 mm, w2 = 150-300, w3=300-450, w4=450-600, w5=600-750, w6=>750, per country, FR = France, SPPT=Iberian Peninsula, lower and upper Gaussian confidence limits based on the t-distribution.

country	sexe_durif	N	Mean(Lower-Upper)	Min	Q3	Median	Q5	Max
FR	female	312	702.0(651.2-752.8)	154.0	362.8	503.5	1 000.0	2 823.0
FR	male	518	115.5(110.9-120.2)	17.0	82.0	104.0	132.0	482.0
PT	female	2	361.8(<0-1 877.5)	242.5	302.1	361.8	421.4	481.1
PT	male	26	84.4(72.9-95.8)	47.0	64.6	79.1	98.0	155.5
SP	female	225	503.5(468.2-538.8)	180.2	315.8	442.5	605.2	1 550.0
SP	male	962	98.8(95.7-101.8)	10.6	70.0	86.1	109.2	398.8

Table 5.3: Weight of silver eel per country and per sex, lower and upper Gaussian confidence limits based on the t-distribution.

country	sexe_durif	size	N	Mean (lower-upper)	Min	Q3	Median	Q5	Max
FR	female	4 - [450-600[	110	336.3 (318.5-354.2)	154.0	279.2	331.0	387.5	925.0
FR	female	5 - [600-750[	117	578.1 (548.3-607.9)	286.0	460.0	551.0	672.0	1 010.0
FR	female	6 - >=750	85	1 345.9 (1 275.5-1 416.2)	698.0	1 112.0	1 258.0	1 527.0	2 823.0
FR	male	2 - [150-300[	14	50.7 (32.7-68.8)	27.0	30.2	38.0	49.0	114.0
FR	male	3 - [300-450[	445	104.5 (101.2-107.9)	17.0	81.0	100.0	120.0	340.0
FR	male	4 - [450-600[	59	214.0 (198.1-229.9)	84.0	179.5	206.0	226.5	482.0
PT	female	4 - [450-600[	1	242.5	242.5	242.5	242.5	242.5	242.5
PT	female	5 - [600-750[	1	481.1	481.1	481.1	481.1	481.1	481.1
PT	male	3 - [300-450[	25	81.5 (71.3-91.8)	47.0	63.5	79.0	97.3	155.5
PT	male	4 - [450-600[	1	155.4	155.4	155.4	155.4	155.4	155.4
SP	female	4 - [450-600[	111	317.7 (301.8-333.6)	180.2	250.0	310.1	354.0	638.0
SP	female	5 - [600-750[	96	603.9 (567.3-640.5)	326.0	484.7	569.5	670.5	1 389.0
SP	female	6 - >=750	18	1 113.8 (1 009.1-1 218.5)	667.0	1 022.8	1 115.5	1 218.2	1 550.0
SP	male	2 - [150-300[	41	54.2 (45.8-62.6)	14.3	43.0	48.0	54.0	136.1
SP	male	3 - [300-450[	853	91.3 (89.0-93.5)	10.6	70.3	85.0	103.0	398.8
SP	male	4 - [450-600[	68	219.4 (208.4-230.3)	39.0	198.3	214.2	243.4	340.0

Table 5.4: Weight of silver eel per sex, per country per size class. Lower and upper Gaussian confidence limits based on the t-distribution.

5.2 Plot of observed and predicted values against response variables

The average presence probably is quite consistent at the spatial scale, by construction for SUDOE area, but also for a spatial variable EMU not included in the Δ model (Figure 5.1).

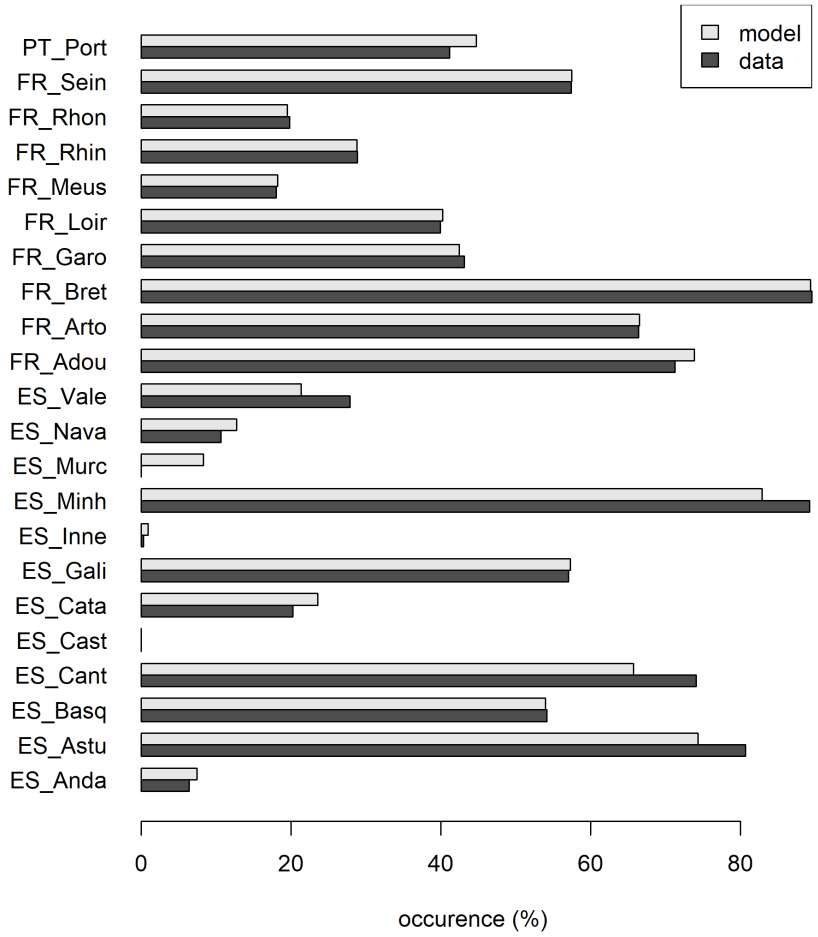

Figure 5.1: Δ model average response and observed values per EMU.

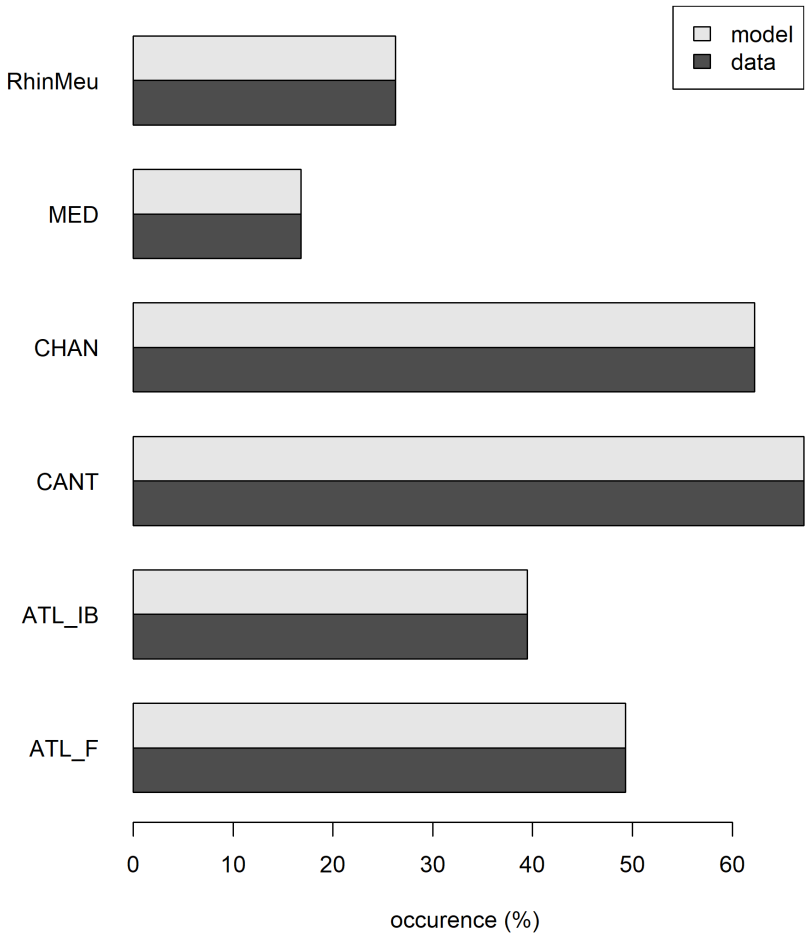

Figure 5.2: Δ model response and observed values per SUDOE area.

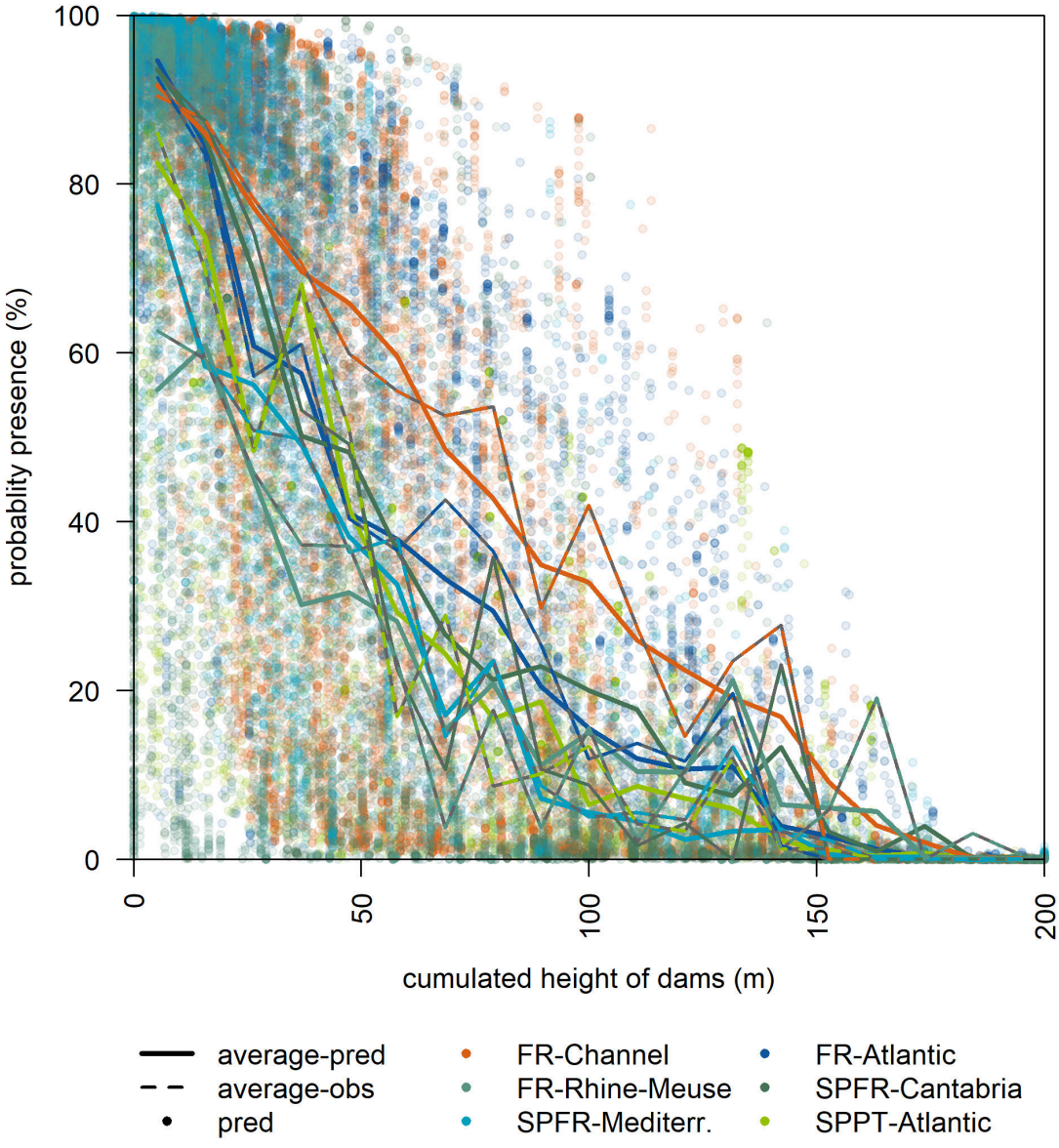

Figure 5.3: Δ model response for cumulated dam height.

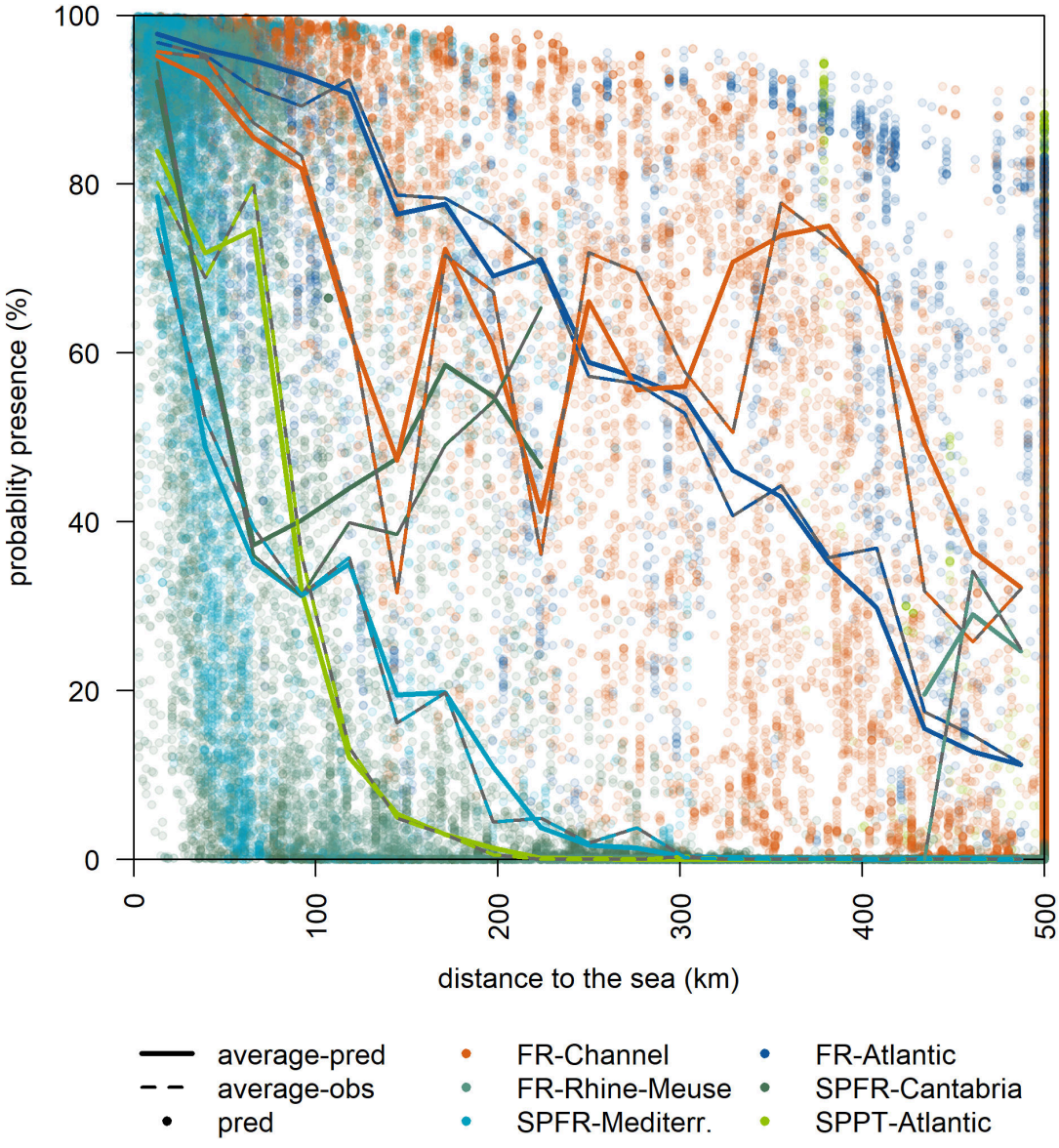

Figure 5.4: Δ model response for distance to the sea.

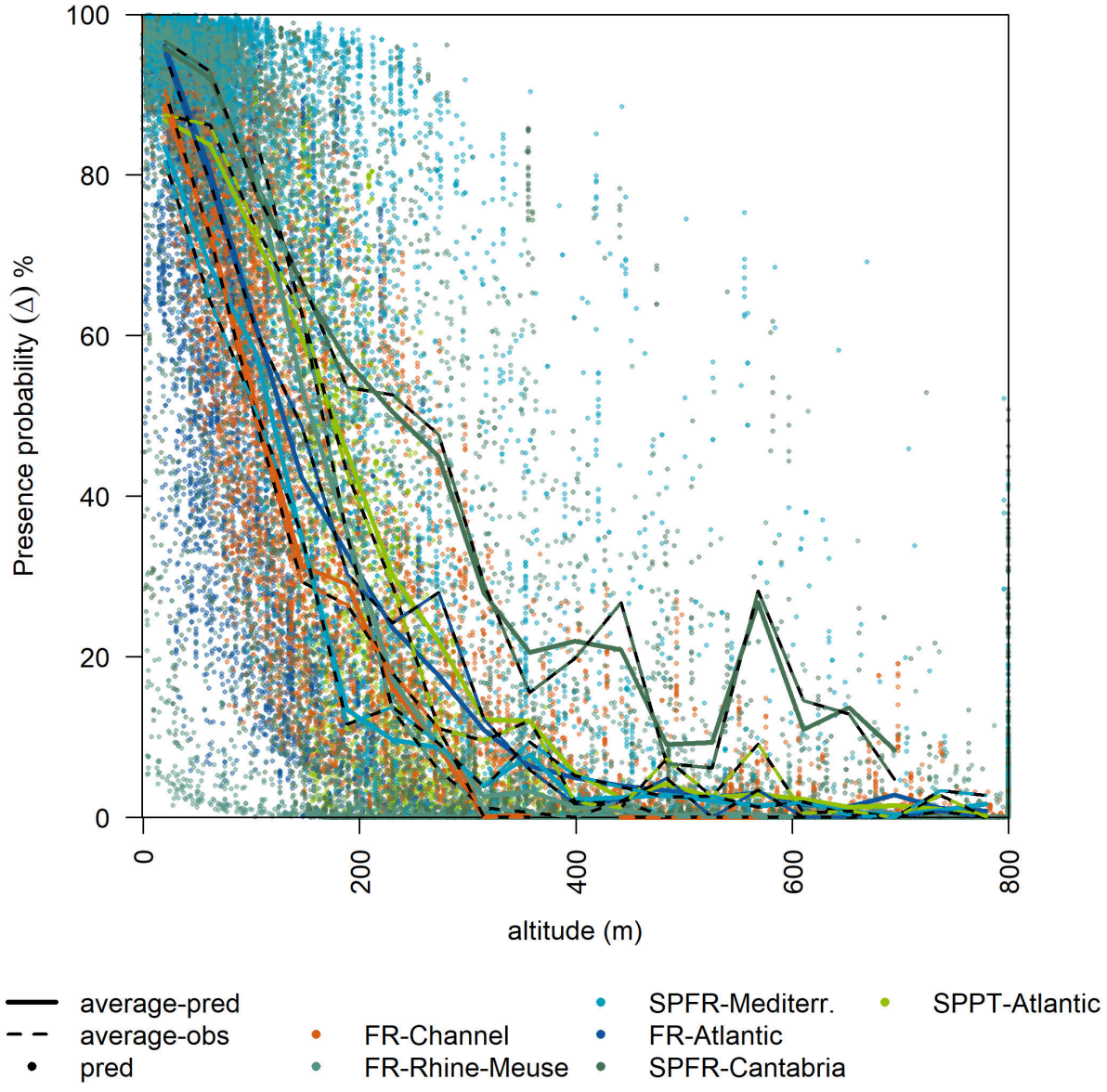

Figure 5.5: Δ model response for altitude.

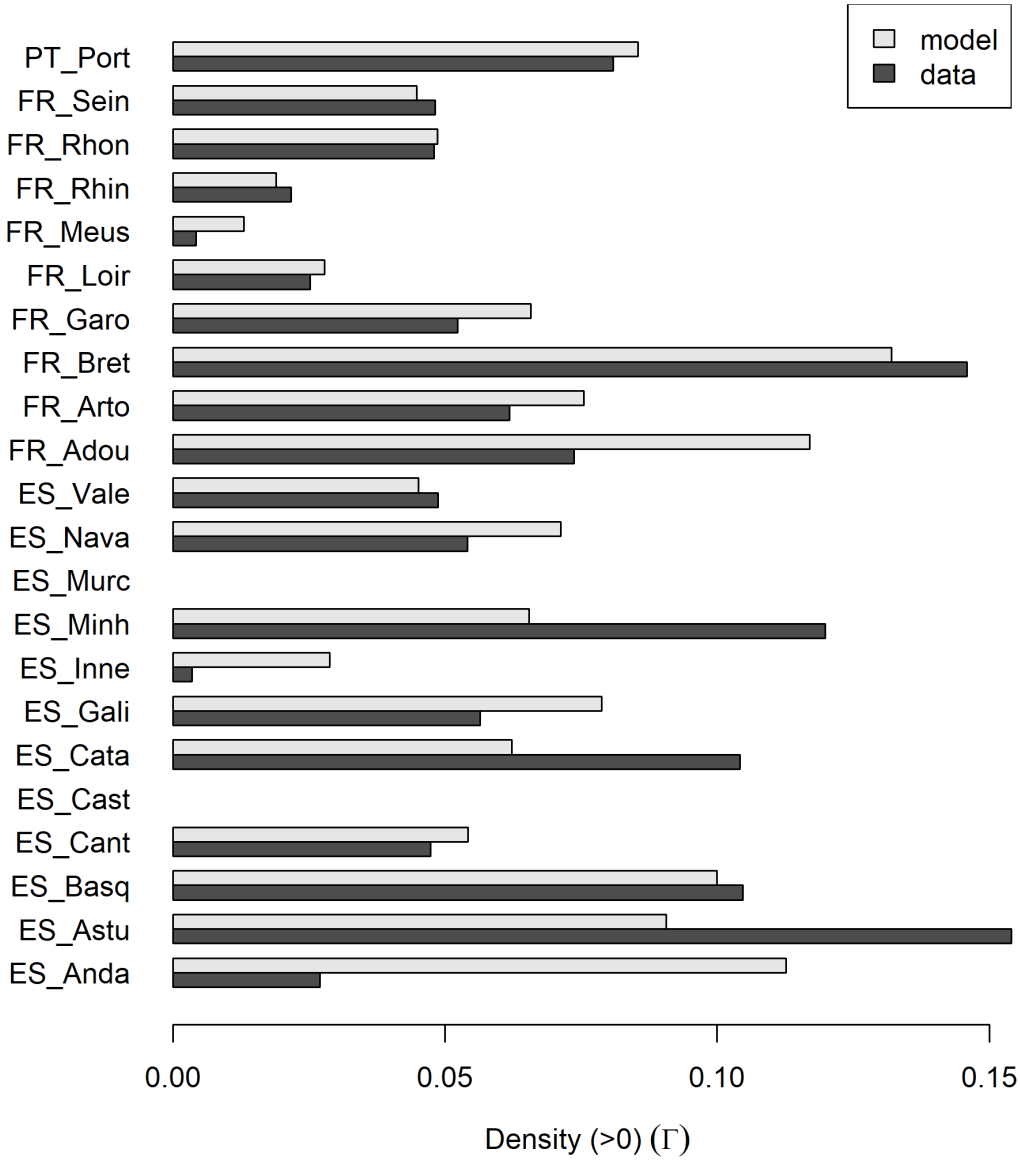

Figure 5.6: Γ model average response and observed values per EMU.

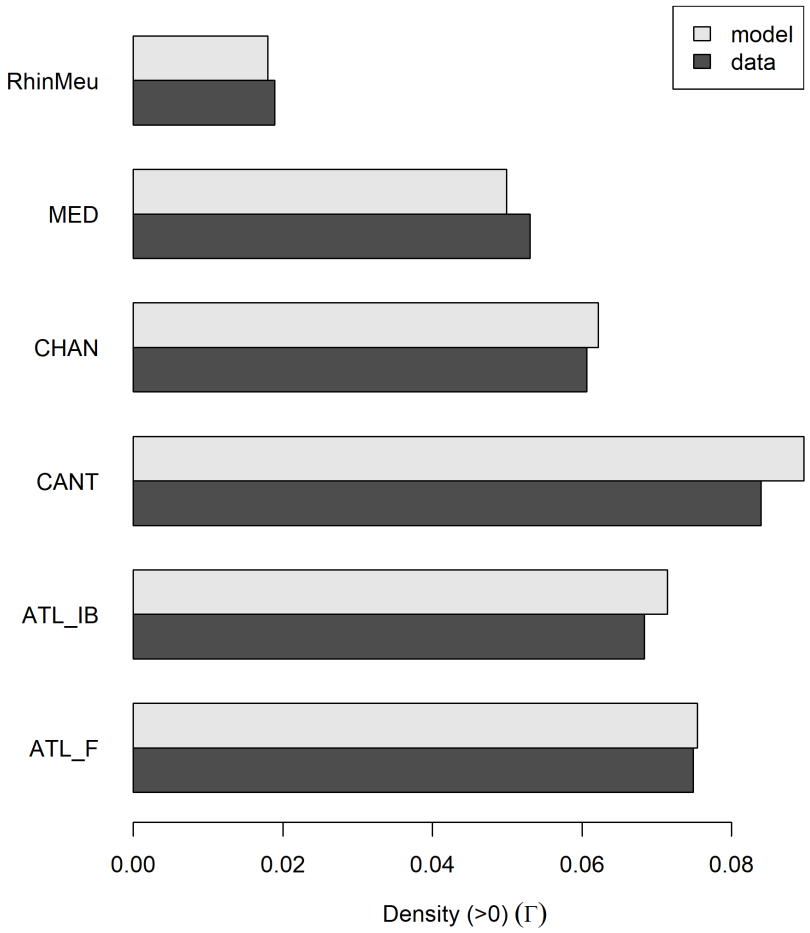

Figure 5.7: Γ model response and observed values per SUDOE area.

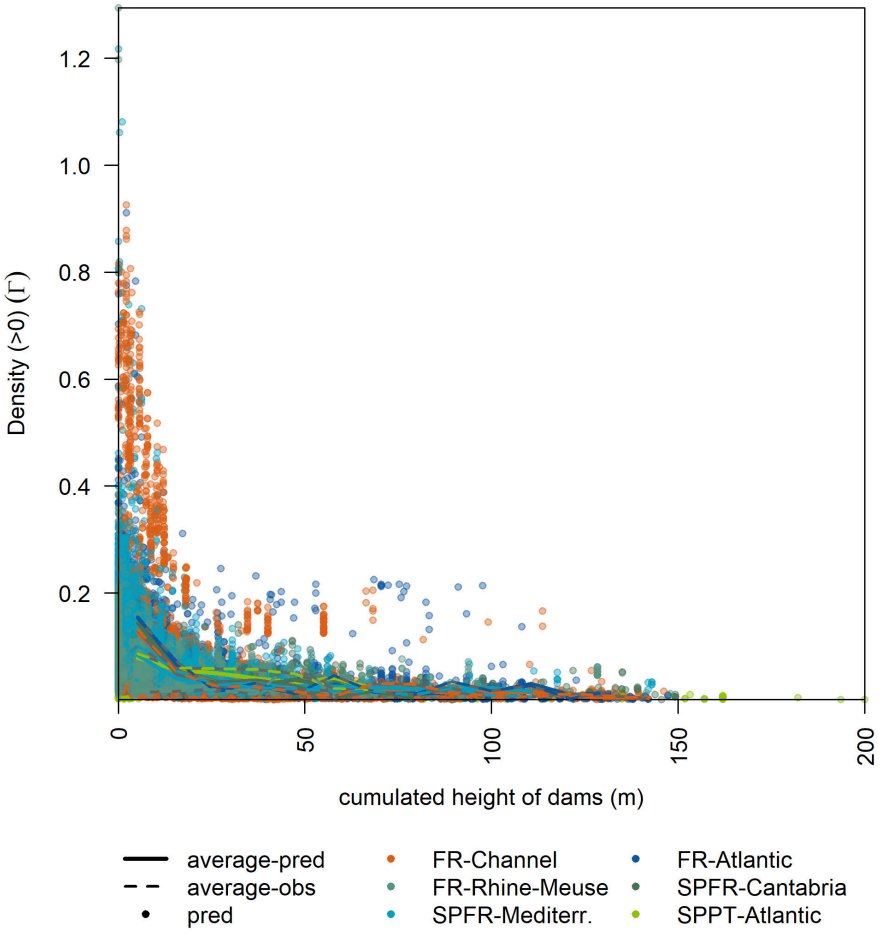

Figure 5.8: Γ model response for cumulated dam height.

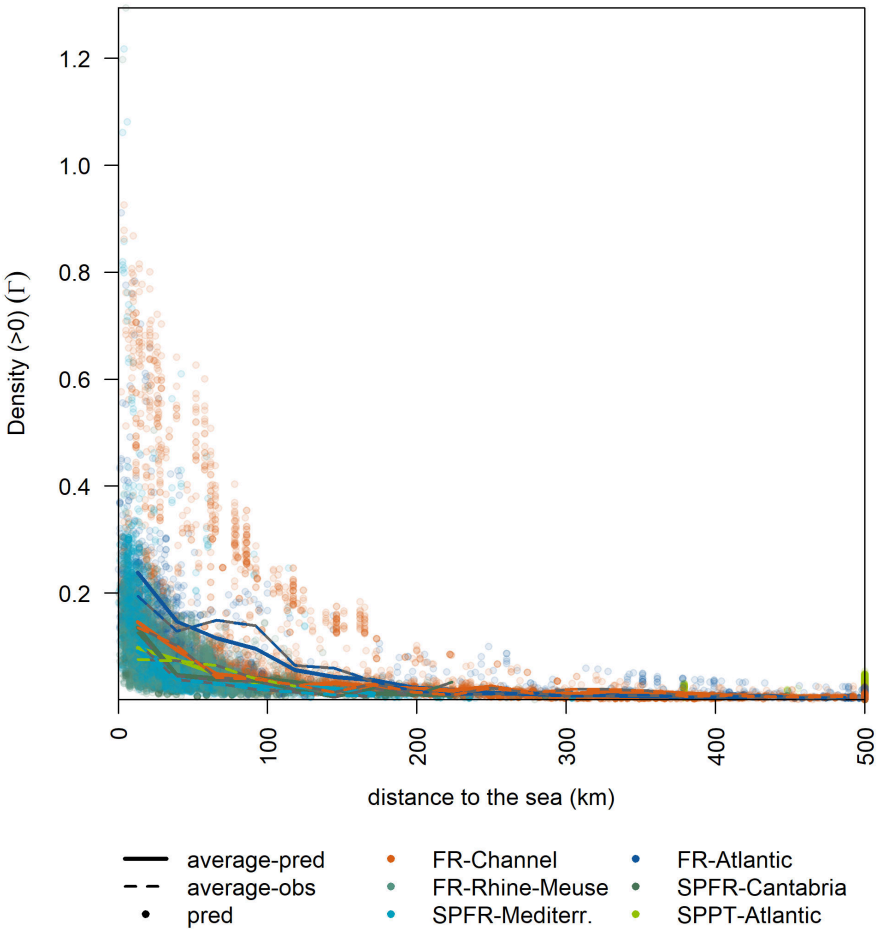

Figure 5.9: Γ model response for distance to the sea.

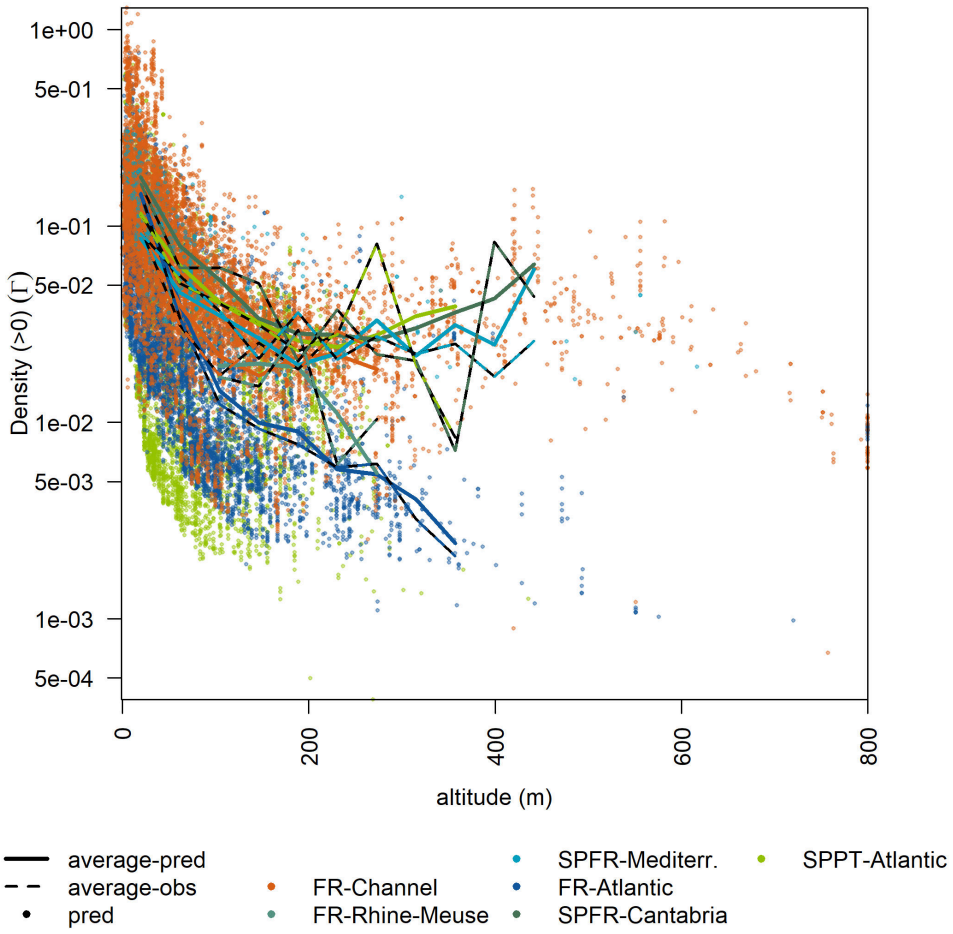

Figure 5.10: Γ model response for altitude.

5.3 Eel density - raw data

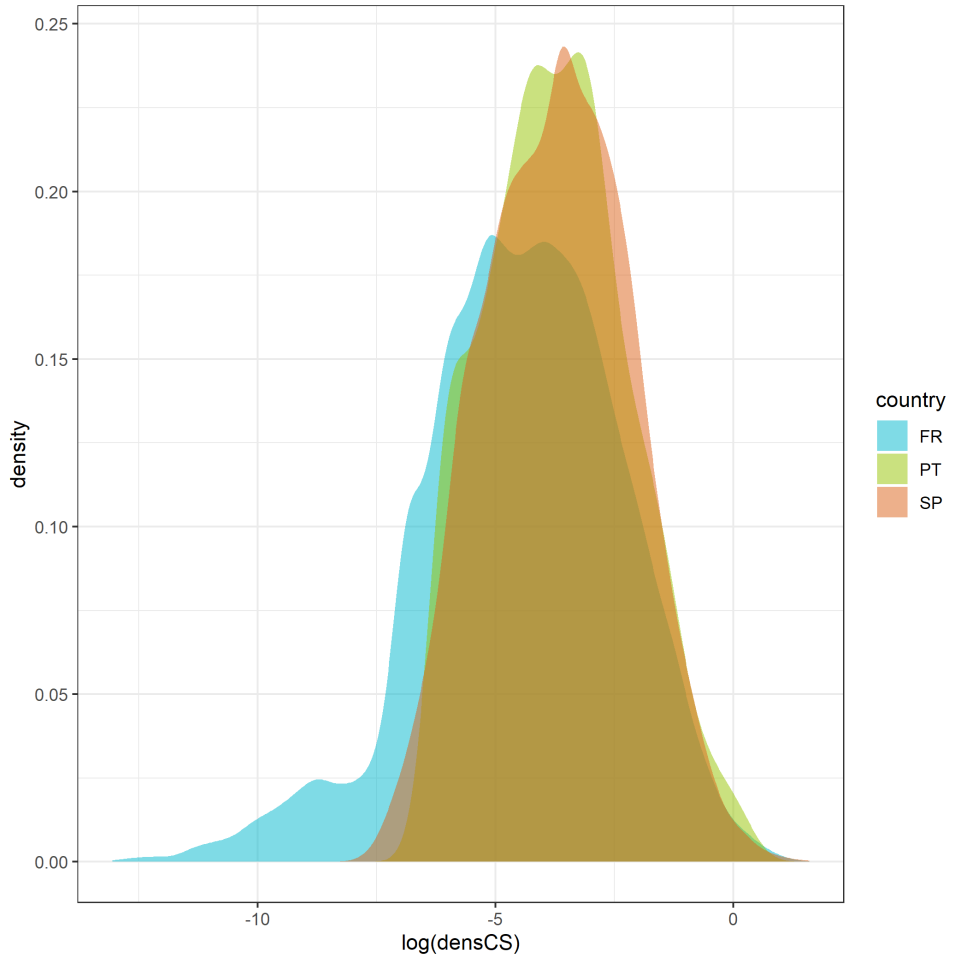

Figure 5.11: Distribution of density per country, log transformed densities

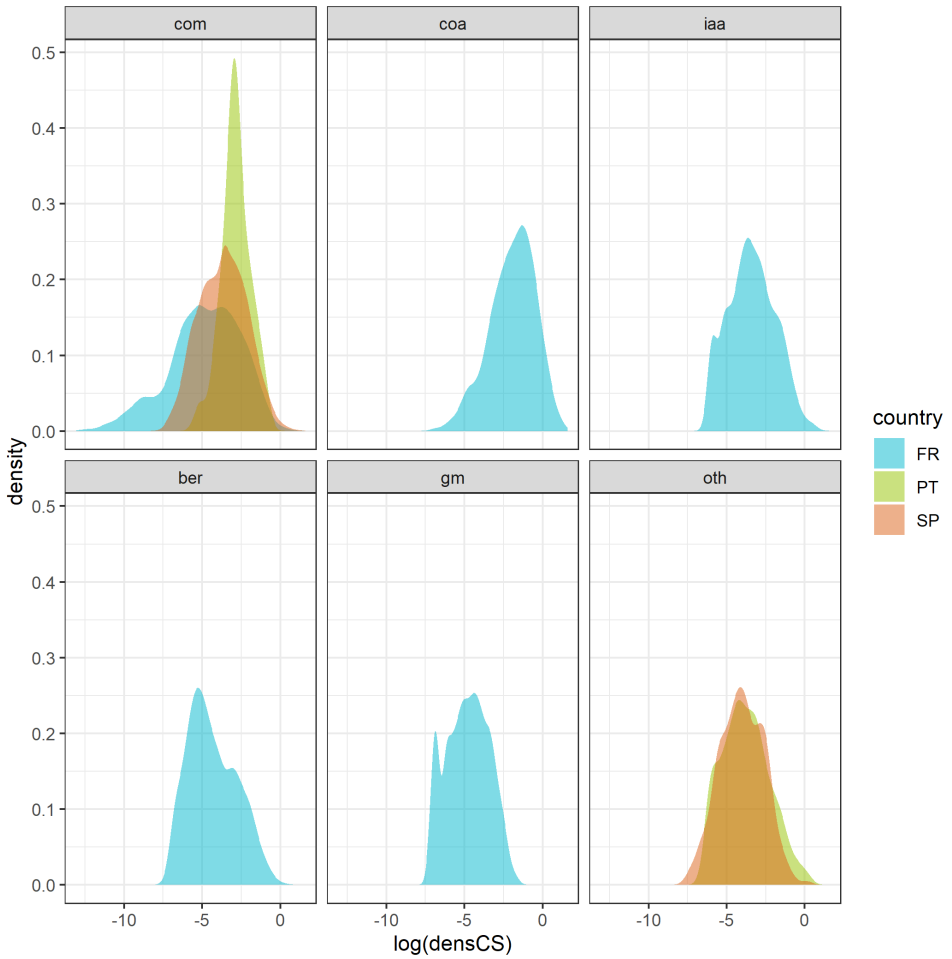

Figure 5.12: Distribution of log transformed density per country per fishing method

5.4 Screening of silvering data

5.4.1 Length

Length measurement correspond to silver, yellow or even glass eel stages. 255 lines have missing data for an initial dataset size of 151 403. Length < 100 mm or >1000 mm are scrutinized for errors by checking weight distribution. This is done to detect and correct length entered in cm that should have been reported in mm. This procedure allowed to correct 32 lines. For some electrofishing operations, repeated lines with the same rounded data were detected as being entered as a default value, thus not measured. Data for which no correction could be provided in an obvious way have also been removed (N = 255). Finally the length distribution per country, as cumulated profile and barplot per country is presented in Figure 5.13.

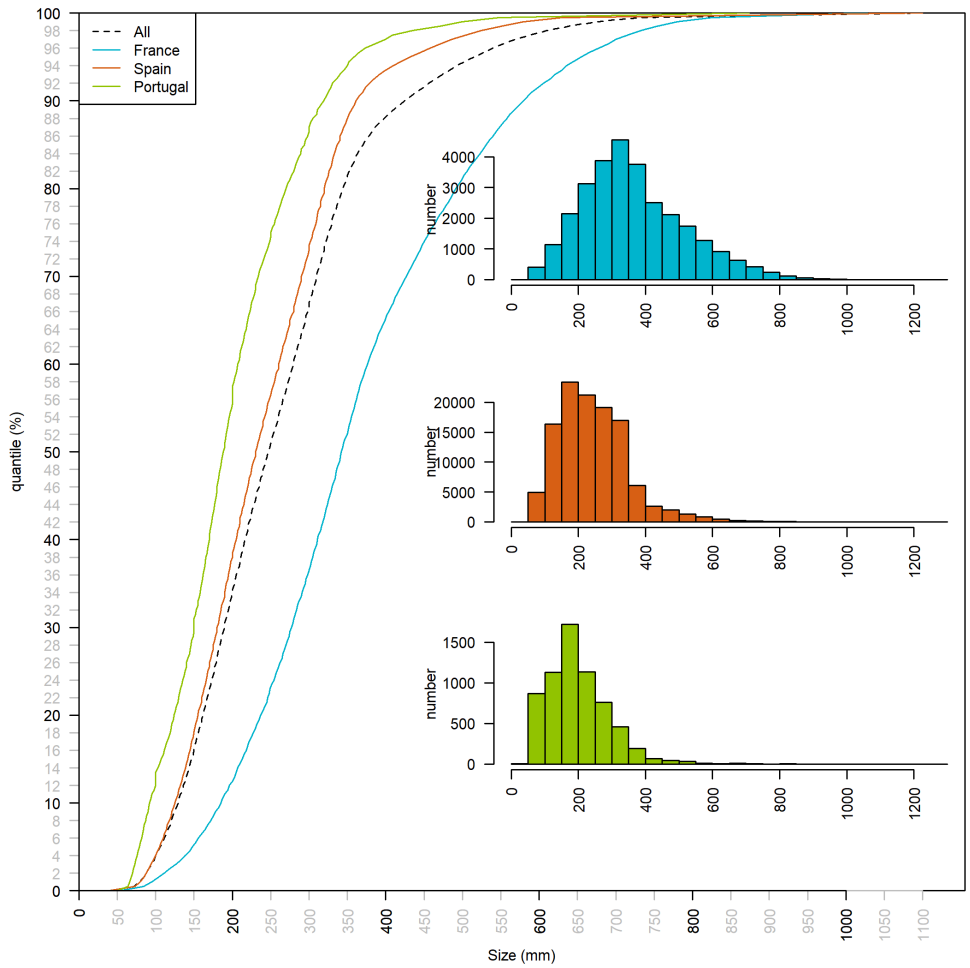

Figure 5.13: Cumulated distributions of size, for France, Spain, Portugal and all data combined, and histogram of size distribution of eels collected to measure the silvering index.

5.4.2 Weight

Some data have been modelled using standard length weight equations in France. Prior to any analysis, these data were excluded from analysis. The number of individ-

uals with weight measurement corresponds to N = 126 185 and the number of missing data [1] is N = 25 218 (Figure 5.14).

A quantile regression is built using:

$$log(W) \sim log(L)$$

and the residuals from 0.5 quantile regression are extracted.

A total of N = 718 individuals with absolute residuals larger than 2 are removed from selection (Koenker, 2020).

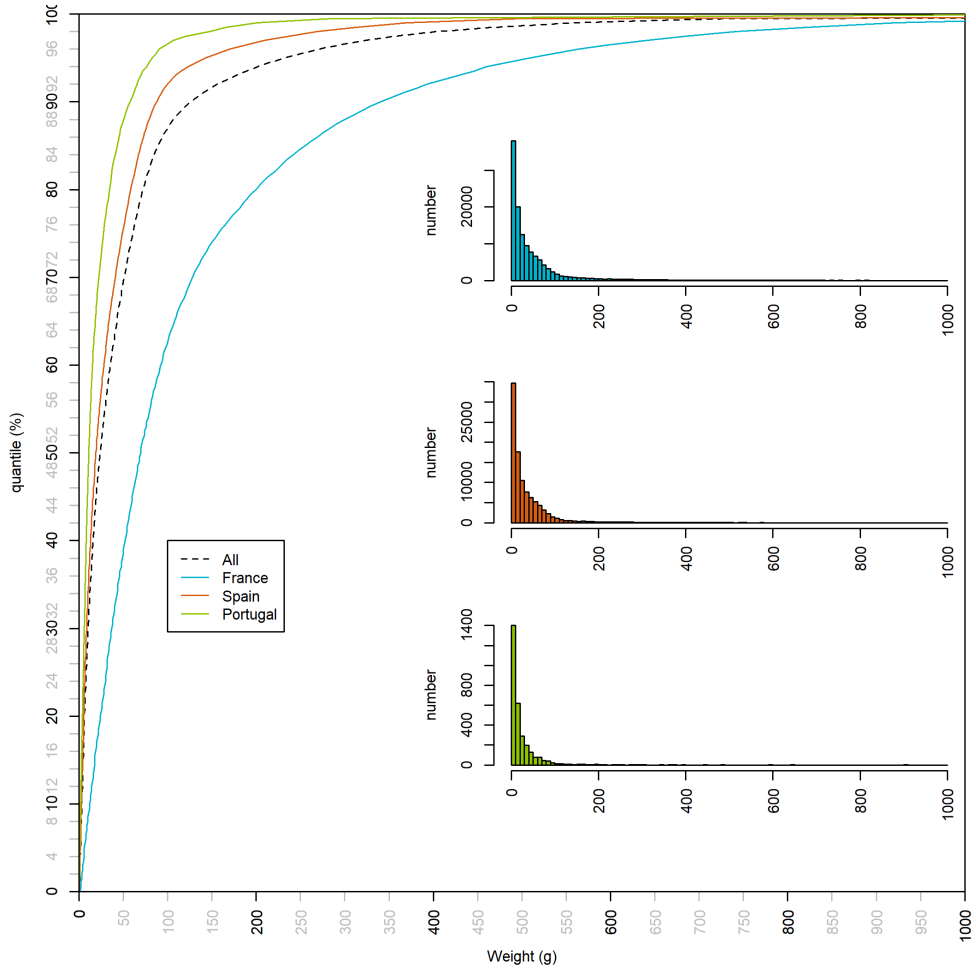

Figure 5.14: Weight cumulated distribution for 126 185 *eels collected in France, Spain and Portugal. Distribution before data selection.*

Weights separated by class are summarized in Table 5.5, a graphical presentation of the selection process is presented in Figure 5.15.

5.4.3 Pectoral fin

Some pectoral fin measurements were clearly to low and have been multiplied by 10 67. Excluded using quantile length - length pectoral regression N = 320. After selec-

[1] this corresponds to missing weight but also missing length as it was not possible to calculate a length weight relationship

country	sexe_durif	N	Mean(Lower-Upper)	Min	Q3	Median	Q5	Max
FR	female	312	702.0(651.2-752.8)	154.0	362.8	503.5	1 000.0	2 823.0
FR	male	518	115.5(110.9-120.2)	17.0	82.0	104.0	132.0	482.0
PT	female	2	361.8(<0-1 877.5)	242.5	302.1	361.8	421.4	481.1
PT	male	26	84.4(72.9-95.8)	47.0	64.6	79.1	98.0	155.5
SP	female	225	503.5(468.2-538.8)	180.2	315.8	442.5	605.2	1 550.0
SP	male	962	98.8(95.7-101.8)	10.6	70.0	86.1	109.2	398.8

Table 5.5: Weight of silver eel per country and per sex, lower and upper Gaussian confidence limits based on the t-distribution.

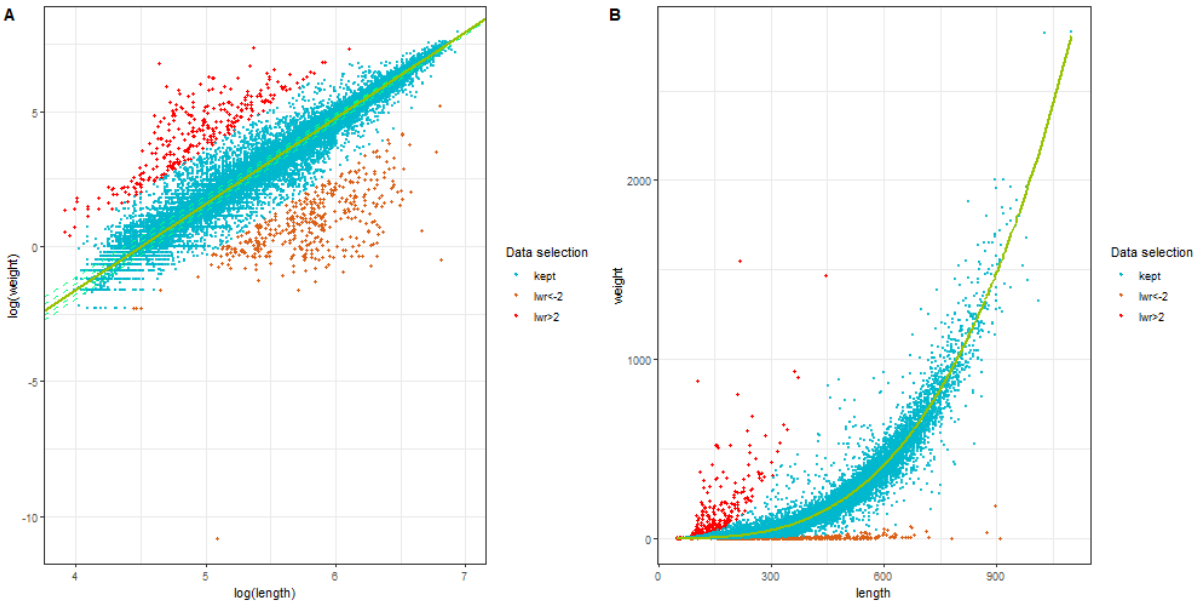

Figure 5.15: Exclusion based on size-weight

tion, the number of eels with pectoral fin measurement allowing to calculate the silver eel is N = 24137 (Figure 5.16).

5.4.4 Eye

For horizontal diameter N = 25219 data are available. Measurements corresponding to eels of eye diameter larger than 20 mm have been corrected by searching for obvious error of a factor 10 or 100 by comparing both eye measurements (N = 83). Finally eels still having eye diameter >20 mm or equal to 1 mm are excluded from the dataset (N = 84), and the dataset is further restricted by removing eels whose length is lower than 250 mm (N = 495) from the analysis. Values lying too far from the regression line (> 5 mm), N = 32 are removed from the analysis (Figure 5.18). The final dataset available for analysis corresponds to N = 24608.

For vertical diameter, N = 25208 individual measurements are available. Measurements corresponding to eels of eye diameter larger than 20 mm have been corrected by searching for obvious error of a factor 10 or 100 by comparing both eye measurements (N=95). Finally eels still having eye diameter >20 mm or equal to 1 mm are

Table 5.6: Weight by size class after selection, min, median, max, and Ws specific weight issued from quantile (0.5) regression on the middle of the size class, and 80 mm for eels > 100mm.

length_class	n	min	Q50	max	Ws
(40,100]	4733	0.1	1.0	10.0	0.7
(100,150]	15536	0.3	3.0	36.2	1.4
(150,200]	22872	0.7	8.1	81.9	5.0
(200,250]	21013	2.0	18.0	150.0	12.5
(250,300]	19817	4.6	34.0	233.0	25.4
(300,350]	18921	6.9	59.6	408.0	45.3
(350,400]	8515	12.7	89.8	467.0	74.0
(400,450]	4256	20.2	131.5	582.0	113.0
(450,500]	3303	30.4	188.0	886.0	164.3
(500,550]	2405	42.3	260.0	773.0	229.5
(550,600]	1619	50.2	345.0	925.0	310.7
(600,650]	1053	76.0	454.8	900.0	409.5
(650,700]	636	211.0	579.0	1280.0	528.0
(700,750]	403	163.3	730.0	1389.0	668.1
(750,800]	200	300.3	893.5	1520.0	831.8
(800,850]	100	529.6	1104.5	1882.0	1020.9
(850,900]	57	793.0	1320.0	2000.0	1237.6
(900,950]	19	1266.0	1638.0	2000.0	1483.9
(950,1e+03]	6	1438.0	1739.0	1961.0	1761.9
(1e+03,1.05e+03]	2	1325.0	2074.0	2823.0	2073.5
(1.05e+03,1.1e+03]	1	2828.9	2828.9	2828.9	2421.0

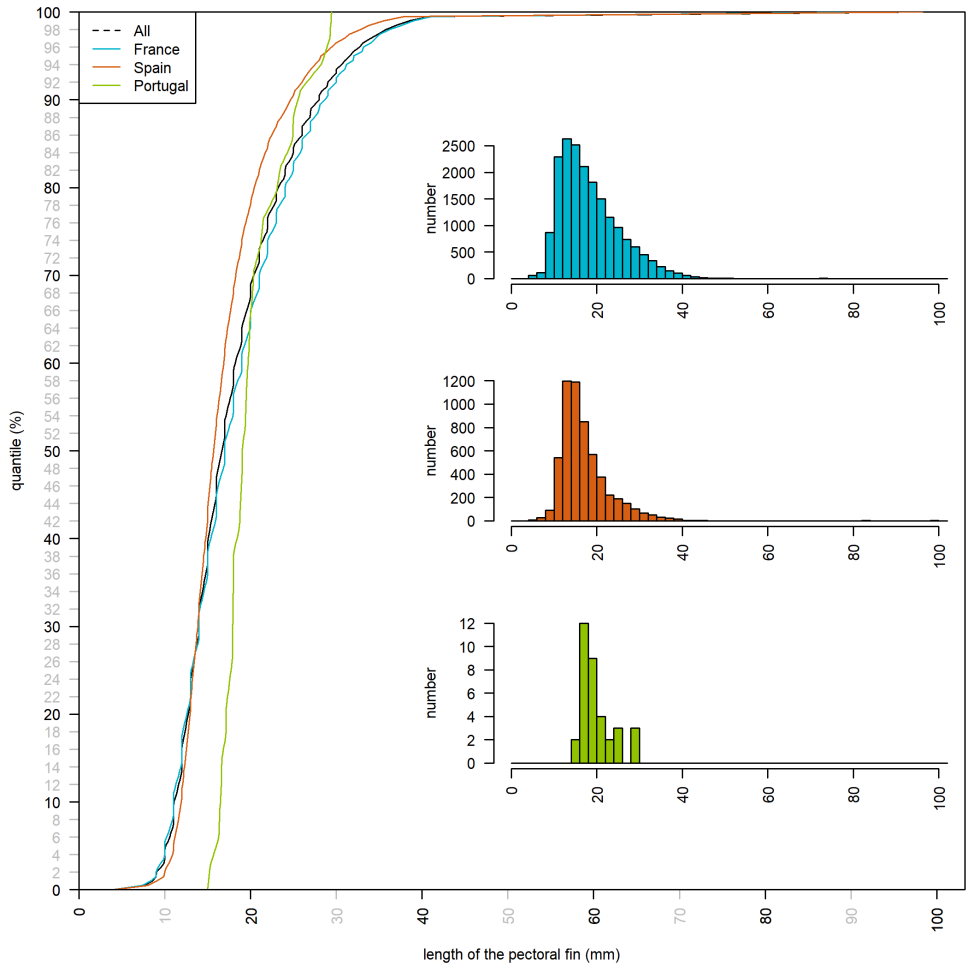

Figure 5.16: Distribution of pectoral fin length.

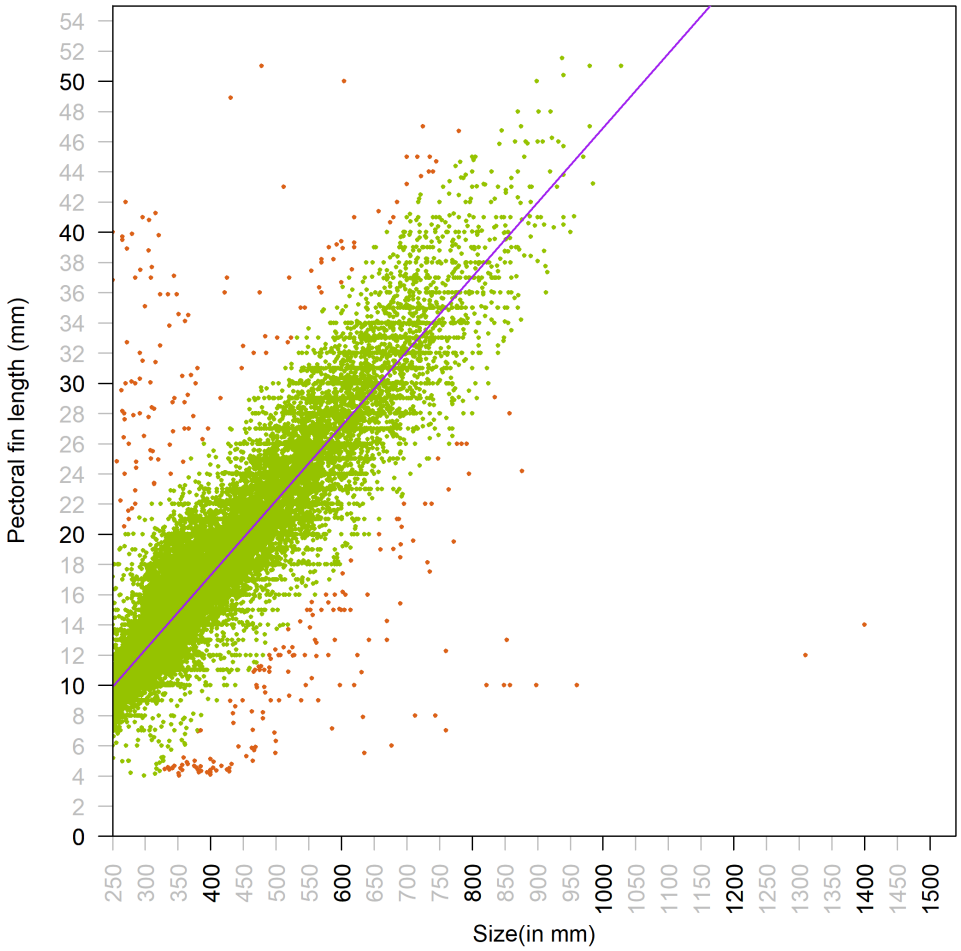

Figure 5.17: Relation between length and pectoral fin length

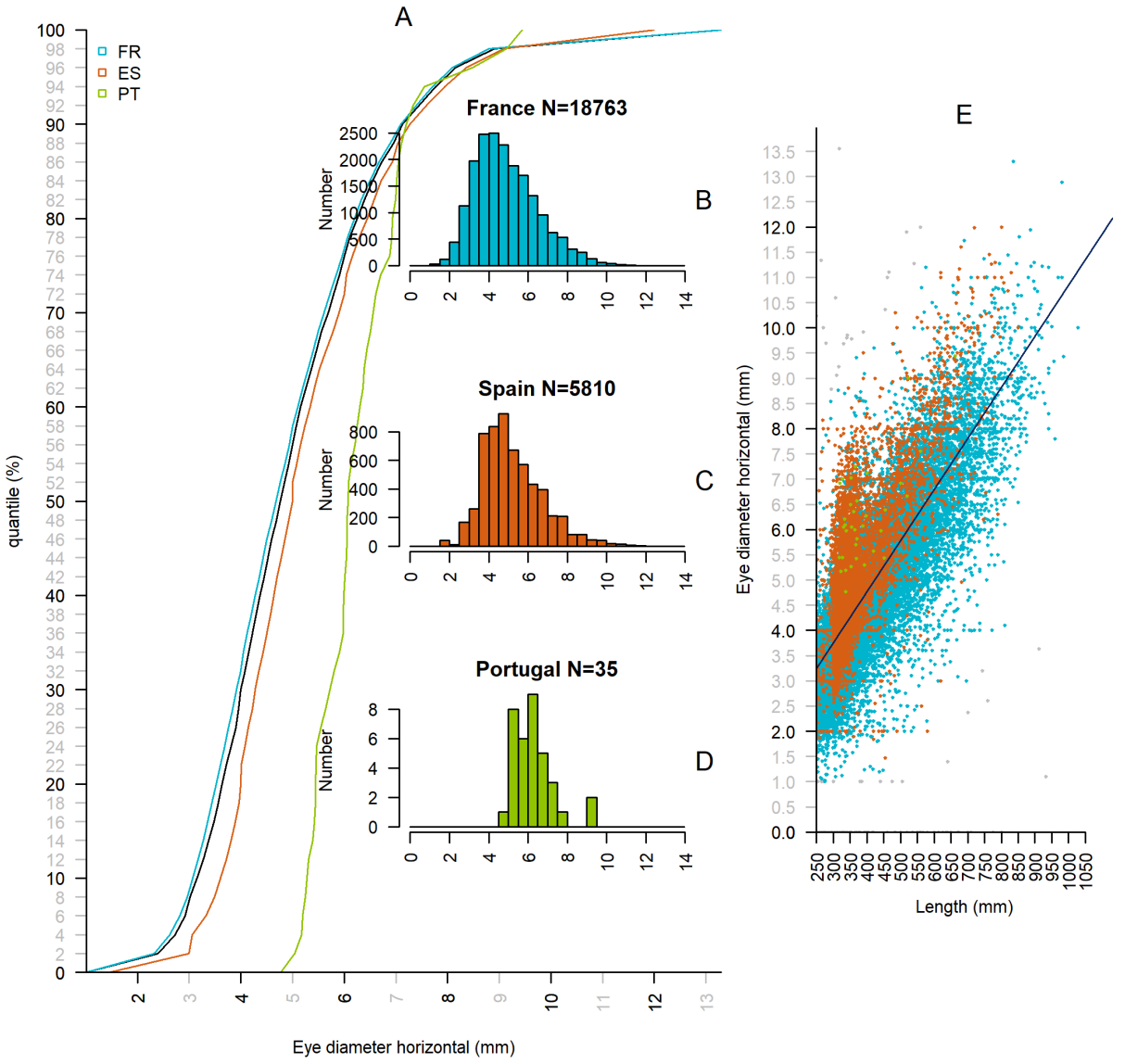

Figure 5.18: Horizontal eye diameter in mm for N = 24608 eels larger than 250 mm, after initial correction and filtering. A. Cumulated distribution for the whole dataset and the three countries (France FR, Spain SP, and Portugal PT). B. C. D. Histograms showing the distribution of horizontal eye diameter (mm) in the three countries, in France a systematic length measurement has been performed on eel >250 mm (by ONEMA) to assess the silvering, while Portuguese measurements were only made on silver eels. E. relation between horizontal eye diameter (mm) and the length of the eels (mm). The black line represents the quantile 0.5 (median) regression. Grey points have residuals larger than 5 mm and are excluded from the analysis. Large values > 12.5 mm not presented.

excluded from the dataset (N = 120). Measurements corresponding to eels of eye diameter larger than 20 mm, or to eels whose length is lower than 250 mm (N = 120) are excluded from the analysis. Values lying too far from the regression line (>5 mm), N = 96 are removed from the analysis (Figure 5.19). Values excluded as eye excentrity >0.8 were N = 64 (Figure 5.20). The final dataset available for analysis is corresponds to N = 24512.

Table 5.7: Number of eels measured per country before a filter is applied to the dataset. FR = France, SP =Spain, PT=Portugal.

year	FR	PT	SP
1988	0	741	605
1989	0	67	392
1991	0	0	152
1995	0	0	2397
1996	0	0	9782
1997	0	0	5425
1998	0	0	1674
1999	0	0	3110
2000	0	0	3181
2001	0	0	2742
2002	0	0	3310
2003	0	0	2948
2004	0	168	4221
2005	0	715	4552
2006	0	182	5117
2007	0	69	4681
2008	0	9	3319
2009	8038	276	3908
2010	7775	3	2821
2011	7060	555	3759
2012	6161	806	5429
2013	0	737	6299
2014	0	488	7434
2015	0	0	5955
2016	0	0	7041
2017	0	1035	7303
2018	0	593	7552
2019	0	0	816
All	29034	6444	115925

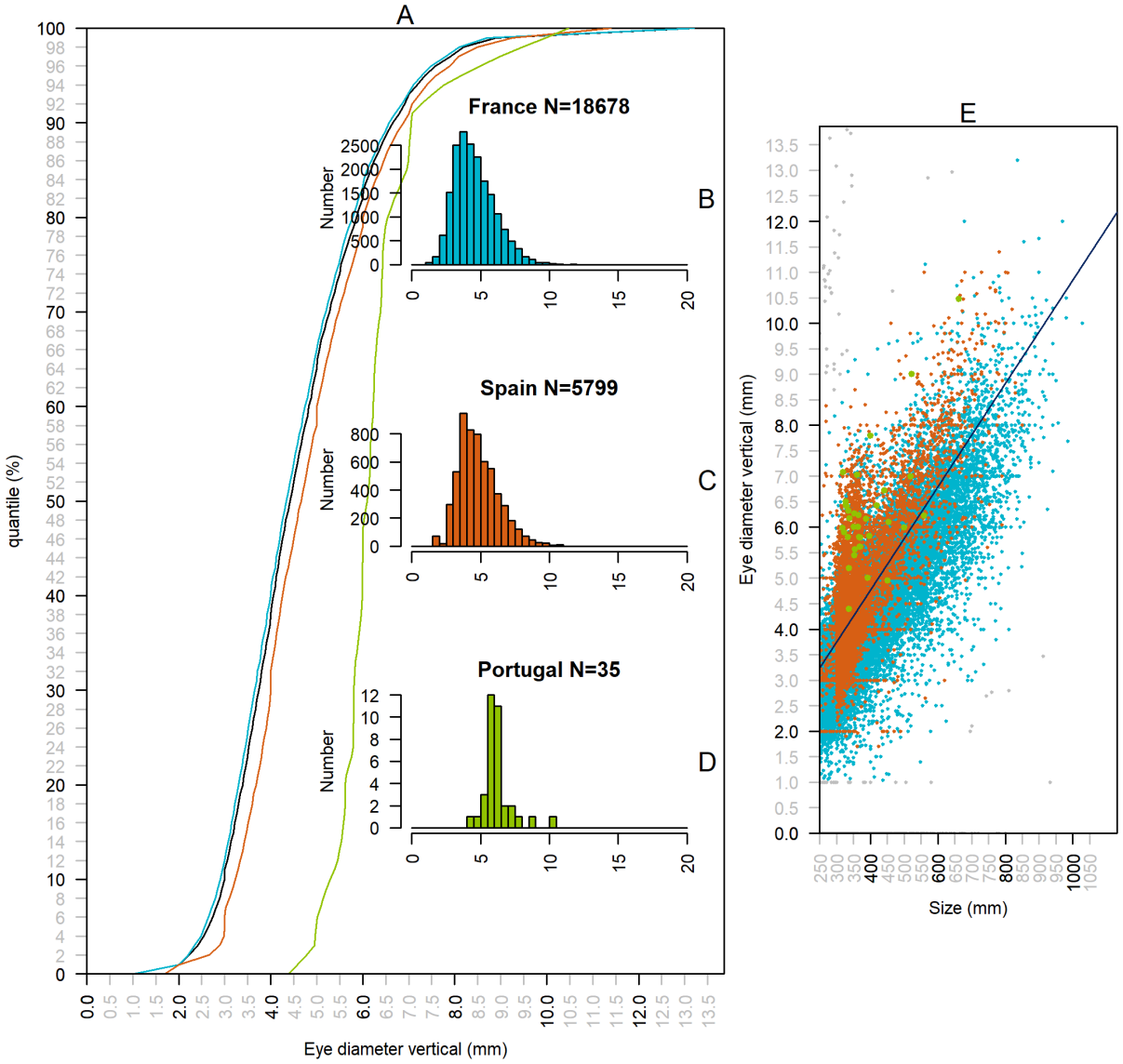

Figure 5.19: Vertical eye diameter in mm for N = 24512 eels larger than 250 mm, after initial correction and filtering. A Cumulated distribution for the whole dataset and the three countries (France FR, Spain SP, and Portugal PT). B, C, D histograms showing the distribution of vertical eye diameter (mm) in the three countries, in France a systematic length measurement has been performed on eel >250 mm (by ONEMA) to assess the silvering, while Portuguese measurements were only made on silver eels. E, relation between vertical eye diameter (mm) and the length of the eels (mm). The black line represents the quantile 0.5 (median) regression. Grey points have residuals larger than 5 mm and are excluded from the analysis. Large values >12.5 mm not presented.

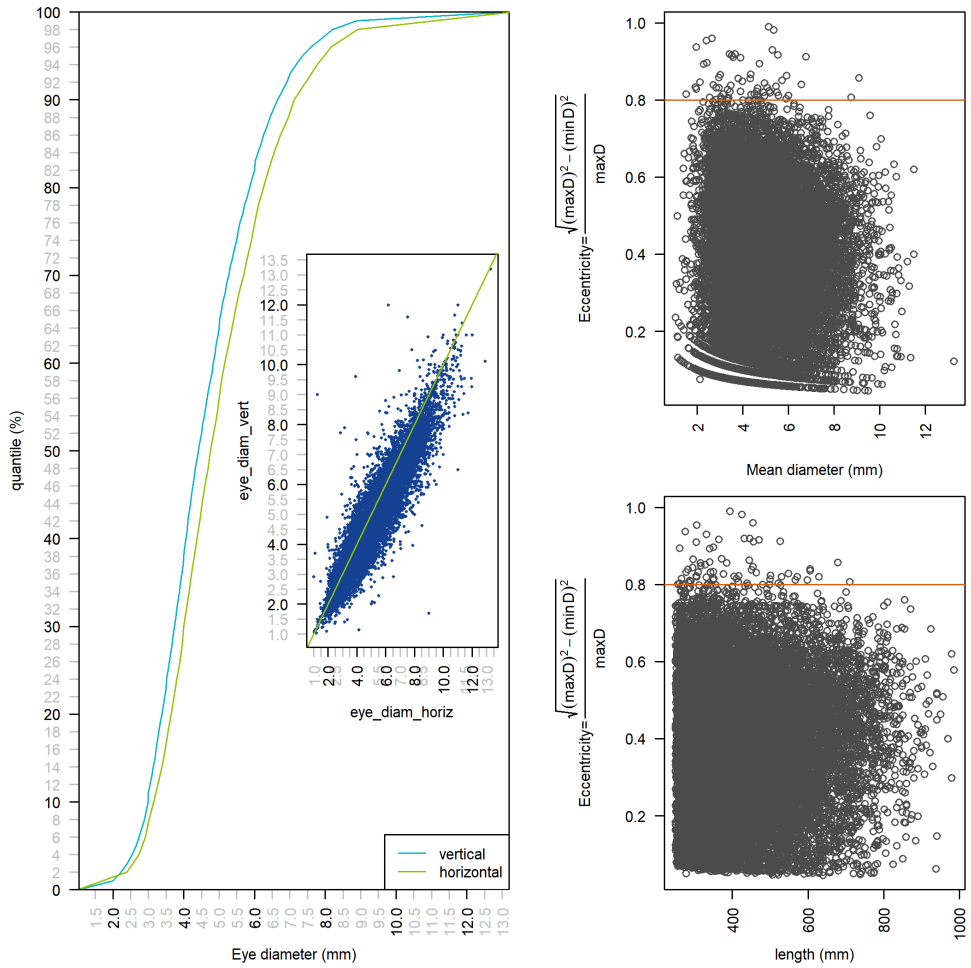

Figure 5.20: Distribution of eye vertical and horizontal measurements and measure of eye eccentricity. Eccentricity values >0.8 (N = 64) are further excluded from analysis.

Table 5.8: Number of eels for which the silvering status was calculated per country, at the end of the quality check process FR = France, SP =Spain, PT=Portugal.

year	FR	PT	SP
2007	0	0	186
2008	0	0	431
2009	4411	0	445
2010	3365	0	328
2011	3721	0	495
2012	3094	0	261
2013	0	0	482
2014	0	17	687
2015	0	0	436
2016	0	0	639
2017	0	12	453
2018	0	5	502
2019	0	0	131
All	14591	34	5476

5.5 transport model

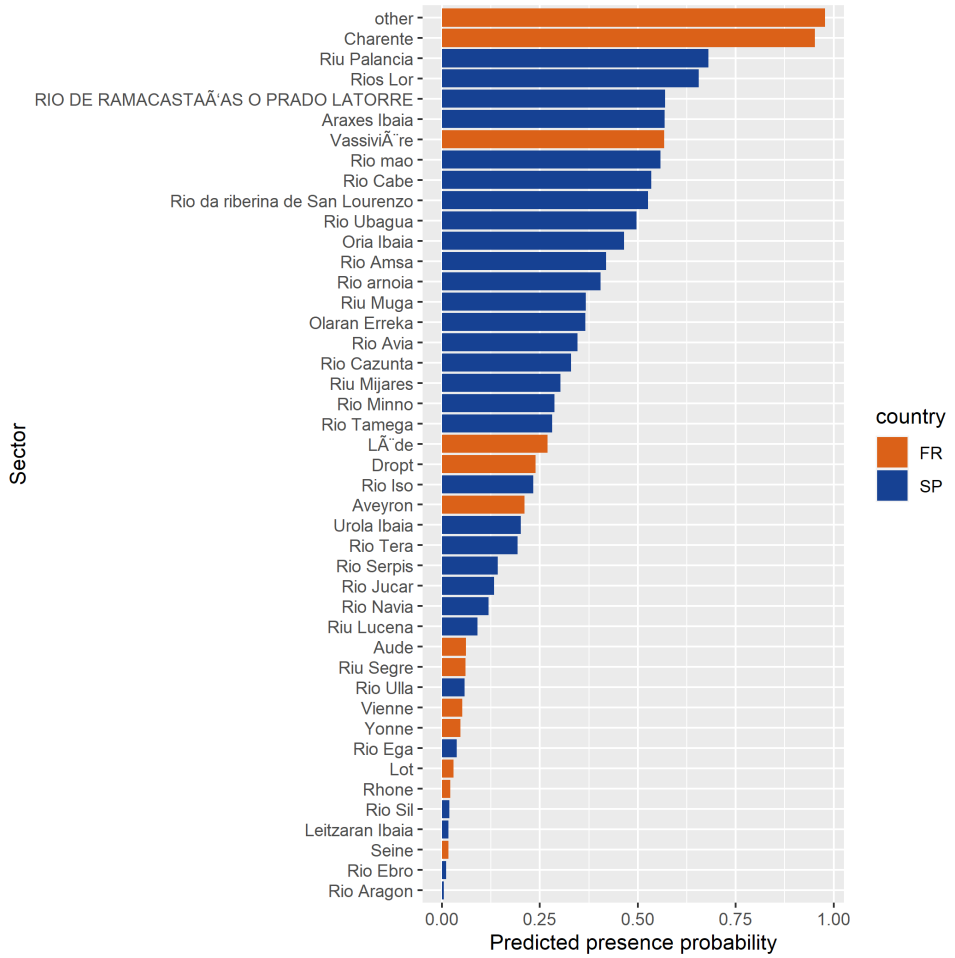

Figure 5.21: Predicted presence probability from transport model.

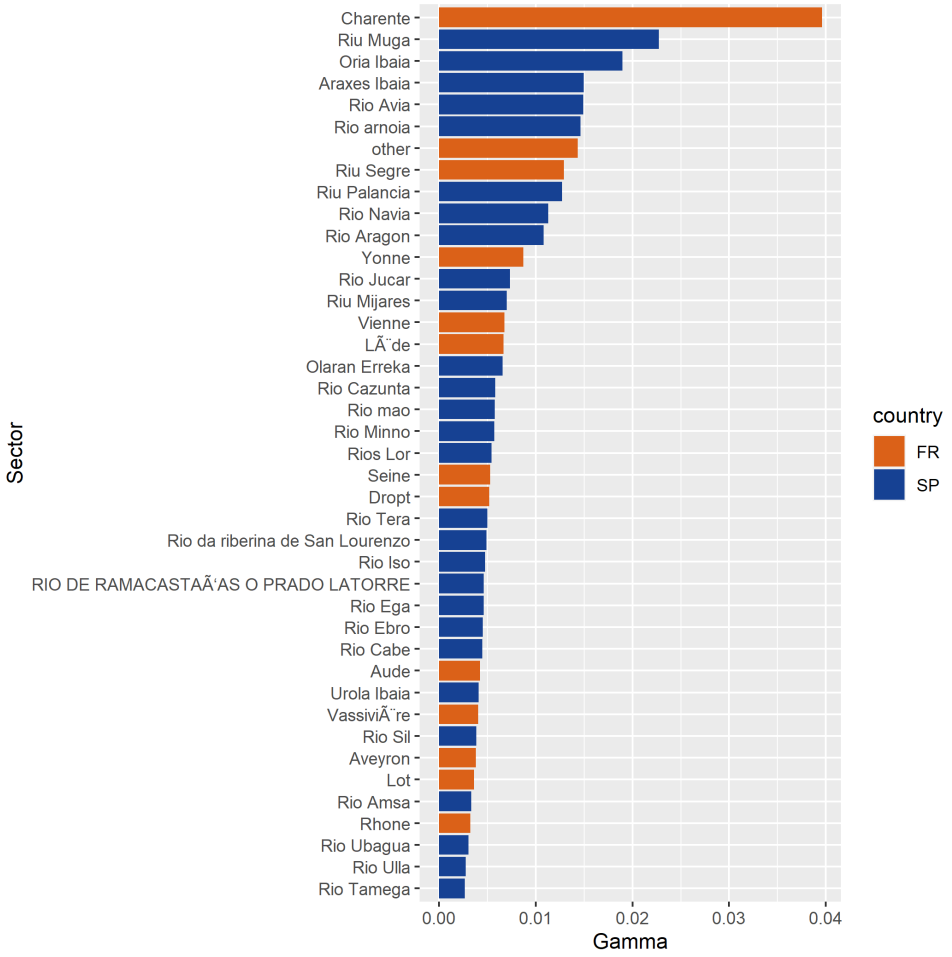

Figure 5.22: Predicted density from transport model.

5.6 Results per Country

Additional results for model transport.

Table 5.9: Silver eel number and wetted area per country in 2015 (with transport model).

country	$\sum Ns_r$	$\sum Ns_o$	$\sum Ns$	$\sum Ns_{♂}$	$\sum Ns_{♀}$	$\sum Bs_{♂}$	$\sum Bs_{♀}$	$\sum Bs$	$\sum Bs_{♀}$	$\sum Bs$
FR	0.85	11.42	12.27	6.53	1.52	581	922	1 504		
PT	1.7	4.15	5.84	4.88	0.12	0	0	0		
SP	0.78	10.93	11.71	11.18	0.78	794	332	1 126		
All	3.3	26.5	29.8	22.6	2.4	1 375			1 254	2 629

5.7 Results per EMU

Table 5.10: Eel number and wetted area per emu in 2015, density eel/^{2}m, $\sum N_r$ *number of eel in the rivers in millions,* $\sum W_r$ *wetted surface in* km, $\sum N_o$ *number of eel in additional waterbodies in millions,* $\sum W_o$ *surface of additional waterbodies* km, $\sum N$ *total number of eel in millions.*

emu	$\bar{d}$	$\sum N_r$	$\sum W_r$	$\sum N_o$	$\sum W_o$	$\sum N$
ES_Anda	0.010	2.6	136.5	131.6	1 063.6	134.2
ES_Astu	0.043	1.2	21.6	5.8	39.0	7.0
ES_Basq	0.034	0.5	13.1	4.2	35.7	4.8
ES_Cant	0.044	0.5	9.1	6.2	61.1	6.7
ES_Cata	0.012	1.6	59.9	3.5	105.6	5.1
ES_Gali	0.023	1.2	46.0	5.0	141.8	6.2
ES_Inne	0.000	0.0	291.8	0.0	755.5	0.1
ES_Minh	0.038	0.6	4.9	4.5	20.6	5.2
ES_Nava	0.002	0.1	29.0	0.0	13.2	0.1
ES_Vale	0.003	0.4	117.4	6.7	386.8	7.1
FR_Adou	0.032	1.4	52.7	3.0	241.7	4.4
FR_Arto	0.026	0.9	32.5	1.0	161.0	2.0
FR_Bret	0.070	3.9	53.9	6.3	222.7	10.2
FR_Garo	0.014	2.3	196.6	9.1	875.6	11.3
FR_Loir	0.012	2.7	241.4	11.1	1 508.9	13.8
FR_Meus	0.000	0.0	20.6	0.0	49.0	0.0
FR_Rhin	0.000	0.0	53.1	0.0	202.5	0.0
FR_Rhon	0.012	2.7	291.9	90.2	2 079.8	92.9
FR_Sein	0.016	3.6	179.3	4.6	668.3	8.2
PT_Port	0.047	21.6	221.2	81.2	1 148.5	102.8
All	0.015	47.8	2 072.5	374.3	9 780.9	422.1

Table 5.11: Silver eel number and wetted area per emu in 2015, $\sum Ns_r$ (million) number of silver eel produced on the river network, $\sum Ns_o$ (million) number of silver eel produced on additional waterbodies, $\sum Ns$ (million) number of silver, $\sum Ns_{♂}$ (million) number of silver males, $\sum Ns_{♀}$ (million) number of silver females, $\sum Bs_{♂}$ (tonnes) biomass of silver males, $\sum Bs_{♀}$ (tonnes) biomass of silver females, $\sum Bs$ (tonnes) biomass of silver eel.

emu	$\sum Ns_r$	$\sum Ns_o$	$\sum Ns$	$\sum Ns_{♂}$	$\sum Ns_{♀}$	$\sum Bs_{♂}$	$\sum Bs_{♀}$	$\sum Bs$
ES_Anda	0.23	8.48	8.71	8.26	0.45	575.68	178.29	753.97
ES_Astu	0.12	0.56	0.68	0.65	0.03	45.15	13.29	58.44
ES_Basq	0.04	0.32	0.37	0.35	0.02	24.48	7.00	31.48
ES_Cant	0.04	0.51	0.55	0.52	0.02	36.44	10.47	46.91
ES_Cata	0.15	0.40	0.55	0.43	0.12	37.76	62.60	100.36
ES_Gali	0.12	0.49	0.61	0.59	0.02	40.18	9.06	49.24
ES_Inne	0.00	0.00	0.01	0.00	0.00	0.17	3.90	4.07
ES_Minh	0.06	0.45	0.52	0.51	0.00	33.25	1.96	35.21
ES_Nava	0.00	0.00	0.00	0.00	0.00	0.36	0.41	0.77
ES_Vale	0.04	0.86	0.90	0.73	0.17	61.85	83.42	145.27
FR_Adou	0.09	0.22	0.31	0.26	0.05	21.43	27.68	49.12
FR_Arto	0.03	0.04	0.07	0.05	0.02	5.11	8.63	13.73
FR_Bret	0.16	0.27	0.44	0.37	0.07	31.49	36.60	68.09
FR_Garo	0.12	0.54	0.67	0.52	0.14	46.21	80.63	126.84
FR_Loir	0.13	0.53	0.66	0.49	0.17	42.89	121.16	164.05
FR_Meus	0.00	0.00	0.00	0.00	0.00	0.00	0.05	0.05
FR_Rhin	0.00	0.00	0.00	0.00	0.00	0.06	0.87	0.93
FR_Rhon	0.17	5.51	5.67	4.66	1.01	417.77	615.65	1 033.42
FR_Sein	0.14	0.17	0.31	0.23	0.08	22.42	43.71	66.12
PT_Port	1.64	5.04	6.68	6.50	0.18	407.38	62.22	469.60
All	3.31	24.39	27.70	25.13	2.57	1 850.08	1 367.60	3 217.68

Table 5.12: Silver eel number and wetted area per emu in 2015 (with transport model).

emu	$\sum Ns_r$	$\sum Ns_o$	$\sum Ns$	$\sum Ns_{♂}$	$\sum Ns_{♀}$	$\sum Bs_{♂}$	$\sum Bs_{♀}$	$\sum Bs$
ES_Anda	0.23	8.09	8.32	8.12	0.44	565.39	172.58	737.97
ES_Astu	0.12	0.47	0.59	0.55	0.02	37.96	8.42	46.38
ES_Basq	0.04	0.25	0.29	0.32	0.01	22.10	5.38	27.48
ES_Cant	0.04	0.40	0.44	0.49	0.02	34.22	8.94	43.15
ES_Cata	0.15	0.33	0.48	0.36	0.09	31.45	46.03	77.49
ES_Gali	0.13	0.47	0.60	0.50	0.01	33.61	6.30	39.91
ES_Inne	0.01	0.03	0.04	0.00	0.00	0.15	1.86	2.01
ES_Minh	0.06	0.16	0.22	0.04	0.00	2.54	0.17	2.71
ES_Nava	0.01	0.00	0.01	0.00	0.00	0.00	0.07	0.07
ES_Vale	0.05	0.76	0.81	0.71	0.16	60.17	79.50	139.68
FR_Adou	0.09	0.85	0.94	0.24	0.05	20.58	26.23	46.81
FR_Arto	0.03	0.23	0.27	0.05	0.02	4.90	8.10	12.99
FR_Bret	0.16	0.80	0.96	0.35	0.07	30.25	35.33	65.58
FR_Garo	0.12	1.51	1.64	0.52	0.14	45.61	80.53	126.13
FR_Loir	0.13	1.46	1.59	0.49	0.17	42.54	119.71	162.25
FR_Meus	0.00	0.00	0.00	0.00	0.00	0.00	0.05	0.05
FR_Rhin	0.00	0.00	0.00	0.00	0.00	0.06	0.85	0.90
FR_Rhon	0.17	5.97	6.14	4.64	1.00	415.13	608.83	1 023.96
FR_Sein	0.14	0.59	0.73	0.23	0.08	22.09	42.83	64.92
PT_Port	1.64	4.11	5.76	4.97	0.13	6.15	2.61	8.77
All	3.33	26.50	29.82	22.58	2.41	1 374.91	1 254.31	2 629.23

5.8 Results per SUDOE area

Table 5.13: Eel number and wetted area per sudoe zone in 2015, $\bar{d}$ eel/^{2}m, $\sum N_r$ number of eel in the rivers in millions, $\sum W_r$ wetted surface in km, *$\sum N_o$ number of eel in additional waterbodies in millions, $\sum W_o$ surface of additional waterbodies* km, *$\sum N$ total number of eel in millions.*

Sudoe area	$\bar{d}$	$\sum N_r$	$\sum W_r$	$\sum N_o$	$\sum W_o$	$\sum N$
ATL_F	0.018	7.9	483.7	26.4	2 681.4	34.2
ATL_IB	0.017	25.3	632.6	218.5	3 095.8	243.8
CANT	0.042	3.8	95.6	20.9	252.9	24.6
CHAN	0.023	6.0	226.8	6.9	869.7	12.9
MED	0.006	4.9	560.2	101.7	2 629.5	106.5
RhinMeu	0.000	0.0	73.7	0.0	251.5	0.0
All	0.015	47.8	2 072.5	374.3	9 780.9	422.1

Table 5.14: Silver eel number and wetted area per sudoe zone in 2015, $\sum Ns_r$ (million) number of silver eel produced on the river network, $\sum Ns_o$ (million) number of silver eel produced on additional waterbodies, $\sum Ns$ (million) number of silver, $\sum Ns_{\male}$ (million) number of silver males, $\sum Ns_{\female}$ (million) number of silver females, $\sum Bs_{\male}$ (tonnes) biomass of silver males, $\sum Bs_{\female}$ (tonnes) biomass of silver females, $\sum Bs$ (tonnes) biomass of silver eel.

Sudoe area	$\sum Ns_r$	$\sum Ns_o$	$\sum Ns$	$\sum Ns_{\male}$	$\sum Ns_{\female}$	$\sum Bs_{\male}$	$\sum Bs_{\female}$	$\sum Bs$
ATL_F	0.38	1.37	1.76	1.37	0.38	119.31	239.39	358.70
ATL_IB	1.97	14.01	15.97	15.37	0.60	1 019.21	222.33	1 241.54
CANT	0.32	1.77	2.10	1.99	0.11	140.18	54.70	194.87
CHAN	0.24	0.27	0.51	0.39	0.12	37.06	62.05	99.11
MED	0.40	6.97	7.37	6.01	1.35	534.25	788.22	1 322.47
RhinMeu	0.00	0.00	0.00	0.00	0.00	0.06	0.92	0.98
All	3.31	24.39	27.70	25.13	2.57	1 850.08	1 367.60	3 217.68

Table 5.15: Silver eel number and wetted area per sudoe area in 2015 (with transport model).

Sudoe area	$\sum Ns_r$	$\sum Ns_o$	$\sum Ns$	$\sum Ns_{♂}$	$\sum Ns_{♀}$	$\sum Bs_{♂}$	$\sum Bs_{♀}$	$\sum Bs$
ATL_F	0.38	4.12	4.50	1.35	0.38	117.04	236.27	353.31
ATL_IB	1.97	12.44	14.41	13.20	0.53	575.26	157.25	732.50
CANT	0.32	1.66	1.98	1.77	0.09	124.52	43.82	168.34
CHAN	0.24	1.02	1.26	0.38	0.11	35.98	60.08	96.06
MED	0.40	7.26	7.67	5.88	1.30	522.07	756.00	1 278.07
RhinMeu	0.00	0.00	0.00	0.00	0.00	0.06	0.89	0.95
All	3.33	26.50	29.82	22.58	2.41	1 374.91	1 254.31	2 629.23

5.9 Model comparison

EDA model version	1.3	2	2.1	2.2	2.2.1	2.3
Framework	Mngt plan 2010	POSE project (FP6)	2012 report	2015 report	2018 report	2021 report
Country	FR	Basins ▼	FR	FR	FR	FR,SP,PT
Year range				1985-2012	1985-2015	1985-2019 ▲
Electrofishing protocols	no	no	no	yes	yes	yes
Size structure	no	no	no	yes	yes	yes
River width source	Electrofishing	Electrofishing	RHT	RHT	RHT	RHT & other ◊
Additional waterbodies	no	no ♣	no	no	no	yes
Obstacles	no	number	number	$\sum height$	$\sum height$ ■	$\sum height$ ■■
River dataset	BD CARTHAGE	CCM	RHT	RHT	RHT	RHT BD TOPAGE, WISE
	Delta model Δ					
Number of observations			9556	24541	29183 ♯	46147
Perc. deviance			54	41.3	40.9	59.8
Kappa ♠			0.71	0.66	0.58	0.75
Reference		Jouanin et al. (2012a); de Eyto et al. (2016)	Briand et al. (2015)	Briand et al. (2018)	Current report	

Table 5.16: Comparison of EDA models implementation.

▼ *Basins modelled in the POSE FP6 project, in FR (Rhone, Brittany), UK, IE, IE (2012), other implementation with the CCM EDA2.0 model have been carried out in the Meuse(BE,FR), whole country IE (2015) (de Eyto et al., 2016).*

▲ *Incomplete reporting for France between 2015 and 2019.* ◊ *The width of RHT dataset has been recaculated with a new model, it correspond to the width of a river predicted without alterations, the width in Spain and Portugal is computed from a model based on electrofishing width, satellite measures, field measures and the width from the MERIT hydro database (Yamazaki et al., 2019).*

♣ *But corrections for lake surface in Ireland.*

■ *The height is transformed using power 1.5 transformation, and then summed. it is combined with distance sea in a variable. It includes a prediction of missing data.*

■■ *The height is not transformed but includes a prediction of missing data using two different models in Spain and Portugal.*

♯ *. Comparison of EDA model Δ implementation, the real number of row for EDA2.2.1 is 175068 as it was built on pseudo size x observation.*

♠ *The Kappa indices is calculated for a threshold of 0.4.*

EDA model version		1.3	2	2.1	2.2	2.2.1	2.3
		Model predictions, comparison for France					
water surface (km^2)	rivers W_r	6727		2114	2114	2114	1122
	other W_o						6001
Yellow eel density ($eel/100m^2$)	2007			3.0	1.62	-	
	2012			-	1.6	1.35	
	2015			-	-	1.63	1.69
Silver eel (million)	2007	15		3.1	2.3		
	2012	-		-	1.8		
	2015	-		-	-		8.13 ⊕
Bpot (tonnes)	2007			2234	819		
	2012			-	613	620	
	2015			-	-	2068 ♠♠	1522
Reference				Briand et al. (2015)	Briand et al. (2018)	Current report	

Table 5.17: Comparison of EDA model results in France

⊕ *0.85 for rivers W_r and 7.28 for other waterbodies W_o.*

♠♠ *In the 2018 report we have 618 for EDA + 1450 as additional expert estimation for wetlands, Mediterranean lagoons and missing estuaries.*

BIBLIOGRAPHY

Aprahamian, M.W., Walker, A.M., Williams, B., Bark, A., and Knights, B. 2007. On the application of models of European eel (Anguilla anguilla) production and escapement to the development of Eel Management Plans: The River Severn. ICES Journal of Marine Science **64**: 1–11.

Baudoin, J.M., Burgun, V., Chanseau, M., Larinier, M., Ovidio, M., Sremski, W., Steinbach, P., and Voegtle, B. 2015. Assessing the passage of obstacles by fish. Concepts, design and application .

Beaulaton, L., Briand, C., and Chapon, P.m. 2015. Analyse des données d'argenture acquises en France. Technical report, ONEMA- EPTB Vilaine, Rennes.

Belletti, B., Garcia de Leaniz, C., Jones, J., Bizzi, S., Börger, L., Segura, G., Castelletti, A., van de Bund, W., Aarestrup, K., Barry, J., Belka, K., Berkhuysen, A., Birnie-Gauvin, K., Bussettini, M., Carolli, M., Consuegra, S., Dopico, E., Feierfeil, T., Fernández, S., Fernandez Garrido, P., Garcia-Vazquez, E., Garrido, S., Giannico, G., Gough, P., Jepsen, N., Jones, P.E., Kemp, P., Kerr, J., King, J., Łapińska, M., Lázaro, G., Lucas, M.C., Marcello, L., Martin, P., McGinnity, P., O'Hanley, J., Olivo del Amo, R., Parasiewicz, P., Pusch, M., Rincon, G., Rodriguez, C., Royte, J., Schneider, C.T., Tummers, J.S., Vallesi, S., Vowles, A., Verspoor, E., Wanningen, H., Wantzen, K.M., Wildman, L., and Zalewski, M. 2020. More than one million barriers fragment Europe's rivers. Nature **588**(7838): 436–441. doi:10.1038/s41586-020-3005-2.

Belliard, J., Ditches, J., and Roset, N. 2008. Guide pratique de mise en oeuvre des opérations de pêche a l'électricité dans le cadre des réseaux de suivi des peuplements de poissons. Technical report, ONEMA.

Briand, C., Beaulaton, L., Chapon, P.m., Drouineau, H., and Lambert, P. 2015. Eel density analysis (EDA 2.2) Estimation de l'échappement en anguilles argentées (Anguilla anguilla) en France. Rapport 2015. Technical report, ONEMA- EPTB Vilaine, La Roche Bernard.

Briand, C., Beaulaton, L., Chapon, P.m., Drouineau, H., and Lambert, P. 2018. Eel density analysis (EDA 2.2.1) Escapement of silver eels (Anguilla anguilla) from French rivers. 2018 report. Technical report, ONEMA- EPTB Vilaine, La Roche Bernard.

Carle, F. and Strub, M. 1978. A New Method for Estimating Population Size from Removal Data. Biometrics **34**: 621–630.

Clavel, J., Poulet, N., Porcher, E., Blanchet, S., Grenouillet, G., Pavoine, S., Biton, A., Seon-Massin, N., Argillier, C., Daufresne, M. et al. 2013. A New Freshwater Biodiversity Indicator Based on Fish Community Assemblages. PloS one **8**(11): e80968.

Clavero, M. and Hermoso, V. 2015. Historical data to plan the recovery of the European eel. Journal of Applied Ecology .

De Eyto, E., Briand, C., Poole, R., and O'Leary, C. 2015. Application of EDA (v 2.0) to Ireland Prediction of silver eel Anguilla anguilla escapement. Report 2015. Technical report, Marine Institute, Westport, Ireland.

de Eyto, E., Briand, C., Poole, R., O'Leary, C., and Kelly, F. 2016. Application of EDA (v 2.0) to Ireland: Prediction of silver eel Anguilla anguilla escapement. Technical Report, Marine Institute.

Degerman, E., Tamario, C., Watz, J., Nilsson, P.A., and Calles, O. 2019. Occurrence and habitat use of European eel (Anguilla anguilla) in running waters: Lessons for improved monitoring, habitat restoration and stocking. Aquatic Ecology pp. 1–12.

Döll, P., Kaspar, F., and Lehner, B. 2003. A global hydrological model for deriving water availability indicators: Model tuning and validation. Journal of Hydrology **270**(1): 105–134. doi:10.1016/S0022-1694(02)00283-4.

Domange, J., Lambert, P., Beaulaton, L., and Drouineau, H. 2018. Flow-wise or path-wise: Diffusion in a fragmented dendritic network and implications for eels. bioRxiv p. 323006.

Drouineau, H., Rigaud, C., Laharanne, A., Fabre, R., Alric, A., and Baran, P. 2015. Assessing the efficiency of an elver ladder using a multi-state mark–recapture model. River research and applications **31**(3): 291–300.

Drouineau, H., Durif, C., Castonguay, M., Mateo, M., Rochard, E., Verreault, G., Yokouchi, K., and Lambert, P. 2018. Freshwater eels: A symbol of the effects of global change. Fish and Fisheries **19**(5): 903–930. doi:10.1111/faf.12300.

Drouineau, H., Marie, V., Diaz, E., Maria, M.S., Maria, K., Carlos, A., Fernández-Delgado, C., Domingos, I., Hernandez, L.M.Z., Laurent, B., Patrick, L., and Briand, C. 2021. Incorporating Stakeholder Knowledge Into a Complex Stock Assessment Model, the Case of Eel Recruitment doi:10.20944/preprints202104.0429.v1.

Durif, C.M., Dufour, S., and Elie, P. 2006. Impact of silvering stage, age, body size and condition on reproductive potential of the European eel. MARINE ECOLOGY-PROGRESS SERIES- **327**: 171.

Durif, C.M., Guibert, A., and Elie, P. 2009. Morphological discrimination of the silvering stages of the European eel. In American Fisheries Society Symposium, volume 58. volume 58, pp. 103–111.

European Commission and Directorate-General for the Environment 2003. Implementing the Geographical Information System Elements (GIS) of the Water Framework Directive No 9. No 9. OPOCE, Luxembourg.

Feunteun, E. 1994. Le Peuplement Piscicole Du Marais Littoral Endigué de Bourgneuf-Machecoul (France Loire-Atlantique). Approche Méthodologique Pour Une Analyse Quantitative de La Distribution Spatiale Du Peuplement Piscicole et de La Dynamique de Certaines de Ses Populations. Thèse 3ème cycle, Université Rennes I.

Feunteun, E., Acou, A., Lafaille, P., and Legault, A. 2000. European eel: Prediction of spawner escapement from continental population parameters. Canadian journal of fisheries and aquatic sciences **57**: 1627:1635.

Feunteun, E., Laffaille, P., Robinet, T., Briand, C., Baisez, A., Olivier, J.M., and Acou, A. 2003. A Review of Upstream Migration and Movements in Inland Waters by Anguillid Eels: Toward a General Theory. In Eel Biology, edited by K. Aida, K. Tsukamoto, and K. Yamauchi, Springer, Tokyo, pp. 181–190.

Germis 2009a. Méthode de pêche électrique par échantillonnage par point au martin pêcheur «indice d'abondance anguille». Technical report.

Germis, G. 2009b. Evaluation de l'état de la population d'anguille en Bretagne par la méthode des indices d'abondance "anguille" de 2003 à 2008. Technical report, Ouest Grand Migrateur.

Graynoth, E., Jellyman, D., and Bonnett, M. 2008. Spawning escapement of female longfin eels. New Zealand Fisheries Assessment Report **7**: 57.

Grill, G., Lehner, B., Thieme, M., Geenen, B., Tickner, D., Antonelli, F., Babu, S., Borrelli, P., Cheng, L., Crochetiere, H., Macedo, H.E., Filgueiras, R., Goichot, M., Higgins, J., Hogan, Z., Lip, B., McClain, M.E., Meng, J., Mulligan, M., Nilsson, C., Olden, J.D., Opperman, J.J., Petry, P., Liermann, C.R., Sáenz, L., Salinas-Rodríguez, S., Schelle, P., Schmitt, R.J.P., Snider, J., Tan, F., Tockner, K., Valdujo, P.H., van Soesbergen, A., and Zarfl, C. 2019. Mapping the world's free-flowing rivers. Nature **569**(7755): 215. doi:10.1038/s41586-019-1111-9.

Halvorsen, S., Korslund, L., Gustavsen, P.Ø., and Slettan, A. 2020. Environmental DNA analysis indicates that migration barriers are decreasing the occurrence of European eel (Anguilla anguilla) in distance from the sea. Global Ecology and Conservation **24**: e01245. doi:10.1016/j.gecco.2020.e01245.

Han, M., Fukushima, M., Kameyama, S., Fukushima, T., and Matsushita, B. 2008. How do dams affect freshwater fish distributions in Japan? Statistical analysis of native and nonnative species with various life histories. Ecological Research **23**(4): 735–743.

Haro, A. and Krueger, W.H. 1991. Pigmentation, otolith rings, and upstream migration of juvenile American eels (Anguilla rostrata) in a coastal rhode island sream. Canadian Journal of Zoology **69**: 812–814.

Hastie, T.J. and Tibshirani, R.J. 1990. Generalized Additive Models, volume 43. CRC Press.

Ibbotson, A., Smith, J., Scarlett, P., and Aprahamian, M. 2002. Colonisation of freshwater habitat by the European eel Anguilla anguilla. Freshwater Biology **47**: 1696–1706.

ICES 2010. Report of the 2010 session of the Joint EIFAC/ICES Working Group on Eels (WGEEL). Technical report, hamburg.

ICES 2013. Report of the Joint EIFAAC/ICES Working Group on Eels (WGEEL), 18–22 March 2013 in Sukarietta, Spain 4–10 September 2013 in Copenhagen, Denmark. Technical Report ICES CM 2013/ACOM: 18, ICES, Sukarieta, Spain, Copehagen, Denmark.

ICES 2020. Joint EIFAAC/ICES/GFCM Working Group on Eels (WGEEL). Technical Report ICES Scientific Reports Volume 2 Issue 85, Virtual.

ICES, Basic, T., Amilhat, E., Beaulaton, L., Belpaire, C., Bernotas, P., Briand, C., Bryhn, A., Capoccioni, F., Ciccotti, E., Dekker, W., Diaz, E., Domingos, I., Drouineau, H., Durif, C.M.F., Evans, D., Giedrojc, L., Gollock, M., van der Hammen, T., Hanel, R., Horn, L., Observer, K.J., Observer, K.K., Leone, C., Lozys, L., Marohn, L., Nermer, T., O'Leary, C., Pedersen, M.I., Pohlmann, J.D., Poole, R., Povliūnas, J., Rosell, R., Rohtla, M., Sapoundis, A., Simon, J., Sundin, J., Svagzydys, A., Thorstad, E.B., Vesala, S., Walker, A.M., and Wickström, H. 2019. Report of the Joint EIFAAC/ICES/GFCM Working Group on Eels (WGEEL). Technical report, ICES, Bergen (Norway).

Imbert, H. 2008. Relationships between locomotor behavior, morphometric characters and thyroid hormone levels give evidence of stage-dependent mechanisms in European eel upstream migration. Hormone and Behaviour **53(1)**: 69–81.

Imbert, H., De Lavergne, S., Gayou, F., Rigaud, C., and Lambert, P. 2008. Evaluation of relative distance as new descriptor of yellow European eel spatial distribution. Ecology of Freshwater Fish **17**(4): 520–527.

Imbert, H., Labonne, J., Rigaud, C., and Lambert, P. 2010. Resident and migratory tactics in freshwater European eels are size-dependent. Freshwater Biology **55**(7): 1483–1493.

Itakura, H., Wakiya, R., Gollock, M., and Kaifu, K. 2020. Anguillid eels as a surrogate species for conservation of freshwater biodiversity in Japan. Scientific Reports **10**(1). doi:10.1038/s41598-020-65883-4.

IUCN 2018. Anguilla anguilla: Pike, C., Crook, V. & Gollock, M.: The IUCN Red List of Threatened Species 2020: E.T60344A152845178. doi:10.2305/IUCN.UK.2020-2.RLTS.T60344A152845178.en.

Jouanin, C., Briand, C., Beaulaton, L., and Lambert, P. 2012a. Eel Density Analysis (EDA2.x) : Un modèle statistique pour estimer l'échappement des anguilles argentées (Anguilla anguilla) dans un réseau hydrographique. Technical report, IRSTEA, Bordeaux, FRANCE.

Jouanin, C., Gommes, p., Briand, C., Berger, V., Bau, F., Drouineau, H., Baran, P., Lambert, P., and Beaulaton, L. 2012b. Evaluation des mortalités d'anguilles induites par les ouvrages hydroélectriques en France. Projet Sea Hope, Silver Eel Escapement

From Hydropower. Rapport final. Parenariat 2011, domaine espèces aquatiques continentales, action 5.2, IRTEA.

Kazuki Yokouchi, Y.K. 2014. Demographic survey of the yellow-phase Japanese eel Anguilla japonica in Japan. Fisheries Science **80**: 543–554. doi:10.1007/s12562-014-0735-9.

Kettle, A.J., Asbjørn Vøllestad, L., and Wibig, J. 2011. Where once the eel and the elephant were together: Decline of the European eel because of changing hydrology in southwest Europe and northwest Africa? Fish and Fisheries **12**(4): 380–411.

Koenker, R. 2020. Quantreg: Quantile Regression.

Kume, M., Terashima, Y., Kawai, F., Kutzer, A., Wada, T., and Yamashita, Y. 2020. Size-dependent changes in habitat use of Japanese eel Anguilla japonica during the river life stage. Environmental Biology of Fishes **103**(3): 269–281. doi:10.1007/s10641-020-00957-w.

Laffaille, P., Acou, A., and Guillouët, J. 2005a. The yellow European eel (Anguilla anguilla L.) may adopt a sedentary lifestyle in inland freshwaters. Ecology of Freshwater Fish **14**: 191–196.

Laffaille, P., Briand, C., Fatin, D., Lafage, D., and Lasne, E. 2005b. Point sampling the abundance of European eel (Anguilla anguilla) in freshwater areas. Archiv f&# 252; r Hydrobiologie **162**(1): 91–98.

Lasne, E. and Laffaille, P. 2007. Analysis of distribution patterns of yellow European eel in the Loire catchment using logistic models based on presence_absence of different classes. Ecology of Freshwater Fish .

Legault, A. 1988. Le franchissement des barrages par l'escalade de l'anguille. Etude en Sèvre Niortaise. Bulletin français de la pêche et de la pisciculture **308**: 1–10.

Linke, S., Lehner, B., Ouellet Dallaire, C., Ariwi, J., Grill, G., Anand, M., Beames, P., Burchard-Levine, V., Maxwell, S., Moidu, H., Tan, F., and Thieme, M. 2019. Global hydro-environmental sub-basin and river reach characteristics at high spatial resolution. Scientific Data **6**(1). doi:10.1038/s41597-019-0300-6.

MacNamara, R. and McCarthy, T.K. 2012. Size-related variation in fecundity of European eel (Anguilla anguilla). ICES Journal of Marine Science: Journal du Conseil p. fss123.

Mateo, M., Drouineau, H., Pella, H., Beaulaton, L., Amilhat, E., Bardonnet, A., Domingos, I., Fernández-Delgado, C., De Miguel Rubio, R.J., Herrera, M., Korta, M., Zamora, L., Diaz, E., and Briand, C. 2021. Atlas of European eel distribution (Anguilla anguilla) in Portugal, Spain and France. GT1 product 1.1. Technical report, AZTI.

Matsushige, K., Yasutake, Y., and Mochioka, N. 2020. Spatial distribution and habitat preferences of the Japanese eel, Anguilla japonica, at the reach and channel-unit scales in four rivers of Kagoshima Prefecture, Japan. Ichthyological Research **67**(1): 68–80. doi:10.1007/s10228-019-00704-x.

Meixler, M., Bain, M., and Todd Walter, M. 2009. Predicting barrier passage and habitat suitability for migratory fish species. Ecological Modelling **220**(20): 2782–2791.

Miller, M.J., Bonhommeau, S., Munk, P., Castonguay, M., Hanel, R., and McCleave, J.D. 2014. A century of research on the larval distributions of the Atlantic eels: A re-examination of the data. Biological Reviews **90**(4): 1035–1064. doi:10.1111/brv.12144.

Morel, M., Booker, D.J., Gob, F., and Lamouroux, N. 2019. Intercontinental predictions of river hydraulic geometry from catchment physical characteristics. Journal of Hydrology p. 124292.

Naismith, I. and Knights, B. 1988. Migrations of elvers and juvenile European eels, Anguilla anguilla L., in the River Thames. Journal of fish biology **33**: 161–175.

Naismith, I.A. and Knights, B. 1993. The distribution, density and growth of the European eel, Anguilla anguilla, in the freshwater catchment of the River Thames. Journal of Fish Biology **42**(2): 217–226. doi:10.1111/j.1095-8649.1993.tb00323.x.

Ogle, D.H., Wheeler, P., and Dinno, A. 2020. FSA: Fisheries Stock Analysis.

Oliveira, K. and McCleave, J.D. 2000. Variation in population and life history traits of the American eel, Anguilla rostrata, in four rivers in Maine. Environmental Biology of Fishes **59**: 141–151.

Pella, H., Lejot, J., Lamouroux, N., and Snelder, T. 2012. Le réseau hydrographique théorique (RHT) fran\ccais et ses attributs environnementaux The theoretical hydrographical network (RHT) for France and its environmental attributes. Géomorphologie : relief, processus, environnement .

Poulet, N., Beaulaton, L., and Dembski, S. 2011. Time trends in fish populations in metropolitan France: Insights from national monitoring data. Journal of Fish Biology **79**(6): 1436–1452.

R Core Team 2020. R: A Language and Environment for Statistical Computing. R Foundation for Statistical Computing, Vienna, Austria.

Schmidt, J. 1909. Remarks on the metamorphosis and distribution of the larvae of the eel (Anguilla vulgaris, Turt.). Meddelester fra Kommissionen for Havundersøgesler, serie Fiskeri Copenhagen **III**(3): 1–17.

Schmidt, J. 1922. The breeding places of the eel. Philosophical Transactions of the Royal Society **211**: 179–208.

Shreve, R.L. 1966. Statistical law of stream numbers. The Journal of Geology **74**(1): 17–37.

Smogor, R., Angermeier, P., and Gaylord, C. 1995. Distribution and abundance of American eels in Virginia streams : Test of null models across spatial scales. Transactions of the American Fisheries Society **124**(6).

Stefánsson, G. 1996. Analysis of groundfish survey abundance data: Combining the GLM and delta approaches. ICES journal of Marine Science **53**(3): 577–588.

Strahler, A.N. 1952. Dynamic basis of geomorphology. Geological society of america bulletin **63**(9): 923–938.

Svedäng, H., Neuman, E., and Wickström, H. 1996. Maturation patterns in female European eel: Age and size at the silver eel stage. Journal of Fish Biology **48**(3): 342–351.

Tamario, C., Calles, O., Watz, J., Nilsson, P.A., and Degerman, E. 2019. Coastal river connectivity and the distribution of ascending juvenile European eel (*Anguilla anguilla* L.): Implications for conservation strategies regarding fish-passage solutions. Aquatic Conservation: Marine and Freshwater Ecosystems **29**(4): 612–622. doi:10.1002/aqc.3064.

Tesch, F. 1980. Occurrence of eel Anguilla anguilla larvae west of the European continental shelf, 1971-1977. Environmental Biology of Fishes **5**(3): 185–190.

Tesch, F.W. and White, R.J. 2008. The Eel. John Wiley & Sons.

Vanacker, M., Briand, C., Mateo, M., and Drouineau, H. 2020. GT3- deliverable E3.1.2 : Technical report on the GEREM model Application. Technical Report E3.12, INRAE.

Velez-Espino, L. and Koops, M. 2010. A synthesis of the ecological processes influencing variation in life history and movement patterns of American eel: Towards a global assessment. Reviews in Fish Biology and Fisheries .

Verdon, R. and Desrochers, D. 2002. Upstream migratory movement of American eel (Anguilla rostrata) between the beauharnois and Moses-Saunders power dam on the St. Lawrence river. Transactions of the American Fisheries Society .

Vogt, J., Colombo, R., Paracchini, M.L., de Jager, A., and Soille, P. 2003. CCM river and catchment database, version 1.0. Institute for Environment and Sustainability, EC Joint Research Centre, Ispra (Varese), Italy p. 31.

Vogt, J., Soille, P., de Jager, A., Rimaviciute, E., Mehl, W., Foisneau, S., Bodis, K., Dusart, J., Paracchini, M., Haastrup, P., and Bamps, C. 2007. A pan-European river and catchment database. Technical report, Joint Research Centre-Institute for Environment and Sustainability, Luxembourg.

Walker, A., Andonegi, E., Apolostolaki, P., Aprahamian, M., Beaulaton, L., Bevacqua, D., Briand, C., Cannas, A., De Eyto, E., Dekker, W., De Leo, G.A., Diaz, E., Doering-Arjes, P., Fladung, E., Jouanin, C., Lambert, P., Poole, R., Oeberst, R., and Schiavina, M. 2011. Pilot projects to estimate potential and actual escapement of silver eel. Technical report, DEFRA.

White, E.M. and Knights, B. 1997. Dynamics of upstream migration of the European eel, *Anguilla anguilla* (L.), in the Rivers Severn and Avon, England, with special reference to the effects of man-made barriers. Fisheries Management and Ecology **4**(4): 311–324. doi:10.1046/j.1365-2400.1997.00050.x.

Wood, S.N. 2003. Thin-plate regression splines. Journal of the Royal Statistical Society (B) **65**(1): 95–114.

Wood, S.N. 2017. Generalized Additive Models: An Introduction with R. Chapman & Hall/CRC Texts in Statistical Science. CRC Press/Taylor & Francis Group, Boca Raton, second edition edition.

Yamazaki, D., Ikeshima, D., Sosa, J., Bates, P.D., Allen, G., and Pavelsky, T. 2019. MERIT Hydro: A high-resolution global hydrography map based on latest topography datasets. Water Resources Research doi:10.1029/2019WR024873.

Yee, T.W. 2013. VGAM: Vector Generalized Linear and Additive Models. R package version 0.9-1. .

6 Glossary

ω_{bf} **bank electrofishing**. In large or deep stream, or in marshes, electrofishing is performed from the banks of the river. 13, 16, 27, 39, 44

ω_{dhf} **deep habitat electrofishing**. In large or deep stream, a point abundance sampling method described as "pe partielle par points" in Belliard (2008). 13, 16, 27, 39, 44

ω_{eai} **Eel abundance index**. Point abundance sampling, performed in wadable streams, with portable equipment using AC current (Germis, 2009) . 13, 16, 27, 39, 44

ω_{fue} **Full electrofishing for eel**. Electrofishing made with two pass with direct current (DC), the electrode is kept for at least 30s at one point. The whole surface of the stream is prospected) . 13, 16, 27, 39, 44

ω_{ful} **Full electrofishing**. Electrofishing in wadable streams with two pass) . 13, 16, 27, 37, 39, 44, 47

ω_{oth} **Other type of electrofishing**, this mostly corresponds to data in Spain and Portugal which lacked a qualifyer for the type of method used.. 13, 16, 27, 39, 44

CCM Catchment characteristation and modelling is a pan-European river database. Based on digital elevation data, it is a hierarchical structured and allows to model the streams in an area from the Atlantic to the Ural. 6, 8, 67, 110

ONEMA Office national de l'eau et des milieux aquatiques. 24

RHT the RHT (rau hydrographique thique - hydrographical theoretical network) is a physico-chemical database associated with all streams in France which have been divided in river segments. It is built on digital elevation data corrected to fit the French streams. It is hierarchically structured (Pella et al., 2012) . 6, 7, 9, 11, 18, 19, 66, 70, 77, 110

ROE Rrentiel des Obstacles 'ulement, a database with all man made obstacles, the models uses an extraction from 19 mai 2014, it has not been updated in 2017. Data concerning "bridges" et "dikes" have been removed from the dataset as those types most often do not create an obstacle to eel migration, link. 18, 70

RSA Eel specific surveys (rau de suivi anguille), eel monitoring framework collected both on index rivers, and in the frame of specific protocols applied to collect eels in some french regions. 13, 15

Adaptive Management of Barriers in European Rivers The AMBER project seeks to apply adaptive management to the operation of barriers in European rivers to achieve a more effective and efficient restoration of stream connectivity. In particular the project has developped a database of obstacles, and shared those data with the SUDOANG project. 17, 29, 69, 71

Akaike Information Criterion The Akaike Information Criterion (1973) is a criteria allowing to select the best model, it is a tradeoff betwee the the goodness of fit and the number of independent parameters used in the model. 21

BD Agglo Database of electrofishing from AFB. This version contains data after 2012. 15

BD CARTHAGE Hydrographical reference system for French streams. This geographical database from water agencies and the environment ministry covers 525 000 km of streams. 7, 17, 28, 110

BD TOPAGE BD TOPO ®hydrographie. Hydrographical reference system for French streams replacing the BD CARTHAGE. 11, 67, 74, 110

BDMAP Database of electrofishing from ONEMA. Historical data used in the model were exported in 2014 and contain data updated to 2012, the most recent data come from another database. 15

DBEEL database for eel, this database stores data related to eel and anthropogenic pressures, and was initally developped during the course of the POSE (Walker et al., 2011) project. It was extended during the SUDOANG project to include more detailed information about dams, and in particular information usefull to describe the downstream migration of eels. 12, 15, 17

EMU Eel management unit, adminitrative unit which sets the geographical level of reporting by EU countries for the Eel Management Plans. Initally based on Water Framework Directive district, they are adapted by european countries to fit the national eel management. In France Loire and Brittany form two separate EMUs of one same district, because migratory fishes are managed by different regional instances. Some countries have chosen to report at the national level, some others at the regional level, mose are using WFD districts. 4, 5, 12, 21, 27, 30, 31, 37, 65, 81, 86

GAM General Additive Model, GLM including a quadratic form in the response curves which allows to adjust a non linear response to some terms in the model. In this report, the adjustment is done using the mgcv package, which also allows to calibrate the degrees of freedom in the smoother, which is related to the number of breakpoint points in the response curve. 20, 21, 24

Gamma Gamma distribution, is a probability distribution for continuous positive data. It uses two parameters to describe different shapes, and in particular is adapted to model density data deviating from the normal distribution. 44, 69

GT1 SUDOANG Task Group on data collection. 4, 12, 17

GT2 SUDOANG Task Group on estimation of eel mortalities in Obstacles. 17

GT5 SUDOANG Task Group on web interactive application. 5

GT6 SUDOANG Task Group on transnational eel monitoring network. 4, 12, 18

ICE The ICE protocol for ecological continuity - Used to Assess the passage of obstacles of different species including eels link. 18, 70

Index river Index sites located in the different EMUs of the national territory, whose objective is to describe eel population. Recruitment, yellow eel standing stock and silver eel escapement are monitored, both qualitatively and quantitatively. Those sites provide data to compare with the current estimated eel numbers by EDA. 25

Kappa Cohen's Kappa coefficient, in EDA it is a measure of the model performance (how well it predicts both presence and absence), when comparing model and observed data (electrofishing). It compares the actual proportions with those that would be expected to occur by chance given the marginal numbers in the table. 35, 36, 69, 70

MERIT Hydro is a global hydrography datasets, developed based on the MERIT DEM and multiple inland water maps. It contains flow direction, flow accumulation, hydrologically adjusted elevations, and river channel width. link . 9, 10, 67

Multinomial Multinomial logistic regression models are models which predict proportions in a categorical variable . 20, 23, 24, 53, 58–61, 71, 75, 76

River segment Elementary unit of the RHT. 4, 6–12, 17, 19, 23–25, 35, 39, 44, 56, 64, 69, 77

Silver eel Subadult eel, which at the end of the continental life, will experiences physiological modifications. Those will prepare it to the marine migration towards the Sargasso Sea. This stage migrates downstream in the rivers to the sea. 3, 4, 10, 20, 21, 24, 25, 31, 32, 34, 57, 58, 64, 65, 67, 69, 76, 99, 101

SUDOE area Areas for recruitment and the EDA model, corresponding to a division of recruitment areas according to expert knowledge of recruitment differences between zones. The final division was also based on the availability of data in each of the zone. The zones correspond to, Atlantic Iberia, Meditteranean, Cantabria, Atlantic coast of France. Two additional areas have been added to build the EDA model which covers the whole of France: Channel, and Rhine-Meuse i.e sectors in France without coastal outlet, where the river mouth drains either in Belgium, or the Netherlands. 4, 8, 12, 21, 23, 25, 27, 37–39, 41, 44, 48, 65, 74, 76, 81, 82, 87

Wise River network format for water framework directive reporting, used as source river network in Spain and Portugal. 10, 110

Yellow eel Resident eel, which performs continental water colonization but may remain in Saline water.. 3, 20, 24, 25

LaTeXreport	
	R packages:
LaTeX:	Hmisc, xtable, stargazer, tables
plot :	StacomiR, ggplot2, lattice, ggpubr, hrbrthemes
database :	sf, sqldf, RPostgresSQL, ggspatial, maptools, mapview, rpostgis, rgdal
treatment :	tidyverse, Hmisc, stargazer, ggrepel, stacomiR, sfsmisc
Last compilation : February 8, 2022	
R version 4.1.2 (2021-11-01)	
plateform x86-64-w64-mingw32	